

OPTIMUM DESIGN OF LOW-RISE STEEL FRAMES MADE OF  
COLD-FORMED THIN-WALLED STEEL SECTIONS

A THESIS SUBMITTED TO  
THE GRADUATE SCHOOL OF NATURAL AND APPLIED SCIENCES  
OF  
MIDDLE EAST TECHNICAL UNIVERSITY

BY

SERDAR ÇARBAŞ

IN PARTIAL FULFILLMENT OF THE REQUIREMENTS  
FOR  
THE DEGREE OF DOCTOR OF PHILOSOPHY  
IN  
ENGINEERING SCIENCES

OCTOBER 2013



Approval of the thesis:

**OPTIMUM DESIGN OF LOW-RISE STEEL FRAMES MADE OF  
COLD-FORMED THIN-WALLED STEEL SECTIONS**

submitted by **SERDAR ÇARBAŞ** in partial fulfillment of the requirements for the degree of **Doctor of Philosophy in Engineering Sciences Department, Middle East Technical University** by,

Prof. Dr. Canan Özgen  
Dean, Graduate School of **Natural and Applied Sciences**

\_\_\_\_\_

Prof. Dr. Murat Dicleli  
Head of Department, **Engineering Sciences**

\_\_\_\_\_

Prof. Dr. Turgut Tokdemir  
Supervisor, **Engineering Sciences Dept., METU**

\_\_\_\_\_

Prof. Dr. Mehmet Polat Saka  
Co-Supervisor, **Civil Engineering Dept., Univ. of Bahrain**

\_\_\_\_\_

**Examining Committee Members:**

Prof. Dr. Murat Dicleli  
Engineering Sciences Dept., METU

\_\_\_\_\_

Prof. Dr. Turgut Tokdemir  
Engineering Sciences Dept., METU

\_\_\_\_\_

Assoc. Prof. Dr. Uğur Polat  
Civil Engineering Dept., METU

\_\_\_\_\_

Assoc. Prof. Dr. Zafer Evis  
Engineering Sciences Dept., METU

\_\_\_\_\_

Assoc. Prof. Dr. Tolga Akış  
Civil Engineering Dept., Atılım University

\_\_\_\_\_

Date: 07.10.2013

**I hereby declare that all information in this document has been obtained and presented in accordance with academic rules and ethical conduct. I also declare that, as required by these rules and conduct, I have fully cited and referenced all materials and rules that are not original to this work.**

Name, Last Name : Serdar arbaş

Signature :

## ABSTRACT

### OPTIMUM DESIGN OF LOW-RISE STEEL FRAMES MADE OF COLD-FORMED THIN-WALLED STEEL SECTIONS

Çarbaş, Serdar

Ph.D., Department of Engineering Sciences

Supervisor: Prof. Dr. Turgut Tokdemir  
Co-Supervisor: Prof. Dr. Mehmet Polat Saka

October 2013, 149 pages

Thin-walled section is the one which is made of thin plates. The thickness of thin plates is quite small compared to other cross-sectional dimensions as well as overall length of the member or substructure. Elements made of thin-walled sections are used extensively in steel and concrete bridges, ships, aircraft, mining head frames, and gantry cranes. One common feature of these members made of thin-walled sections is that they are very light compared with alternative sections and, therefore, they are used extensively in long-span structures where the economy is of prime consideration. Thin-walled sections may have a closed or open form. The open thin-walled sections possess small torsional rigidity and they undergo warping deformation when subjected to torsional moments. The warping deformation in turn generates significant normal stresses that are to be considered in the design of such sections. In this thesis, at first an optimum design algorithm is developed for thin-walled beams with open sections when they are subjected to bi-axial bending and torsion. The dimensions of thin plates joined together to constitute the thin-walled section including their thickness are taken as design variables. The displacement, stress and local buckling constraints are considered in the formulation of the design problem. Vlasov's theory is used to calculate the normal and shear stresses that occur due to warping. Besides, this study also aims to produce optimum design of cold-formed thin-walled open sections and optimum design of steel frame made of these kinds of sections given in AISI-LRFD. For this purpose, a different optimum design algorithm is developed which imposes the behavioral and performance constraints in accordance with AISI-LRFD. Moreover, due to the slenderness and the presence of imperfections in cold-formed thin-walled open sections and steel frames built up with these sections, it is necessary to take cognizance of the geometric nonlinearity into account in the prediction of their response under the external loading in both cases. Afterwards, the optimum design problems obtained turn out to be mixed integer and discrete programming problem. Artificial bee colony algorithm is used to obtain their solution. This technique is a recent numerical

optimization technique which mimics the intelligent behavior of honey bee swarm. The recent studies with the artificial bee colony method have shown its effectiveness and robustness in finding the optimum solution of combinatorial optimization problems. Number of design examples is included to demonstrate the competence of the optimum design algorithms developed.

**Keywords:** Cold-Formed Thin-Walled Open Sections, Optimum Size Design, Artificial Bee Colony Algorithm, Warping, Geometric Nonlinearity, Steel Frames.

## ÖZ

### SOĞUK ŞEKİLLENDİRİLMİŞ İNCE CİDARLI ÇELİK KESİTLERDEN YAPILAN AZ KATLI ÇELİK ÇERÇEVELERİN OPTİMUM TASARIMI

Çarbaş, Serdar

Doktora, Mühendislik Bilimleri Bölümü

Tez Yürütücüsü: Prof. Dr. Turgut Tokdemir  
Ortak Tez Yürütücüsü: Prof. Dr. Mehmet Polat Saka

Ekim 2013, 149 sayfa

İnce cidarlı kesitler ince levhalardan yapılırlar. İnce levhaların kalınlıkları, diğer kesitsel boyutlarının yanında elemanın toplam uzunluğu ile karşılaştırıldığında oldukça küçüktür. İnce cidarlı kesitlerden yapılmış olan elemanlar çelik ve beton köprülerde, gemilerde, uçaklarda, maden şövalmanlarında ve gezer vinçlerde yaygın olarak kullanılırlar. İnce cidarlı kesitlerden yapılmış olan bu elemanların ortak bir özelliği, alternatif kesitlerle karşılaştırıldıklarında çok hafif olmaları ve bu yüzden ekonominin asıl etken olduğu uzun açıklıklı yapılarda yaygın olarak kullanılmalarıdır. İnce cidarlı kesitler kapalı veya açık formda olabilirler. Açık ince cidarlı kesitler küçük burulma direncine sahiptirler ve burulma momentine tabi tutuldukları zaman çarpılma deformasyonuna maruz kalırlar. Çarpılma deformasyonu bu tip kesitlerin tasarımında önemli ölçüde dikkate alınması gereken normal gerilmeler oluşturur. Bu tezde, ilk olarak çift eksenli eğilme ve burulmaya maruz bırakılan ince cidarlı açık kesitlerin optimum tasarımını yapan bir algoritma geliştirilmiştir. İnce cidarlı kesiti oluşturmak için kalınlıklarını muhteva ederek birleştirilmiş ince plakaların ölçüleri tasarım değişkenleri olarak alınırlar. Tasarım probleminin formülasyonunda yer değiştirme, gerilme ve lokal burkulma sınırlayıcıları göz önünde tutulur. Çarpılmadan dolayı oluşan normal ve kesme gerilmelerinin hesabında Vlasov teoremi kullanılır. Bunun yanında, bu çalışmanın diğer bir amacı da soğuk şekillendirilmiş ince cidarlı açık kesitlerin ve bu tür kesitlerden yapılmış olan çelik çerçevelerin optimum tasarımlarını AISI-LRFD tasarım yönetmeliğine göre yapmaktır. Bu amaçla, geliştirilen farklı bir optimum tasarım algoritması AISI-LRFD'ye uygun olan davranış ve performans sınırlayıcılarını uygular. Soğuk şekillendirilmiş ince cidarlı açık kesitlerde ve bu kesitlerden inşa edilen çelik çerçevelerde narinlikten ve kusurların var olmasından dolayı, bu yapıların dış yükler altında vereceği tepkiyi tahmin ederken geometrik doğrusalsızlığı göz önüne almak gerekmektedir. Daha sonra, elde edilen optimum tasarım problemleri tam sayı ve ayrık programlama probleminin karışımına döner. Bu problemlerin çözümlerini elde etmek için yapay arı kolonisi yöntemi

kullanılmıştır. Bu teknik bal arısı kolonilerinin zeka davranışlarını taklit eden yeni optimizasyon tekniklerinden biridir. Yapay arı kolonisi metodu ile yapılan güncel çalışmalar bu tekniğin birleşimsel optimizasyon problemlerinin çözümünde ne kadar etkin ve sağlam olduğunu göstermiştir. Geliştirilen optimum tasarım algoritmalarının yetkinliği belirli tasarım örnekleri çözülerek gösterilmiştir.

**Anahtar Sözcükler:** Soğuk Şekillendirilmiş İnce Cidarlı Açık Kesitler, Optimum Boyut Tasarımı, Yapay Arı Kolonisi Algoritması, Çarpılma, Geometrik Doğrusalsızlık, Çelik Çerçeveler.



To My Lovely Daughter and My Family....  
*For your endless support and love*

## ACKNOWLEDGMENTS

I wish to express my deepest appreciation to Prof. Dr. Mehmet Polat Saka, for his support and tremendous encouragement during my research life in METU. He was not only my co-supervisor, but also is one of my friends and especially my second father. I thank him very much for everything. It's an honor for me to work with him. Words cannot express my gratitude to him.

I owe great thanks to Prof. Dr. Turgut Tokdemir for his help, technical support and answering my questions anytime, besides thank his kind friendship for not only his support throughout my studies but also treated me like his son.

I also would like to thank Prof. Dr. Ruşen Gecit, Prof. Dr. Murat Dicleli, Prof. Dr. Ertuğrul Taciroğlu, and Prof. Dr. Stanley B. Dong for their endless encourage.

My special thanks are due Assoc. Prof. Dr. Oğuzhan Hasançebi from Civil Engineering Department, Engineering Faculty, METU for his great advices and discussions in performing my researches.

I wish especially thank Assist. Prof. Dr. İbrahim Aydoğdu for his endless help, never-ending support and trust during my thesis studies even though he is thousands of kilometers away.

Special thanks go to my dear friends, Assist. Prof. Dr. Semih Erhan, Assist. Prof. Dr. Fuat Korkut, Assist. Prof. Dr. Erkan Doğan, Assist. Prof. Dr. Okan Tarık Komesli, Assist. Prof. Dr. Ali Sinan Dike, Dr. Hakan Bayrak, Dr. Ferhat Erdal, Dr. Alper Akın, Refik Burak Taymuş, Memduh Karalar, Kaveh Hassanzehtab, Eras Eraslan, Başar Akdemir, M. Ali Çolak, A. Cem Gel, M. Nuri Katkat, Harun Bakkal, A. Özgür Cırıkçı and Hakan Efe for their useful conversations and cooperation.

I also wish to thank all my colleagues in Engineering Sciences Department, METU. I would also like to thank the staff at this department for their efforts and helps.

I thank to my parents Hayriye and Süreyya Çarbaş for believing in me and giving me endless support. My parents without whom, I would not be the person that I am today. My love for them is eternal. Also, many thank due my elder sister, Ayşegül Çarbaş, for her priceless support during my lifetime. I also want to thank to my second family; Gülser and Mustafa Yaşar Bezin for their support and love.

Finally, I give my special thanks to my wife, Buket, for her endless love and support no matter how unbearable I get. She is the source of my inspiration and my ultimate. At least I dedicate this thesis to my daughter, Buse, who is the joy and soul of my life.

## TABLE OF CONTENTS

<b>ABSTRACT .....</b>	<b>v</b>
<b>ÖZ.....</b>	<b>vii</b>
<b>ACKNOWLEDGMENTS.....</b>	<b>x</b>
<b>TABLE OF CONTENTS .....</b>	<b>xi</b>
<b>LIST OF FIGURES .....</b>	<b>xiv</b>
<b>LIST OF TABLES .....</b>	<b>xvi</b>
<b>CHAPTERS</b>	
<b>1. INTRODUCTION.....</b>	<b>1</b>
1.1. Cold-Formed Thin-Walled Steel Sections.....	1
1.2. Literature Survey.....	3
1.3. Objectives .....	5
1.4. Outline.....	6
<b>2. STRUCTURAL OPTIMIZATION.....</b>	<b>9</b>
2.1. A Brief Introduction to Optimization .....	9
2.2. Mathematical Model of a Typical Optimization Problem .....	9
2.3. A General Outlook on the Issue of Structural Optimization.....	10
2.3.1. Structural Optimization Techniques.....	11
2.3.1.1. Genetic Algorithms (GAs).....	12
2.3.1.2. Evolutionary Strategies (ES) .....	12
2.3.1.3. Evolutionary Programming (EP) .....	13
2.3.1.4. Simulating Annealing (SA) .....	13
2.3.1.5. Particle Swarm Optimizer (PSO).....	13
2.3.1.6. Tabu Search (TS) .....	14
2.3.1.7. Ant Colony Optimization (ACO).....	15
2.3.1.8. Firefly Algorithm (FFA).....	15
2.3.1.9. Cuckoo Search (CS).....	16
2.3.1.10. Bee-Inspired Algorithms .....	16
2.3.1.10.1 Artificial Bee Colony (ABC) Algorithm .....	17
<b>3. TORSIONAL ANALYSIS OF THIN-WALLED SECTIONS.....</b>	<b>19</b>
3.1. General Definition of Torsion.....	19
3.2. Matrix Displacement Method for 3D Steel Structures .....	20
3.2.1 Relationship Between Member End Forces and Member End Displacements	21
3.2.2 Coordinate Transformation.....	23
3.2.2.1. Rotation of $\gamma$ about x axis .....	24

3.2.2.2. Rotation of $\alpha$ about y axis .....	25
3.2.2.3. Rotation of $\beta$ about z axis.....	26
3.2.2.4. Space Frame Members Along the Y-Axis.....	31
3.2.3 Relationship between External Loads and Member End Forces .....	33
3.2.4 Overall Stiffness Matrix .....	34
3.2.5 Member End Conditions .....	35
3.2.5.1. Type 1: Frame member both ends are moment resisting.....	35
3.2.5.2. Type 2: Frame member having a hinge connection at its first end .....	36
3.2.5.3. Type 3: Frame member having a hinge connection at its second end.....	39
3.2.5.4. Type 4: Frame member having a hinge connections at both ends .....	43
3.3 Theory of Thin-Walled Open Members Including Warping Effect.....	45
3.3.1. Twisting Moment and Bimoment .....	46
3.3.2. Cross-Sectional Properties of a Thin-Walled Section.....	48
3.3.3. Stresses Due to Bi-moment and Flexural Twist .....	52
3.3.4. Torsional Stiffness Matrix.....	55
<b>4. GEOMETRIC NONLINEARITY AND STABILITY FUNCTIONS.....</b>	<b>61</b>
4.1. Geometric Nonlinearity.....	61
4.2. Stability Functions .....	63
4.2.1. Effect of Flexure on Axial Stiffness.....	63
4.2.2. Effect of Axial Force on Flexural Stiffness.....	68
4.2.2.1. Bending in X-Y Plane .....	68
4.2.2.2. Bending in X-Z Plane.....	69
4.2.2.3. Effect of Axial Force on Stiffness Against Translation .....	70
4.2.2.3.1. Translation in X-Y Plane.....	71
4.2.2.3.2. Translation in X-Z Plane .....	73
4.3. Analysis of 3-D Frames Including Geometric Nonlinearity.....	76
4.4. Numerical Examples .....	77
4.4.1. Example 1 .....	77
4.4.2. Example 2.....	78
<b>5. OPTIMUM DESIGN OF COLD-FORMED THIN-WALLED OPEN SECTIONS</b>	<b>81</b>
5.1. Definitions.....	81
5.1.1. Yield Point, Tensile Strength, and Stress-Strain.....	81
5.1.2. Modulus of Elasticity, Tangent Modulus, and Shear Modulus.....	82
5.1.2.1. Modulus of Elasticity, $E$ .....	82
5.1.2.2. Tangent Modulus, $E_t$ .....	83
5.1.2.3. Shear Modulus, $G$ .....	83
5.2. Optimum Design of Cold-Formed Thin-Walled Beams with Open Steel Sections	83
5.3. Optimum Design of Steel Frames of Cold-Formed Thin-Walled Open Sections to	86
AISI-LRFD .....	86
5.3.1. Discrete Optimum Design Process .....	86
5.3.1.1. Objective Function.....	87
5.3.1.2. Strength Constraints.....	87
5.3.1.2.1. Effective Slenderness Ratio.....	87
5.3.1.2.2. Computation of Nominal Axial Strength, $P_n$ .....	88

5.3.1.2.2.1. Nominal Buckling Stress, $F_n$ .....	88
5.3.1.2.2.2. Nominal Load, $P_n$ , Based On Flexural Buckling .....	89
5.3.1.2.2.3. Nominal Load, $P_n$ , Based On Distortional Buckling .....	90
5.3.1.2.3. Computation of Allowable Strength, $M_n$ .....	90
5.3.1.2.3.1. Nominal Section Strength, $M_n$ .....	90
5.3.1.2.3.2. Distortional Buckling Strength, $M_n$ .....	91
5.3.1.2.4. Checking Combined Tension Axial Load and Bending .....	91
5.3.1.2.5. Checking Combined Compressive Axial Load and Bending (Beam- Columns) .....	92
5.3.1.3. Deflection and Drift Constraints .....	94
5.3.1.4. Serviceability Constraints .....	95
5.3.1.5. Geometric Constraints .....	95
<b>6. ARTIFICIAL BEE COLONY OPTIMIZATION.....</b>	<b>97</b>
6.1. Introduction .....	97
6.2. Mathematical Formulation of Structural Optimization Problem .....	98
6.2.1. Objective Function .....	98
6.2.2. Design Constraints .....	99
6.3. Steps of Artificial Bee Colony Algorithm .....	99
6.4. Optimum Design Algorithm .....	102
<b>7. DESIGN EXAMPLES.....</b>	<b>105</b>
7.1. Introduction .....	105
7.2. A Thin-Walled Z-Lip Cantilever Beam.....	105
7.3. A Thin-Walled Simply Supported Beam with an Arbitrary Open Section.....	108
7.4. A Thin-Walled Column with a L-Lip Open Section .....	111
7.5. Cold-Formed Thin-Walled Cantilever Beam with C-sections with Lips to AISI-LRFD.....	113
7.6. Cold-Formed Thin-Walled Column with C-sections with Lips to AISI-LRFD ..	116
7.7. Plane Portal Frame Design to AISI-LRFD .....	118
7.8. 302-Member Lightweight Steel Frame Built Up With Cold-Formed Thin-Walled Sections .....	121
7.9. 106-Member Industrial Building Made of Cold-Formed Thin-Walled Sections to AISI-LRFD.....	125
<b>8. SUMMARY AND CONCLUSIONS.....</b>	<b>131</b>
<b>REFERENCES.....</b>	<b>135</b>
<b>CURRICULUM VITAE .....</b>	<b>145</b>

## LIST OF FIGURES

### FIGURES

Figure 1.1. A Typical Roll-Former.....	2
Figure 1.2. Steel Frame Skeleton Made of Cold-Formed Thin-Walled Open Sections.....	2
Figure 3.1. Definition of Torsion.....	19
Figure 3.2. Torsion in a circular member.....	19
Figure 3.3. 3-D frame.....	20
Figure 3.4. Joint end displacements, end forces and end moments of a space frame member.....	21
Figure 3.5. Member forces and moments for each degree of freedom; (a) $u_1=1$ and $u_7=1$ , (b) $u_2=1$ and $u_8=1$ , (c) $u_3=1$ and $u_9=1$ , (d) $u_4=1$ and $u_{10}=1$ , (e) $u_5=1$ and $u_{11}=1$ , (f) $u_6=1$ and $u_{12}=1$ .....	23
Figure 3.6. Rotation of $\gamma$ about x axis.....	25
Figure 3.7. Rotation of $\alpha$ about y axis.....	26
Figure 3.8. Rotation of $\beta$ about z axis.....	28
Figure 3.9. Coordinate transformation from local axis to global axis.....	28
Figure 3.10. Calculation of the length of an element in space.....	30
Figure 3.11. Local coordinates of vertical member in +Y direction.....	32
Figure 3.12. Local coordinates of vertical member in -Y direction.....	33
Figure 3.13. 3-D frame member having a hinge connection at its first end.....	36
Figure 3.14. 3-D frame member having a hinge connection at its second end.....	40
Figure 3.15. 3-D frame member having a hinge connections at both ends.....	43
Figure 3.16. Clarification of Vlasov's Theory.....	46
Figure 3.17. I-section beam distorted by twisting moment.....	47
Figure 3.18. Physical interpretation of bimoment.....	48
Figure 3.19. Sectorial co-ordinate on a thin-walled section.....	49
Figure 3.20. Thin-walled structure and a rectangular coordinate system's origin on its centroid.....	49
Figure 3.21. The cross-section of a thin-walled beam.....	51
Figure 3.22. The sign convention of internal forces on a thin-walled beam.....	53
Figure 3.23. Thin-walled section subjected to torsion.....	54
Figure 3.24. Beam element subjected to the torsion.....	56
Figure 3.25. Twisting torque acting on beam element.....	57
Figure 4.1. P-Delta effects.....	62
Figure 4.2. Effect of Flexure on Axial Stiffness: (a) Bending in X-Y plane; (b) Bending in X-Z plane.....	64
Figure 4.3. Effect of Axial Force on Stiffness Against Translation.....	70
Figure 4.4. Nonlinear stiffness matrix of a three-dimensional steel element.....	75
Figure 4.5. Nonlinear response of a structure obtained through successive elastic linear analysis.....	76
Figure 4.6. 8-member three dimensional steel frame.....	77

Figure 4.7. 8-member, 3D steel frame with crosswise columns. ....	78
Figure 5.1. Stress–strain curves of carbon steel sheet or strip (a) Sharp-yielding; (b) Gradual-yielding. ....	82
Figure 5.2. Thin-walled steel beam with unsymmetrical channel shape. ....	84
Figure 5.3. Beam–columns; (a) subject to eccentric loads, (b) subject to axial and transverse loads, (c) subject to axial loads and end moments. ....	86
Figure 5.4. Geometric constraints for a typical beam-column. ....	96
Figure 6.1. Sharing the fitness of solutions between employed bees and onlooker bees. .	97
Figure 6.2. A Bee Colony Model. ....	98
Figure 6.3. Flowchart of the Artificial Bee Colony (ABC) algorithm. ....	102
Figure 7.1. A thin-walled Z-lip cantilever beam; (a) Z-lip cantilever beam, (b) Design variables. ....	105
Figure 7.2. Loading of thin-walled Z-lip cantilever beam. ....	106
Figure 7.3. Optimum designs of cold-formed thin-walled Z-lip cantilever beam; a) without warping, b) with warping. ....	107
Figure 7.4. Design history graph of cold-formed thin-walled Z-lip cantilever beam. ....	108
Figure 7.5. A thin-walled simply supported beam with arbitrary open section. ....	109
Figure 7.6. Loading of thin-walled simply supported beam with arbitrary open section. ....	109
Figure 7.7. Design history graph of cold-formed thin-walled simply supported beam with an arbitrary open section. ....	110
Figure 7.8. A thin-walled L-lip column; (a) Design variables, (b) Loading of the column. ....	111
Figure 7.9. Design history graph of thin-walled column with L-lip cross-section. ....	112
Figure 7.10. Comparison of the optimum design weights obtained by ABC algorithm. ....	113
Figure 7.11. Cold-formed thin-walled cantilever beam with C-section. ....	114
Figure 7.12. Loading of cold-formed thin-walled cantilever beam with C-section. ....	114
Figure 7.13. Optimum design of cold-formed thin-walled cantilever beam with C-section. ....	115
Figure 7.14. Design history graph of thin-walled cantilever beam with C-section. ....	115
Figure 7.15. Cold-formed thin-walled column; a) Column with C-section, b) Loading of the column. ....	116
Figure 7.16. Optimum designs of cold-formed thin-walled column with C-section. ....	117
Figure 7.17. Design history graph of cold-formed thin-walled column with C-section. ....	118
Figure 7.18. Geometry of a plane portal frame with cold-formed steel sections. ....	118
Figure 7.19. Loading and geometry of the plane portal frame. ....	119
Figure 7.20. Optimum design of plane portal frame. ....	120
Figure 7.21. Design history graph of plane portal frame. ....	121
Figure 7.22. 302-Member Lightweight Steel Frame; a) 3D View, b) Front View, c) Side View, d) Member Grouping. ....	123
Figure 7.23. Design history graph of 302-Member Lightweight Steel Frame. ....	125
Figure 7.24. 106-member industrial building; a) 3D view, b) front view, c) first floor plan and column orientations view, d) side view, e) member grouping. ....	128
Figure 7.25. Design history graph of 106-member industrial building. ....	129

## LIST OF TABLES

### TABLES

Table 3.1. Hinge condition types. ....	35
Table 4.1. Joint displacements obtained by the nonlinear analysis using SAP2000 v14 and nonlinear analysis by the routine developed in this study for 8-members three dimensional steel frame.....	78
Table 4.2. Joint displacements obtained by the nonlinear analysis using SAP2000 v14 and nonlinear analysis by the routine developed in this study for 8-member, 3D steel frame with crosswise columns.....	79
Table 5.1. Displacement limitations for steel frames.....	95
Table 7.1. Optimum design results of thin-walled Z-lip cantilever beam. ....	107
Table 7.2. Optimum design results of cold-formed thin-walled simply supported beam with an arbitrary open section. ....	110
Table 7.3. Optimum design results of thin-walled column with L-lip cross-section. ....	112
Table 7.4. Optimum design results of cold-formed thin-walled cantilever beam.....	114
Table 7.5. Optimum design results of cold-formed thin-walled column.....	117
Table 7.6. Optimum design results of plane portal frame. ....	119
Table 7.7. Optimum design results of 302-member lightweight steel frame. ....	124
Table 7.8. Optimum design results of 106-member industrial building.....	129



# CHAPTER 1

## INTRODUCTION

### 1.1. Cold-Formed Thin-Walled Steel Sections

Thin-walled sections are defined as those where the wall thickness is assumed to be much smaller than a representative dimension of the cross section. This means that the thickness over the width of the section must be much smaller than one. Thin-walled structures may consist of closed or open sections, or a combination of both. Obviously for a beam theory to be reasonable approximation to the structural behavior, the thin-walled beam must be long which means that the ratio of the width over length of the beam must be much smaller than one. Sections of this kind are used extensively in steel and concrete bridges, ships, aircraft, mining head frames, and gantry cranes. They are seen in the form of box girders, plate girders, box columns, purlins (Z and channel (C) sections), pallet stacks, and stud walls [1]. Thin-walled sections can be designed to exhibit great torsional rigidity, for example, as box girders, or they have very little torsional rigidity as, for example, in the case of a plate girder. However, one property they all have in common is that they are very light compared with alternative sections and, therefore, they are used extensively in log-span bridges and other sections where weight and cost are prime considerations.

Structural members used in steel construction can be grouped in two main families. The first and most known group is so-called hot-rolled shapes and members built up of plates. The other, less familiar but of growing importance, is composed of sections cold-formed from steel sheet, strip, plates, or flat bars in roll-forming machines or by press brake or bending brake operations [2]. These are cold-formed steel structural members. The thickness of steel sheets or strip generally used in cold-formed steel structural members ranges from 0.0149 in. (0.4 mm) to about 0.25 in. (6.4 mm). Steel plates and bars with a thickness of 1 in. (25 mm) can be successfully formed into a structural shape by using cold forming process.

The cold-formed steel sections are produced from steel coils by roll-formers or hydraulic press machine. Production with roll-formers is faster and more accurate because in roll-formers the whole production process is controlled by a computer. Today it is possible by the developments in roll-former technology (Figure 1.1 (courtesy of custompart.net)) to produce the frames of several houses in a day and finish hundreds of houses in a few months. Especially the wall frames are assembled in factory and transported to the site as frames and at site these frames are assembled to each other. According to scale of project, the roll-formers can be moved to site and the production can be done in a workshop at site, which results in great savings in transportation costs.

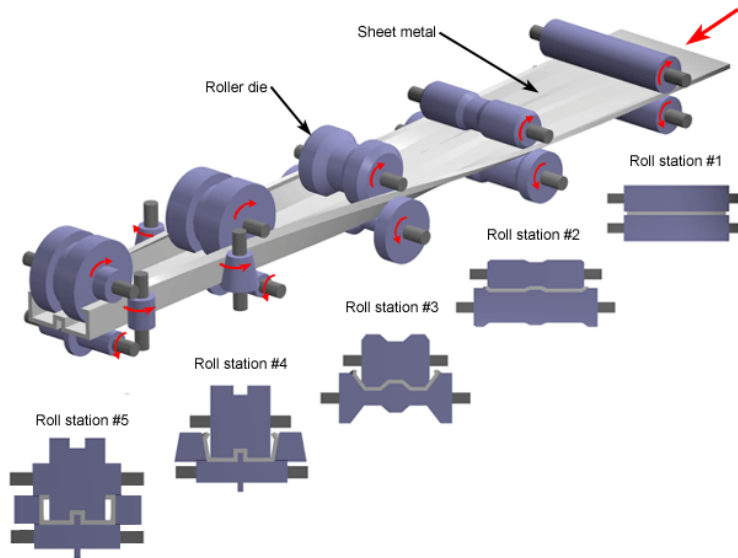


**Figure 1.1.** A Typical Roll-Former.

Cold-formed steel sections has been widely used in construction of residential districts all over the world and light gauge steel housing is becoming very popular in the world since last severe earthquakes occurred. The main advantages of such construction are its high strength, low weight ratio, short construction time, extraordinary standing to earthquake due to its low weight, environmentally friendly, high sound and heat isolation. (Figure 1.2 (courtesy of structure.com)).



**Figure 1.2.** Steel Frame Skeleton Made of Cold-Formed Thin-Walled Open Sections.

The above advantages increased the utilization of cold-formed steel sections in the construction of new residential buildings in last two decades. As the cold-formed steel sections bring into play increasingly, it will become even more indispensable for design procedures and methods to accurately predict the behavior of such structural elements. This will guarantee structures constructed with cold-formed steel sections to be safe and cost-effective [3].

Thin-walled box-sections are also replacing massive reinforced concrete beams in many types of bridge construction and torsionally stiff thin-walled cellular decks are replacing conventional lattice girder designs suspension bridges. Thin-walled hollow box-sections are also used as columns and beams in building construction while many forms of crane framework include this type of structural member [4]. Thin-walled sections are not, of course, restricted box-sections; built-up plate girders form open I-section thin-walled beams and even heavy rolled steel joists may be analyzed by thin-walled theory in certain circumstances.

The sections which are subjected to general loading can be classified in two groups; i ) Closed Sections, ii ) Open Sections.

Another classification concerning the sections is given in the following;

- 1) If the thickness of the section is not very small comparatively to its width, they are called *Thick-Walled* sections.
- 2) If the ratio of thickness over depth is small, they are called *Thin-Walled* sections.

## **1.2. Literature Survey**

Many studies have been conducted on design of cold-formed thin-walled steel sections;

In 1961, the behavior of uniform thin-walled beams under bending and torsion is studied by Vlasov [5]. The derivations of the differential equations of non-uniform torsion for thin-walled members with open cross-section were given in 1961 by Timoshenko [6, 7].

Paz et al. [8], in 1976, developed a computer program which determines the properties of open and closed thin-walled steel section areas of rectangular segments and in a similar vein for determination of torsional and flexural properties of thin-walled beams, Ghersi et al. [9] calculated geometrical properties using a computer code in 2002.

In 1982, Pedersen and Gunnlaugsson [10] offered a finite element model for calculation of stresses and deformations of beams with thin-walled steel cross-sections. Warping effect is considered by a modified sectorial coordinate formulation. Prismatic elements with seven degree of freedom on each node were used in the theory. As a means of

transition matrices, various types of prismatic beam segments could be represented in the global stiffness matrix with efficient kinetic compatibility.

Meek and Ho [11], in 1983, introduced another finite element method for the solution of warping torsion problems of thin-walled structures including the stiffness equations with warping displacements.

Tralli [12], in 1986, tackled a hybrid finite element model for calculation of stresses and deformations of steel beams constructed with thin-walled open, closed and mixed cross sections. The suggested model considers shear deformations and lets one to deal with beams with sharp variations of the cross section. Uniform and mixed type thin-walled structures searched.

A solution for torsional analysis of open cross-section beams is studied by Eisenberger [13], in 1995. This study focused on an analytical method to form the stiffness matrix of the beam including the warping effect. The method proposed based upon the solution of the differential equation for any polynomial variation of the cross-section properties.

Al-Mosawi and Saka [14], in 1999, developed an algorithm which obtains the optimum cross-sectional dimensions of cold-formed thin-walled steel beams subjected to general loading. This study includes the effect of warping in the calculation of normal stresses which is included using Vlasov's theory.

Lee et al. [15, 16], in 2004 and 2006, presented a micro genetic algorithm to find an optimum cross-section of cold-formed steel beams and columns. The shape optimization of cold-formed steel channel sections under uniformly distributed load and axial compression were presented for beams and columns, respectively. The design curves are generated for optimum values of the thickness, the web flat-depth-to-thickness ratio, and the flange flat-width-to-thickness ratio for beams and columns under uniformly distributed load.

Magnucki and Monczak [17], in 2000, Magnucki [18] in 2002, Magnucka et al. [19] in 2004 determined optimum shapes of selected mono-symmetrical open cross-sections of cold-formed thin-walled beams. In these studies, optimal design of thin-walled beams under strength and stability constraints is investigated.

Adeli and Karim [20] applied the neural network method to optimize cold-formed steel beams and Karim and Adeli [21] implemented the optimization for the hat section of cold-formed steel beams under uniformly distributed loading via a comprehensive parametric study. The beams may be fully braced, unbraced, or braced at a specified number of points according to the AISI-ASD and the LRFD specifications.

In 2006, a global optimization method for designing the cross-section of channel beams under uniformly distributed transverse loading is presented by Tran and Li [22]. The optimization of the cross-section is managed by using the trust-region method (TRM)

based on the failure modes of yielding strength, deflection limitation, local buckling, distortional buckling and lateral–torsional buckling.

Geometric nonlinear analysis of thin-walled space frames is investigated by Chang et al. [23] using of incremental equilibrium equations based on the updated Lagrangian formulation and Vlasov’s assumption. In this study, the improved displacement field for non-symmetric thin-walled cross-sections is demonstrated based upon inclusion of second order terms of finite rotations and the potential energy corresponding to the semi-tangential rotations and moments.

Stasiewicz et al. [24] formulated local buckling of a bent flange of a thin-walled beam. In classical approach each segment of the flange is considered as a simple plate. However, an analytical description of the whole flange as a thin-walled structure with the use of an energetic method is introduced by the authors. Silvestre and Camotim [25,26] presented the derivation of generalized beam theory based on full analytical formula to provide distortional critical length and bifurcation stress resultant estimates in cold-formed steel C-section and Z-section members; (i) subjected to uniform compression (columns), pure bending (beams) or a combination of both (beam–columns), (ii) with arbitrary sloping single-lip stiffeners and (iii) displaying four end support conditions. These formulas incorporate genuine folded-plate theory, which is a feature that is responsible for their generality and high accuracy. Camotim et al. [27] presented the general beam theory (GBT) formulation, and corresponding finite element implementation to analyze local and global buckling behavior of thin-walled members with arbitrary loading and support conditions. Macdonald et al. [28] described the main types of cold-formed steel members and discussed the particular characteristics affecting their design.

Lim and Nethercot [29] defined some of the benefits of using a cold-formed steel portal framing system over conventional hot-rolled steel portal frames and authors considered the behavior and design of bolted moment-connections between cold-formed steel members, formed by using brackets bolted to the webs of the section [30].

### **1.3. Objectives**

In this study, an optimum design algorithm is developed for cold-formed thin-walled open sections where the effect of geometric nonlinearity as well as effect of warping is taken into consideration when they are subjected to axial load, bi-axial bending and torsion. Due to the slenderness and the presence of imperfections in cold-formed thin-walled steel sections it is necessary to consider the geometric nonlinearity in the prediction of their response to external loading in order to attain realistic results in their design. The dimensions of thin plates of cold-formed sections such as their length and thickness are treated as design variables. The displacement and stress constraints are included in the formulation of the design problem. The effect of cross sectional warping in the computation of normal and shear stresses is considered by using Vlasov’s theory.

Moreover, a different design algorithm is proposed to optimum design of cold-formed thin-walled open sections and low-rise steel frames made use of these sections to AISI-LRFD design provisions. The strength and stability constraints are adapted from the design provisions of the 2007 edition of the North American (AISI) specification for the design of beam–columns. It is estimated that cold-formed steel beam-column members will be comprised of standard C-sections with lips. Once the loading of the beam-column members is established then the design problem turns out to be the selection of appropriate C-sections from the available section list.

The objective function is selected as the minimum weight for both cases. The optimum design problem obtained in such formulation turns out to be mixed integer and discrete programming problem. The Artificial Bee Colony (ABC) algorithm which is one of the recent metaheuristic techniques is used to obtain the solution of the optimum design problem. The optimum design algorithm developed is used to determine the optimum dimensions of number of steel members and frames made of cold-formed thin-walled open sections.

#### **1.4. Outline**

The outline of thesis can be categorized as follows;

In Chapter I, a cursory definition is given about cold-formed thin-walled steel sections and advantageous of these sections to be selected as structural component is mentioned. Addition to this, manufacturing procedure and application areas of cold-formed thin-walled steel sections is discussed briefly. Besides, a literature survey on the design of cold-formed thin-walled steel sections and structures made of using these sections is included. At last, objectives and outline of the current study is stated.

In Chapter II, engineering design optimization, structural optimization and the methods of structural optimization are discussed. Also, general definitions about optimization, elements of optimization problems that are used in optimization problems are pointed out in this chapter. In addition, mathematical formulation of a typical optimization problem is defined.

In Chapter III, the matrix displacement method for 3D frames and the theory of the effect of warping are described. In addition to these, a computer program encoded in FORTRAN which has the feature of analysis of cold-formed thin-walled open sections excluding or including effect of warping is developed.

In Chapter IV, a detail derivation and definition of stability functions used to calculate the nonlinear stiffness matrix of a three dimensional steel structure is figured out. Besides, geometric nonlinearity is described in this section.

In Chapter V, the optimum design of cold-formed thin-walled beams with open steel sections is formulated and defined. Besides, optimum design of cold-formed thin-walled open sections including geometric nonlinearity that are subjected to axial load as well as biaxial bending moments according to design code AISI-LRFD is described. In addition, optimum design of low-rise steel frames built up with cold-formed thin-walled sections to AISI-LRFD is represented. The objective function and design constraint functions of these kinds of steel frames are described in detail.

In Chapter VI, artificial bee colony algorithm is adopted to obtain the solution of the optimum design problem described and formulated in Chapter 5. Also, optimum design algorithm based on artificial bee colony is defined in this chapter.

In Chapter VII, the robustness and effectiveness of proposed ABC algorithm is tested on design examples related with the optimization process defined in Chapter 5.

In Chapter VIII, principal conclusions and remarks summarized of this study is provided.





## CHAPTER 2

### STRUCTURAL OPTIMIZATION

#### 2.1. A Brief Introduction to Optimization

The engineering design optimization has emerged in the middle of 20<sup>th</sup> century and it has found many applications almost in every branch of industry involving civil, mechanical, and industrial and aerospace engineering. The applications covered complete systems as well as components for products ranging from steel sections to wings of aircrafts. In today's world, optimization has been broadly implemented in operational research, artificial intelligence and computer science, and is used to develop processes in the field of management and various other disciplines other than engineering. The main objective of the optimization is to find values of the decision or design variables that minimize or maximize the objective function while satisfying the certain limitations or constraints. The basic objective of the optimization process is to reach the best solution from the possible combination of variables defined in mathematical problem. Objective function of an optimization problem represents some quantity, such as profit or cost that is to be maximized or minimized. The first step in formulating the mathematical model of an optimization problem is to identify the design variables and describe the constraints in terms of these design variables. Design variables depend on the class of problems and requirements. Constraints usually composed of either system restrictions or physical and economic rules that the solution must satisfy. A general optimization problem can be defined as selecting optimal values of the design variables so that the specified objective function has the minimum value and constraints which are generally functions of these variables, are satisfied.

Over the past decade, with the development of computer-based analysis methods, the enhancement of optimization subjects has been revolutionized. In conjunction with the quick progress of high-performance computers and development of computational methods, it became possible to deal with more and more large-scale optimization problems that designers face every day's practice.

#### 2.2. Mathematical Model of a Typical Optimization Problem

The mathematical statement of an optimization problem includes determination of design variables, and expression of objective function and constraints. The general mathematical formulation of an optimal design problem may be phrased as follows;

$$\text{Minimize } F(x) \tag{2.1}$$

Subject to:

$$m_l(\mathbf{x}) = 0, \quad l = 1, 2, \dots, 0 \quad (2.2)$$

$$g_j(\mathbf{x}) \leq 0, \quad j = q+1, \dots, n \quad (2.3)$$

$$\mathbf{x}_k \in X, \quad X = \{x_1, x_2, \dots, x_d\} \quad (2.4)$$

where  $F(\mathbf{x})$  is the objective function and  $\mathbf{x}$  is design variable vector. In general optimization problems, some constraints can be expressed as equality constraints  $m_l$  and some others may be stated as inequality constraints  $g_j$ . Furthermore some optimization problems requires the use of lower and upper bound constraints for each or some design variables that vary depending on the type of the problem.  $X$  represents the set of design variables and  $d$  is the total number of these variables. Number of constraints which limit the objective function is presented by  $n$  [31].

### 2.3. A General Outlook on the Issue of Structural Optimization

Contemporary structural optimization has its roots in the 1960s [32]. Early structural optimization algorithms were based on mathematical programming techniques. Structural design problems are formulated as decision making problems where the objective function is selected as the minimum cost or weight of the structure. The displacement and allowable stress constraints are introduced to the mathematical model. The cross sectional areas of structural members are treated as design variables. Such formulation has transformed the structural design problem into a decision making problem. The design constraints in these structural design problems are nonlinear functions of the design variables. Therefore one of the nonlinear programming techniques can be used to obtain the solution of these programming problems. By making use of mathematical programming techniques several structural optimization algorithms were developed and they were applied wide area of structural design problems [33]. Initially the design problems solved were small size problems where the total number of design variables were not more than ten. Later when these techniques are applied to large size structural design problems designed faced with convergence difficulties. Furthermore one of the assumption which is necessary to be made in mathematical programming techniques is the assumption of continuous design variables which produced optimum solutions for the cross sectional areas that were not available in the steel sections list. The techniques that were based on mathematical programming techniques which were capable of handling discrete variables were complicated and not easy to code for programming. Hence researchers had to move to develop another kind of optimization techniques which did not suffer the above discrepancies [34, 35].

To remove all of these drawbacks of mathematical programming a-state-of-art optimization methods, so-called *Metaheuristic* or *Stochastic* search techniques were brought into play. These methods are class of search methods which includes heuristics and an element of non-determinism in traversing the search space [36]. Unlike the search algorithms introduced so far, a metaheuristic and/or stochastic search algorithm moves from one point to another in the search space in a nondeterministic manner, guided by heuristics. The next move is partly determined by the outcome of the previous move. These search techniques deal with situations where some or all of the parameters of the optimization problem are described by random or probabilistic variables rather than by deterministic quantities. The source of random variables may be several, depending on the nature and the type of problem.

These techniques do not require gradient information of the objective function and constraints, and use probabilistic transition rules not deterministic ones. They employ random number call, and incorporate a set of parameters that require to be adjusted prior to their use. These novel and innovative metaheuristic search algorithms make use of ideas inspired from the nature. The essential phenomena lay over the behind of these methods is to mimic the natural events, such as survival of the fittest, immune system, swarm intelligence and the cooling process of molten metals through annealing into a numerical algorithm [37-44]. The optimum structural design algorithms that are based on these techniques are robust and quite effective in finding solutions to discrete programming problems. A detailed review of these algorithms as well as their applications in optimum structural design is carried out by Saka [45].

### **2.3.1. Structural Optimization Techniques**

Optimum structural design algorithms provide a useful tool to steel designers. The optimum topology, the optimum geometry and the optimum steel profiles for the members of a steel structure can be determined such that the steel structure can be constructed by using adequate steel material but not more. Structural design optimization achieves these aims such that design constraints defined by steel design standards are satisfied under the applied loads and the weight or the cost of the steel structure under consideration is the minimum. When formulated, two types of structural optimization problems may be categorized. In some design problems the design variables might have continuous values. But in some others it is required that the values of design variables have to be chosen from a set of discrete values. The optimum design problem of steel structures falls into the second class. Designer has to select steel sections for the members of steel frames from a discrete set which contains certain designations of steel profiles that are produced by steel mills. Hence the formulation of the steel frame design optimization problem turns out to be a discrete programming problem [46]. Obtaining solutions to discrete programming problems is more difficult than finding solutions to programming problems with continuous variables [47]. This may be one of the reasons why early mathematical programming techniques developed have dealt with continuous variables [48-50]. Later some of these algorithms have been extended to address discrete

optimization problems as well. The algorithms that are based on mathematical programming techniques are deterministic. They need an initial design point to initiate a search for the optimum solution and require gradient computations in the exploration process. Some of the recent metaheuristic techniques are summarized in the following.

### **2.3.1.1. Genetic Algorithms (GAs)**

Genetic algorithm (GA) is one of the recent metaheuristic search algorithm inspired by evolutionary biology such as inheritance, mutation, selection, and crossover. GAs is a particular class of evolutionary algorithms that categorized as global search heuristics. The basic techniques of the GAs are designed to simulate processes in natural systems necessary for evolution, especially those following the first laid down by Charles Darwin of survival of the fittest [51, 52]. GAs is composed of three essential phases [53]. These are, (i) coding and decoding variables into strings, (ii) evaluating the fitness of each solution string, and (iii) applying genetic operators to generate the next generation of solution strings.

GAs are used to determine the optimum solution of large amount of optimization problems, such as optimal control problems, job scheduling, transportation problems, economic models, structural engineering, etc. This technique is implemented to handle optimization problems including both discrete and continuous variables. GA has been quite successful in finding the optimum solutions of both constrained and unconstrained optimization problems [54]. Therefore this technique is one of famous optimization method applied for structural engineering problems.

### **2.3.1.2. Evolutionary Strategies (ES)**

The evolution strategies (ES) were developed by Rechenberg [55] and Schwefel [56] in 1964. These algorithms were originally developed for continuous optimization problems. This optimization technique is based upon phenomena of adaptation and evolution has very complex mutation and replacement functions. Initial populations consisting of  $\mu$  parent individuals are randomly generated in evolution strategies algorithm. After generating process, a new population is produced by mutation, recombination, and selection operators.

Rajasekaran et al. [57] has used evolutionary strategies technique to determine the optimum solution of large size steel frames. It is reported in this study that ES presents good performance in the optimum design of large size structures. Ebenaua et al. [58] and Hasançebi et al. [59] also used ES in the optimum design of large scale structures. It is reported in these studies that ES performed effectively to obtain the optimum solutions of large scale structures. It is concluded that ES is one of the robust and efficient optimization methods that can be employed for finding the optimum solutions of structural optimization problems.

### **2.3.1.3. Evolutionary Programming (EP)**

Evolutionary programming (EP) is one of the stochastic search techniques introduced by Fogel [60]. This method is alike to ES. EP has three basic steps that are listed as follows [61, 62]; (i) Initial design is generated randomly, (ii) each design variable in the design is reproduced into new designs as off springs. Each of this off-spring is mutated according to a distribution of mutation types, ranging from minor to extreme with a continuum of mutation types between. The acuteness of mutation is judged on the basis of the functional change forced upon parents, (iii) each off-spring solution is assessed by computing its values. Typically a stochastic tournament is held to determine those to be retained in the next population. There is no requirement that the population size be held constant or that only a single off spring be generated from each parent [63].

### **2.3.1.4. Simulating Annealing (SA)**

Simulated annealing (SA) [64] employs a simulative model of the annealing process of physical systems, establishing a direct analogy to the elementary principles of thermodynamics and statistical mechanics. It simulates the cooling process of a physical system, taking advantage of the fact that if this cooling procedure is performed slowly enough, the system will end up in the optimum state (e.g., a flawless crystal). Name of this method comes from annealing strategy in metallurgy. This technique involves heating and controlled cooling of a material in order to expand the size of its crystals and decrease their defects. The heat causes the atoms to leave from their initial positions (a local minimum of the internal energy) and move randomly through states of higher energy; the slow cooling gives the atoms enough time to find positions that minimize a steady state is reached. Simulating Annealing algorithm starts with initial design which is randomly created. Then initial value of the temperature is set. Candidate designs are generated in the close neighbor of the current design. Candidate designs are evaluated and temperature is decreased. This process is repeated when the system is frozen in the optimum state at a low temperature.

There are many applications of SA in structural optimization problems. In 1991 and 1992, Balling [65, 66] used SA for the discrete optimum design of three dimensional steel frames. Topping [67], Hasańcebi and Erbatur [68, 69] applied simulated annealing method for optimum design truss systems. It can be concluded that this method is efficient tool for structural optimization problems.

### **2.3.1.5. Particle Swarm Optimizer (PSO)**

Particle swarm optimizer is based on the social behavior of animals such as fish schooling, insect swarming and birds flocking. The method considers an artificial swarm which consists of particles (agents). The behavior of each agent in the swarm is simulated

according to three rules. This method is originated in 1995 by James Kennedy and Russell C. Eberhart [70] inspiring social behavior of bird flocking or fish schooling.

The particle swarm optimizer selects a number of particles to represent a swarm. Each particle in the swarm is a potential solution to the optimization problem under consideration. A particle explores the search domain by moving around. This move is decided by making use of its own experience and the collective experience of the swarm. Best candidate solution is defined as the local best or the best particle. Each individual stores value of its best candidate solution and where its best success is stored. This information can be also seen from its neighbors. These in formations guide the movements in the design space, with the population usually converging, by the end of a trial, on a problem solution better than that of non-swarm approach using the same methods.

In the past fifteen years, there are many studies have been done with PSO method. Fourie and Groenwold [71] used particle swarm optimization method for optimum design of structures with sizing and shape variables. Perez and Behdinan [72] presented a study about optimum design algorithm for pin jointed steel frames by using particle swarm optimization method. It is reported from studies that PSO shows good performance in structural optimization method.

#### **2.3.1.6. Tabu Search (TS)**

Tabu search (TS) implements a simple yet an efficient iterative based local search strategy for solving combinatorial optimization problems. At each step a number of candidate solutions are sampled in the close vicinity of the current design by perturbing a single design variable called a move. The best candidate is chosen and replaced with the current design even if it offers a non-improving solution, and the move leading to this candidate is recognized as a successful move. To protect the search against cycling within the same subset of solutions, information regarding most recently visited solutions is collected in a list referred to as tabu list. It is actually a set of restricted moves the search is prohibited to be transmitted to. This method was first developed by Glover [73] in 1989. TS uses a neighbor search procedure. New solution is obtained by moving iteratively from a solution in the neighborhood [74].

Degertekin et al. conducted some studies about optimum design of steel frames using TS [75-79]. Hasançebi et al. [59] have applied TS method in optimum design of real-sized pin-jointed structures. Similar to aforementioned stochastic search methods TS is very popular among designers for structural optimization problems.

### **2.3.1.7. Ant Colony Optimization (ACO)**

Ant colony optimization (ACO) [80] simulates the foraging behavior of social ants. ACO uses pheromone as a chemical messenger and the pheromone concentration as the indicator of quality solutions to a problem of interest. Since the solution is often linked with the pheromone concentration, the search algorithms often produce routes and paths signed by the higher pheromone concentrations, and therefore, ants-based algorithms are particular suitable for discrete optimization problems.

The movement of an ant is controlled by pheromone which vaporizes over time. Without such time-dependent evaporation, the algorithms cause premature convergence to the (often infeasible) solutions. With proper pheromone evaporation, they usually act very well.

There are two fundamental issues here: the probability of choosing a path, and the vaporization rate of pheromone. There are few ways of solving these problems, although it has popularity as a field of active research. Camp and Bichon [81] first developed a design algorithm with ACO to size steel space trusses for minimum weight subject to stress and deflection limitations. Later, they extended this work to optimize rigid steel frames in Camp et al. [82]. Kaveh and Shojaee [83] also presented an ACO integrated solution algorithm for discrete optimum design problem of steel frames with design constraints consisting of combined bending and compression, combined bending and tension and deflection limitations. In some studies in the literature, attempts were made to accelerate the performance of ACO by hybridizing it with another meta-heuristic technique, namely particle swarm method [84-86]. In Aydogdu and Saka [87], ACO is employed to seek optimum design of three dimensional (3D) irregular steel frames, taking into account warping deformations of thin-walled sections.

### **2.3.1.8. Firefly Algorithm (FFA)**

The Firefly Algorithm (FFA) is a very recent heuristic optimization algorithm developed by Yang [88] and is inspired by the flashing behavior of fireflies. According to Yang [88], FFA algorithm has three basic rules; (i) All fireflies are unisex, so that one firefly is attracted to other fireflies regardless of their sex, (ii) Attractiveness is proportional to brightness, so for any two flashing fireflies, the less bright firefly will move towards the brighter firefly. Both attractiveness and brightness decrease as the distance between fireflies increases. If there is no firefly brighter than a particular firefly, that firefly will move randomly, (iii) The brightness of a firefly is affected or determined by the landscape of the objective function. There are two essential components of FFA; the variation of light intensity and the formulation of attractiveness. The latter is assumed to be determined by the brightness of the firefly, which in turn is related to the objective function of the problem under study. As light intensity and attractiveness decrease and the distance from the source increases, the variation of light intensity and attractiveness should be a monotonically decreasing function.

Engineering design application of firefly algorithm is given in [89, 90]. Firefly Algorithm [FA] is used to determine optimum solution of six engineering design problem that are taken from the literature and its performance is compared with other metaheuristic algorithms such as particle swarm optimizer, differential evolution, genetic algorithm, simulated annealing, harmony search method and others [89]. It is stated that the results attained from the optimum solutions of these design examples, firefly algorithm is more efficient than particle swarm optimizer, genetic algorithm, simulated annealing and harmony search method. In [90], the permutation flow shop is formulated as a mixed integer programming problem which is classified as hard to solve nonlinear programming problem.

### **2.3.1.9. Cuckoo Search (CS)**

Cuckoo search (CS) algorithm is firstly introduced by Yang and Deb [91]. This technique mimics the reproduction mechanism of some kind of cuckoo birds. A cuckoo bird deposits its eggs in another bird's nest in order that the eggs are hatched and fledglings are fed by the other birds. This type of cuckoo birds, sometimes, chucks out the host birds' eggs from nest to create more hatching chance to their own eggs. Some female cuckoos has very special characteristic to simulate the color and pattern of the eggs of a host birds so that its eggs are not recognized to be alien eggs and safely hatched by the host bird. If a host bird perceives conflict with the intruding different eggs in its nest, the cuckoos' eggs can be removed away or host bird can rebuilt its nest on a different place. In cuckoo search (CS) algorithm cuckoo egg represents a potential solution to the design problem which has a fitness value. The algorithm uses three idealized rules as given in [91]. These are: a) each cuckoo lays one egg at a time and dumps it in a randomly selected nest. b) the best nest with high quality eggs will be carried over to the next generation. c) the number of available host nests is fixed and a host bird can discover an alien egg with a probability of  $P_a \in [0,1]$ . The performance of cuckoo search algorithm is compared with particle swarm optimizer, differential evolution and artificial bee colony algorithms in [92]. Fifty different benchmark problems are taken from literature and solved using the above mentioned metaheuristic algorithms. Optimum design of tall steel frames based on cuckoo search algorithm is carried out in [93]. The design problem is formulated according to Load and Resistance Factor Design code of American Institute of Steel Construction. The optimum designs obtained by cuckoo search algorithm are compared with those attained by other algorithms on benchmark frames. Cuckoo search algorithm is extended to deal with multi-objective optimization problems under complex nonlinear constraints in [94].

### **2.3.1.10. Bee-Inspired Algorithms**

Bee-inspired algorithms are various and some use pheromone and most do not [95-98]. Almost all bee-inspired algorithms imitate the foraging behavior of honey bees in nature. Interesting features such as waggle dance, polarization and nectar maximization are often



used to mimic the allocation of the foraging bee along flower patches and thus different search regions in the search space. In order to comprehend this process, one should understand well the life of the Parpinelli and Honey bees in a colony and the foraging and storing the honey in their constructed colony. Honeybees make contact by pheromone and ‘waggle dance’. As an example, an alarming bee may release a chemical message (pheromone) to warn attack response in other bees. Moreover, when some bees find a good food source and bring some nectar back to the hive, they will communicate the location of the food source by performing the so-called ‘waggle dances’ as a signal system. Such signaling dances vary from species to species; on the other hand, they try to conscript more bees by using directional dancing with varying strength so as to contact with the direction and distance of the found food resource. For multiple food sources such as flower patches, studies present that a bee colony is capable of allocating forager bees among different flower patches so as to maximize their total nectar intake.

In the honeybee-based algorithm, forager bees are allocated to different food sources (or flower patches) so as to maximize the total nectar intake. The colony has to ‘optimize’ the overall efficiency of nectar collection; the allocation of the bees is thus depending on many factors such as the nectar richness and the proximity to the hive.

The most popular bee-inspired algorithm is known as “Artificial Bee Colony (ABC)” which is widely applied to every branch of engineering design optimization problems.

#### **2.3.1.10.1 Artificial Bee Colony (ABC) Algorithm**

The artificial bee colony (ABC) algorithm is originated by Karaboga and Basturk [99-102]. This algorithm is based on characteristic behavior of honey bee swarms. ABC algorithm uses only common control parameters such as colony size and maximum cycle number as in Particle Swarm Optimizer and Ant Colony Optimization methods. ABC as an optimization tool provides a population-based search procedure in which individuals called foods positions are modified by the artificial bees with time and the bee’s aim is to discover the places of food sources with high nectar amount and finally the one with the highest nectar. In ABC system, artificial bees fly around in a multidimensional search space and some (employed and onlooker bees) choose food sources depending on the experience of themselves and their nest mates, and adjust their positions. Some (scouts) fly and choose the food sources randomly without using experience. If the nectar amount of a new source is higher than that of the previous one in their memory, they memorize the new position and forget the previous one. Thus, ABC system combines local search methods, carried out by employed and onlooker bees, with global search methods, managed by onlookers and scouts, attempting to balance exploration and exploitation process.

In this study, optimum design of low-rise steel frames made of cold-formed steel sections is determined by using artificial bee colony algorithm. The main steps of this technique are discussed in detail in Chapter 6.



## CHAPTER 3

### TORSIONAL ANALYSIS OF THIN-WALLED SECTIONS

#### 3.1. General Definition of Torsion

Torsion can be expressed as twisting of a structural member, when it is loaded by couples that produce rotation about its longitudinal axis [103] as shown in Figure 3.1.

$$T_1 = P_1 d_1 ; T_2 = P_2 d_2 \quad (3.1)$$

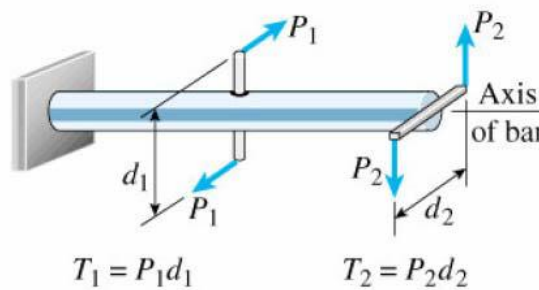


**Figure 3.1.** Definition of Torsion.

where the couples  $T_1$  and  $T_2$  are called torques, twisting couples or twisting moments (Figure 3.2.). The unit of  $T$  is N-m and/or lb-ft.



a ) Torques Occured;  $T_1$  and  $T_2$ .

b) A circular member subjected to torsion.

**Figure 3.2.** Torsion in a circular member.

Analysis of more complicated steel section shapes required more advanced method than a simple solution process. This chapter first introduces the matrix displacement method for 3D frames, and then summarizes the theory of thin-walled members including warping effect and cross-sectional properties of thin-walled sections and finally extends the matrix displacement method for thin-walled members so that effect of warping can be taken into consideration in the analysis of steel frames having such members.

### 3.2. Matrix Displacement Method for 3D Steel Structures

A 3D steel frame is shown in Figure 3.3. The coordinates of joints in this frame are defined according to the XYZ Cartesian system which is called global axis system. Each joint of this frame has six degrees of freedom as shown in the figure. These are the usual three translations ( $d_1, d_2, d_3$ ) along X, Y, and Z axes and three rotations ( $d_4, d_5, d_6$ ) about these axes as shown Figure 3.3. Therefore, the displacement vector of any joint  $i$  in the frame is  $D_i = d_1 d_2 d_3 d_4 d_5 d_6$  in the global axis. The corresponding loading vector applied on joint  $i$  has the form of  $P_i = p_1 p_2 p_3 p_4 p_5 p_6$ , where, ( $p_1, p_2, p_3$ ) are the force components along X, Y, and Z axis respectively and ( $p_4, p_5, p_6$ ) are moment components along X, Y, and Z axis, respectively.

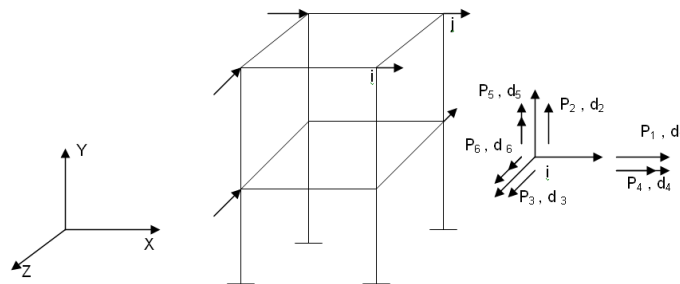


**Figure 3.3.** 3-D frame.

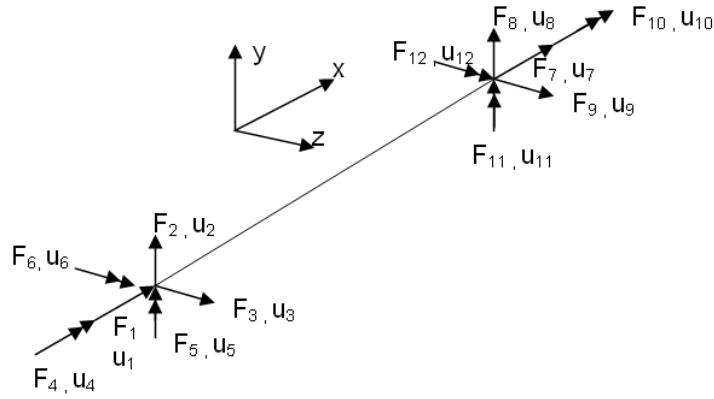


**Figure 3.4.** Joint end displacements, end forces and end moments of a space frame member.

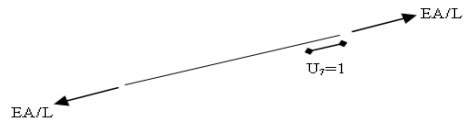
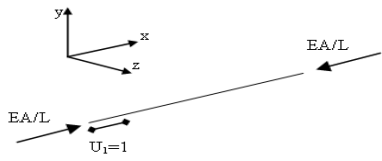
When a space structure is subjected to external forces its joints moves in the three dimensional space and internal forces occur at the ends of its members. Joint displacements and end forces are defined in local axis as shown in Figure 3.4. In this figure, first end forces and moments of the member  $k$ , are represented as vector  $F_k = f_1 f_2 f_3 f_4 f_5 f_6$  where;  $(f_1, f_2, f_3)$  are the axial force, shear forces y and z axis respectively and  $(f_4, f_5, f_6)$  are end moments of the first end of the member  $k$ . The member end displacement vector in the first end of member  $k$  is described as  $U_i = u_1 u_2 u_3 u_4 u_5 u_6$  in the local coordinate system. Consequently, six end joint displacements and six end forces develop at each end of the member.

### 3.2.1 Relationship Between Member End Forces and Member End Displacements

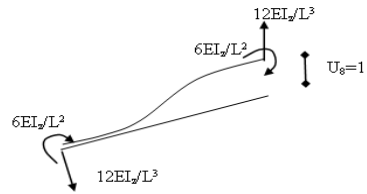
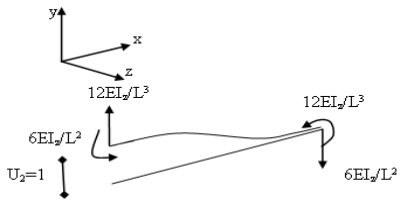
The relationship between member end forces and member end deformations is described as follows.

$$F_i = [k_i] U_i \quad (3.2)$$

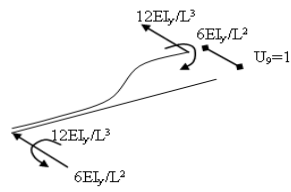
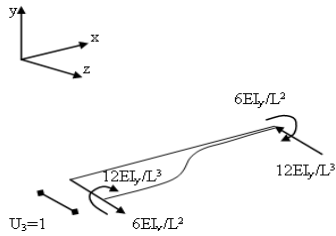
where,  $[k_i]$  is the stiffness matrix of member  $i$ , in the local coordinate system. Member stiffness matrix has twelve rows and twelve columns for 3D space frames systems. Each row of this matrix can be obtained by assigning unit value to the each degree of freedom, while restraining the remaining degree of freedoms, respectively. When unit value is assigned to the degree of freedom,  $i$ , twelve end forces and end moments are obtained which constitutes the  $i^{th}$  column of the stiffness matrix. By assigning unit value to all the degree of freedoms as shown in Figure 3.5., the member stiffness matrix shown in Equation (3.3) is obtained.



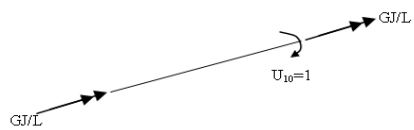
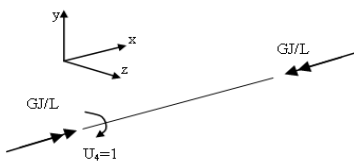
(a)



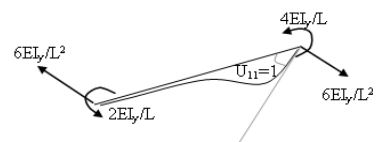
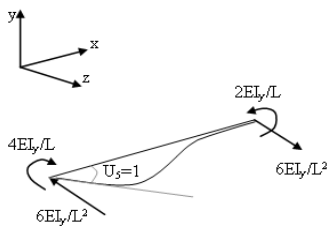
(b)



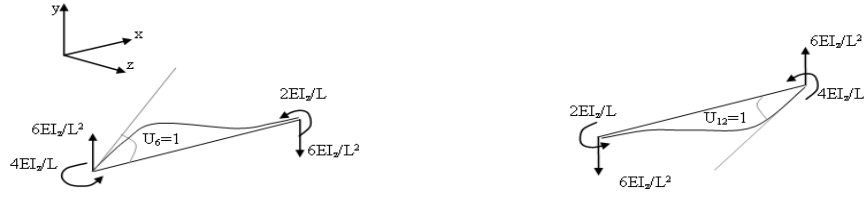
(c)



(d)



(e)



(f)

**Figure 3.5.** Member forces and moments for each degree of freedom; (a)  $u_1=1$  and  $u_7=1$ , (b)  $u_2=1$  and  $u_8=1$ , (c)  $u_3=1$  and  $u_9=1$ , (d)  $u_4=1$  and  $u_{10}=1$ , (e)  $u_5=1$  and  $u_{11}=1$ , (f)  $u_6=1$  and  $u_{12}=1$ .

$$k = \begin{bmatrix} \frac{EA}{\ell} & 0 & 0 & 0 & 0 & 0 & -\frac{EA}{\ell} & 0 & 0 & 0 & 0 & 0 \\ 0 & \frac{12EI_z}{\ell^3} & 0 & 0 & 0 & \frac{6EI_z}{\ell^2} & 0 & -\frac{12EI_z}{\ell^3} & 0 & 0 & 0 & \frac{6EI_z}{\ell^2} \\ 0 & 0 & \frac{12EI_y}{\ell^3} & 0 & -\frac{6EI_y}{\ell^2} & 0 & 0 & 0 & -\frac{12EI_y}{\ell^3} & 0 & -\frac{6EI_y}{\ell^2} & 0 \\ 0 & 0 & 0 & \frac{GJ}{\ell} & 0 & 0 & 0 & 0 & 0 & -\frac{GJ}{\ell} & 0 & 0 \\ 0 & 0 & -\frac{6EI_y}{\ell^2} & 0 & \frac{4EI_y}{\ell} & 0 & 0 & 0 & \frac{6EI_y}{\ell^2} & 0 & \frac{2EI_y}{\ell} & 0 \\ 0 & \frac{6EI_z}{\ell^2} & 0 & 0 & 0 & \frac{4EI_z}{\ell} & 0 & -\frac{6EI_z}{\ell^2} & 0 & 0 & 0 & \frac{2EI_z}{\ell} \\ -\frac{EA}{\ell} & 0 & 0 & 0 & 0 & 0 & \frac{EA}{\ell} & 0 & 0 & 0 & 0 & 0 \\ 0 & -\frac{12EI_z}{\ell^3} & 0 & 0 & 0 & -\frac{6EI_z}{\ell^2} & 0 & \frac{12EI_z}{\ell^3} & 0 & 0 & 0 & -\frac{6EI_z}{\ell^2} \\ 0 & 0 & -\frac{12EI_y}{\ell^3} & 0 & \frac{6EI_y}{\ell^2} & 0 & 0 & 0 & \frac{12EI_y}{\ell^3} & 0 & \frac{6EI_y}{\ell^2} & 0 \\ 0 & 0 & 0 & -\frac{GJ}{\ell} & 0 & 0 & 0 & 0 & 0 & \frac{GJ}{\ell} & 0 & 0 \\ 0 & 0 & \frac{6EI_y}{\ell^2} & 0 & \frac{2EI_y}{\ell} & 0 & 0 & 0 & \frac{6EI_y}{\ell^2} & 0 & \frac{4EI_y}{\ell} & 0 \\ 0 & \frac{6EI_z}{\ell^2} & 0 & 0 & 0 & \frac{2EI_z}{\ell} & 0 & -\frac{6EI_z}{\ell^2} & 0 & 0 & 0 & \frac{4EI_z}{\ell} \end{bmatrix} \quad (3.3)$$

### 3.2.2 Coordinate Transformation

The joint displacements in the local axis and the joint displacements in the global axis are related to each other given below. This relation is obtained by carrying out coordinate transformations between the local and global axis.

$$U_i = [B_i] D_i \quad (3.4)$$

where,  $B_i$  is coordinate transformation matrix obtained from multiplication of the  $[B_x],[B_y],[B_z]$  matrices.  $[B_x],[B_y],[B_z]$  matrices are called the transformation matrices corresponding to the rotation about x, y, z local axis, respectively. These matrices are obtained as described in the following.

### 3.2.2.1. Rotation of $\gamma$ about x axis

Consider that x axis is rotated amount of  $\gamma$ . In this case the new coordinates of point A can be expressed in terms of the old ones as in the following.

$$\begin{aligned} x &= X \\ y &= \overline{OB} = \overline{OC} + \overline{BC} = Y \cos \gamma + Z \sin \gamma \\ z &= \overline{AB} = \overline{AD} - \overline{BD} = Z \cos \gamma - Y \sin \gamma \end{aligned} \quad (3.5)$$

by writing Equations (3.5) in matrix form:

$$\begin{bmatrix} x \\ y \\ z \end{bmatrix} = \begin{bmatrix} 1 & 0 & 0 \\ 0 & \cos \gamma & \sin \gamma \\ 0 & -\sin \gamma & \cos \gamma \end{bmatrix} \begin{bmatrix} X \\ Y \\ Z \end{bmatrix} \quad (3.6)$$

Hence, transformation matrix corresponding to the rotation  $\gamma$  about x axis is obtained as;

$$B_x = \begin{bmatrix} 1 & 0 & 0 \\ 0 & \cos \gamma & \sin \gamma \\ 0 & -\sin \gamma & \cos \gamma \end{bmatrix} \quad (3.7)$$



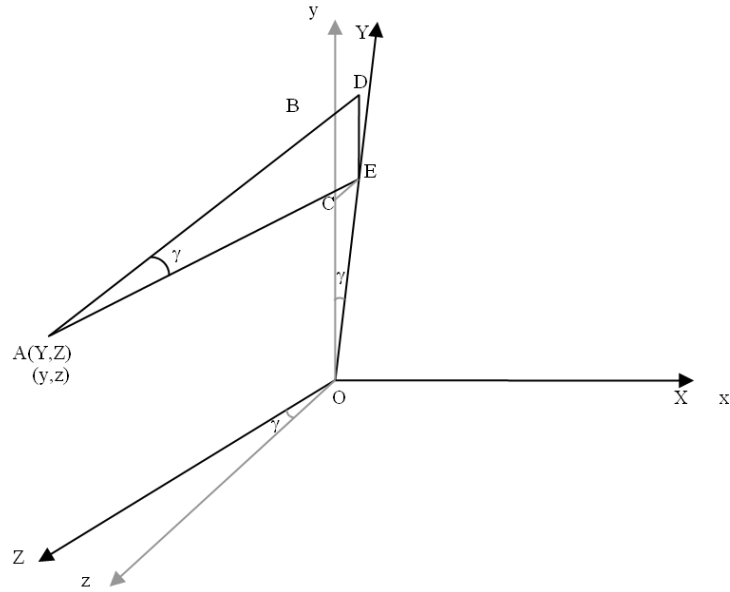


**Figure 3.6.** Rotation of  $\gamma$  about x axis.

### 3.2.2.2. Rotation of $\alpha$ about y axis

For this case y axis is rotated by the amount of  $\alpha$  the coordinates of point A in both x, z and X, Z axis are related to each other as follows:

$$\text{In } \triangle AED \rightarrow \overline{BC} = \overline{ED} = \overline{AD} \sin \alpha = Z \sin \alpha,$$

$$\text{In } \triangle ODC \rightarrow \overline{OC} = \overline{OD} \cos \alpha = X \cos \alpha.$$

It follows that:

$$\begin{aligned} x &= \overline{OB} = \overline{OC} - \overline{BC} = Y \cos \alpha - Z \sin \alpha \\ y &= Y \\ z &= \overline{AB} = \overline{AD} + \overline{BD} = Z \cos \alpha + Y \sin \alpha \end{aligned} \quad (3.8)$$

by writing Equations (3.8) in matrix form;

$$\begin{bmatrix} x \\ y \\ z \end{bmatrix} = \begin{bmatrix} \cos \alpha & 0 & -\sin \alpha \\ 0 & 1 & 0 \\ \sin \alpha & 0 & \cos \alpha \end{bmatrix} \begin{bmatrix} X \\ Y \\ Z \end{bmatrix} \quad (3.9)$$

Hence, transformation matrix corresponding to the rotation  $\alpha$  about y axis is obtained as;

$$B_y = \begin{bmatrix} \cos \alpha & 0 & -\sin \alpha \\ 0 & 1 & 0 \\ \sin \alpha & 0 & \cos \alpha \end{bmatrix} \quad (3.10)$$

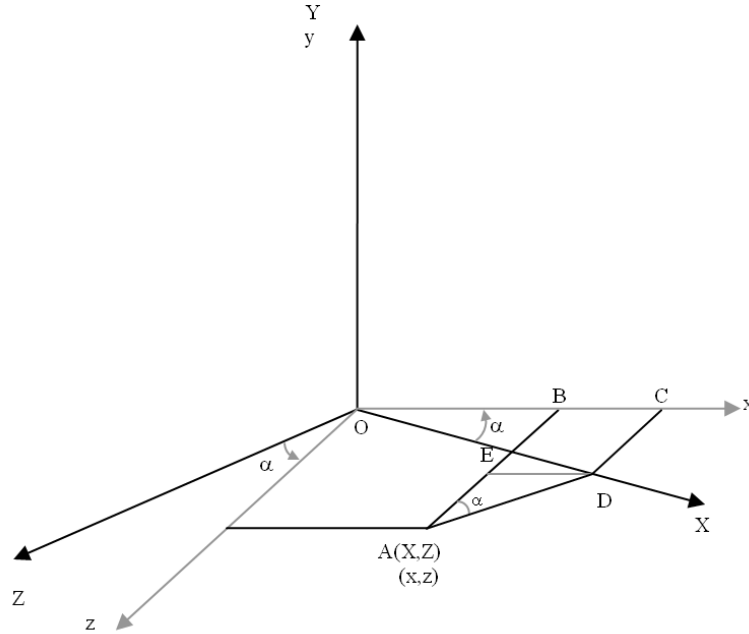


**Figure 3.7.** Rotation of  $\alpha$  about y axis.

### 3.2.2.3. Rotation of $\beta$ about z axis

In this case the coordinates of point A can be expressed in terms of the old ones as in the following.

$$\text{In } \triangle AED \rightarrow \bar{ED} = \bar{ED} = \bar{AE} \sin \beta = Y \sin \beta, \bar{AD} = Y \cos \beta$$

$$\text{In } \triangle ODE \rightarrow \bar{OC} = \bar{OE} \cos \beta = X \cos \beta, \bar{BD} = \bar{CE} = \bar{OE} \cos \beta = X \cos \beta$$

It follows that:

$$\begin{aligned} x &= \bar{OB} = \bar{OC} + \bar{ED} = X \cos \beta + Y \sin \beta \\ y &= \bar{AB} = \bar{AD} - \bar{BD} = -X \cos \beta + Y \sin \beta \\ z &= Z \end{aligned} \quad (3.11)$$

by writing write equations (3.11) in matrix form;

$$\begin{bmatrix} x \\ y \\ z \end{bmatrix} = \begin{bmatrix} \cos\beta & \sin\beta & 0 \\ -\sin\beta & \cos\beta & 0 \\ 0 & 0 & 1 \end{bmatrix} \begin{bmatrix} X \\ Y \\ Z \end{bmatrix} \quad (3.12)$$

Hence, transformation matrix corresponding to the rotation  $\beta$  about z axis is obtained as;

$$B_z = \begin{bmatrix} \cos\beta & \sin\beta & 0 \\ -\sin\beta & \cos\beta & 0 \\ 0 & 0 & 1 \end{bmatrix} \quad (3.13)$$

The overall transformation matrix which corresponds to the case where the x axis rotates amount of  $\gamma$ , y axis amount of  $\alpha$  and z axis amount of  $\beta$  is obtained by multiplying the above three transformation matrices  $[B_x]$ ,  $[B_y]$ ,  $[B_z]$  as shown in Equation (3.14).

$$B = \begin{bmatrix} 1 & 0 & 0 \\ 0 & \cos\gamma & \sin\gamma \\ 0 & -\sin\gamma & \cos\gamma \end{bmatrix} \cdot \begin{bmatrix} \cos\alpha & 0 & -\sin\alpha \\ 0 & 1 & 0 \\ \sin\alpha & 0 & \cos\alpha \end{bmatrix} \cdot \begin{bmatrix} \cos\beta & \sin\beta & 0 \\ -\sin\beta & \cos\beta & 0 \\ 0 & 0 & 1 \end{bmatrix} \quad (3.14)$$

$$B = \begin{bmatrix} \cos\beta \cdot \cos\alpha & \sin\beta & -\cos\beta \cdot \sin\alpha \\ \sin\alpha \cdot \sin\gamma - \cos\alpha \cdot \sin\beta \cdot \cos\gamma & \cos\beta \cdot \cos\gamma & \cos\alpha \cdot \sin\gamma + \sin\alpha \cdot \sin\beta \cdot \cos\gamma \\ \sin\alpha \cdot \cos\gamma + \cos\alpha \cdot \sin\beta \cdot \sin\gamma & -\cos\beta \cdot \sin\gamma & \cos\alpha \cdot \cos\gamma - \sin\alpha \cdot \sin\beta \cdot \sin\gamma \end{bmatrix} \quad (3.15)$$

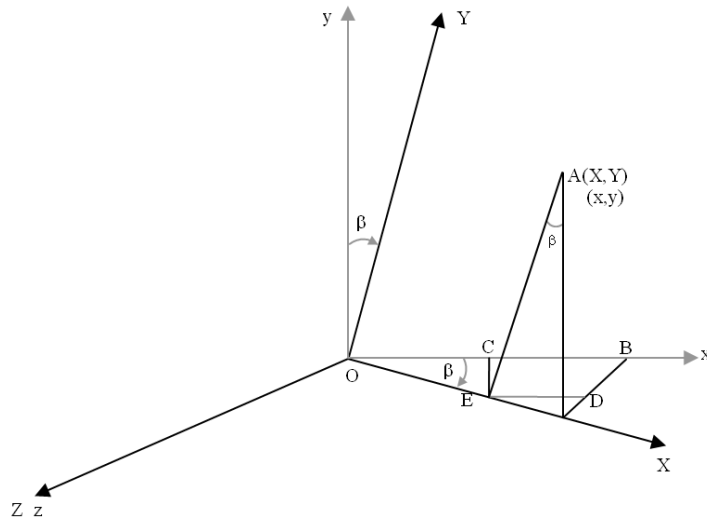


**Figure 3.8.** Rotation of  $\beta$  about z axis.

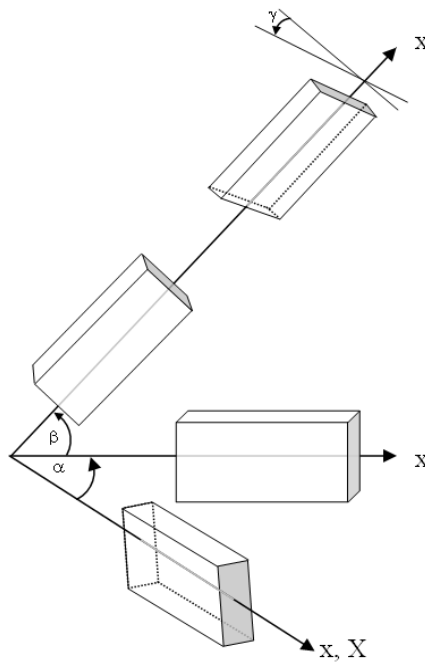


**Figure 3.9.** Coordinate transformation from local axis to global axis.

It is apparent from Equations (3.14) and (3.15) that terms of the coordinate transformation matrix depend on angles  $\alpha$ ,  $\beta$ , and  $\gamma$ .  $\gamma$  angle is not related to the joint coordinates of a space frame member. Therefore, value of  $\gamma$  angle is entered manually in the program.

Whereas,  $\alpha$  and  $\beta$  angles are related to joint coordinates of space frame member. It is possible to re-write the coordinate transformation matrix in terms of length of space frame members by using relationships between  $\alpha$  and  $\beta$  angles and joint coordinates as shown in the following.

The length of a space frame member as shown Figure 3.10 is calculated as follows.

$$AB=l=\sqrt{\Delta x^2 + \Delta y^2 + \Delta z^2} \quad (3.16)$$

$$A_1B_1=l_1=\sqrt{\Delta x^2 + \Delta z^2} \quad (3.17)$$

When the terms  $\cos \alpha$ ,  $\cos \beta$ ,  $\sin \alpha$ ,  $\sin \beta$  are written in terms of the length of element.

$$\cos(-\alpha)=\cos\alpha=\frac{\Delta x}{l_1}, \sin(-\alpha)=-\sin\alpha=-\frac{\Delta z}{l_1} \quad (3.18)$$

$$\cos\beta=\frac{l_1}{l}, \sin\beta=\frac{\Delta z}{l_1} \quad (3.19)$$

where,  $\Delta_x$ ,  $\Delta_y$ , and  $\Delta_z$  are shown in Figure 3.10. When these terms are substituted in to the coordinate transformation matrix, following expression is obtained.

$$[B^*] = \begin{bmatrix} \frac{\Delta x}{l} & \frac{\Delta y}{l} & \frac{\Delta z}{l} \\ \frac{-l \cdot \Delta z \cdot \sin \gamma - \Delta x \cdot \Delta y \cdot \cos \gamma}{l \cdot l_1} & \frac{l_1 \cdot \cos \gamma}{l} & \frac{l \cdot \Delta x \cdot \sin \gamma - \Delta z \cdot \Delta y \cdot \cos \gamma}{l \cdot l_1} \\ \frac{\Delta x \cdot \Delta y \cdot \sin \gamma - l \cdot \Delta z \cdot \cos \gamma}{l \cdot l_1} & -\frac{l_1 \cdot \cos \gamma}{l} & \frac{l \cdot \Delta x \cdot \sin \gamma + \Delta z \cdot \Delta y \cdot \cos \gamma}{l \cdot l_1} \end{bmatrix} \quad (3.20)$$

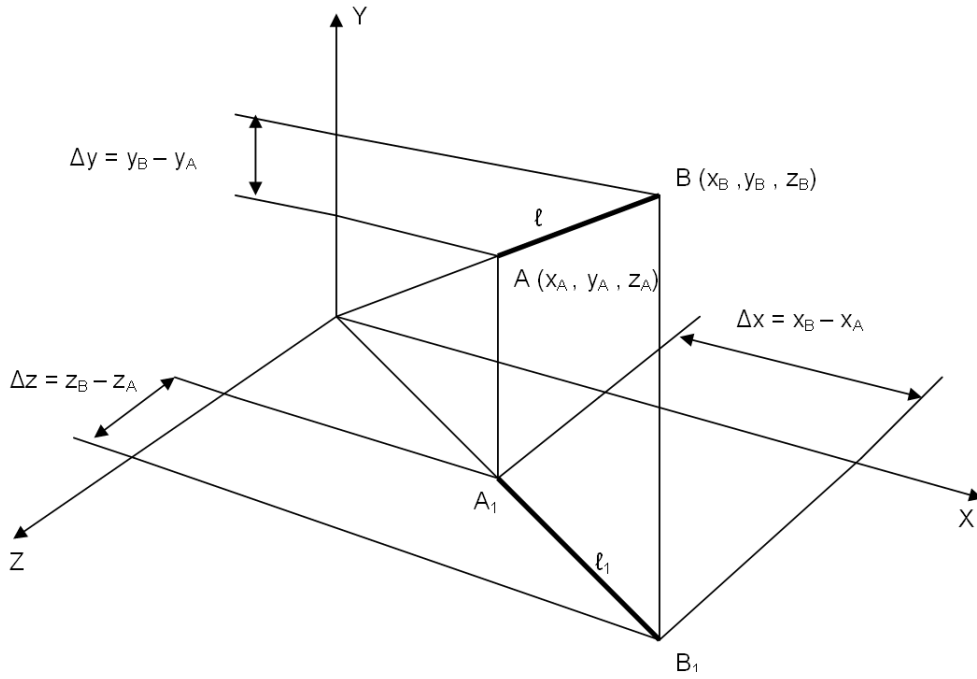


**Figure 3.10.** Calculation of the length of an element in space.

The coordinate transformation matrix described in Equation (3.20) represents transformations at one end of the space frame member. The complete displacement transformation matrix for the degrees of freedom of both ends of the frame member has twelve columns and twelve rows as shown in Equation (3.21).

$$B = \begin{bmatrix}
 b_{11} & b_{12} & b_{13} & 0 & 0 & 0 & 0 & 0 & 0 & 0 & 0 & 0 \\
 b_{21} & b_{22} & b_{23} & 0 & 0 & 0 & 0 & 0 & 0 & 0 & 0 & 0 \\
 b_{31} & b_{32} & b_{33} & 0 & 0 & 0 & 0 & 0 & 0 & 0 & 0 & 0 \\
 0 & 0 & 0 & b_{11} & b_{12} & b_{13} & 0 & 0 & 0 & 0 & 0 & 0 \\
 0 & 0 & 0 & b_{21} & b_{22} & b_{23} & 0 & 0 & 0 & 0 & 0 & 0 \\
 0 & 0 & 0 & b_{31} & b_{32} & b_{33} & 0 & 0 & 0 & 0 & 0 & 0 \\
 0 & 0 & 0 & 0 & 0 & 0 & b_{11} & b_{12} & b_{13} & 0 & 0 & 0 \\
 0 & 0 & 0 & 0 & 0 & 0 & b_{21} & b_{22} & b_{23} & 0 & 0 & 0 \\
 0 & 0 & 0 & 0 & 0 & 0 & b_{31} & b_{32} & b_{33} & 0 & 0 & 0 \\
 0 & 0 & 0 & 0 & 0 & 0 & 0 & 0 & 0 & b_{11} & b_{12} & b_{13} \\
 0 & 0 & 0 & 0 & 0 & 0 & 0 & 0 & 0 & b_{21} & b_{22} & b_{23} \\
 0 & 0 & 0 & 0 & 0 & 0 & 0 & 0 & 0 & b_{31} & b_{32} & b_{33}
 \end{bmatrix} \quad (3.21)$$

where,  $b_{i,j}$ ,  $i=1, 2, 3$  and  $j=1, 2, 3$  are the terms of the coordinate transformation matrix described as follows.

$$\begin{aligned}
 b_{11} &= \frac{\Delta x}{\ell} \quad , \quad b_{12} = \frac{\Delta y}{\ell} \quad , \quad b_{13} = \frac{\Delta z}{\ell} \\
 b_{21} &= \frac{-\ell \cos \gamma \sin \gamma - \Delta x \cos \gamma}{\ell l_1} \quad , \quad b_{22} = \frac{l_1 \cos \gamma}{\ell} \quad , \quad b_{23} = \frac{\ell \cos \gamma \sin \gamma - \Delta z \cos \gamma}{\ell l_1} \\
 b_{31} &= \frac{\Delta x \sin \gamma - \ell \cos \gamma}{\ell l_1} \quad , \quad b_{32} = -\frac{l_1 \sin \gamma}{\ell} \quad , \quad b_{33} = \frac{\ell \sin \gamma \cos \gamma - \Delta y \sin \gamma}{\ell l_1}
 \end{aligned} \tag{3.22}$$

#### 3.2.2.4. Space Frame Members Along the Y-Axis

It is apparent from Equations (3.16) and (3.17) that for a frame member along Y-axis,  $\Delta_x = \Delta_y = 0$ ,  $\Delta_z = l$  and  $l_1 = 0$ . This causes division by zero in the expressions given in Equation (3.22) which turns them to undefined and indeterminate form as shown in Equation (3.23). In order to eliminate this discrepancy displacement transformation matrix is required to be re-constructed. These special matrices are given in Equations (3.24) and (3.25). When x axis of space frame member is along to +Y axis, transformation matrix of Equation (3.24) is used. When x axis of space frame member is along to -Y axis, the transformation matrix of Equation (3.25) is used. Directions of these members are shown in Figures 3.11 and 3.12. [104].

$$B = \begin{bmatrix} 0 & 1 & 0 \\ 0 & 0 & 0 \\ 0 & 0 & 0 \\ 0 & 0 & 0 \\ 0 & 0 & 0 \end{bmatrix} \tag{3.23}$$

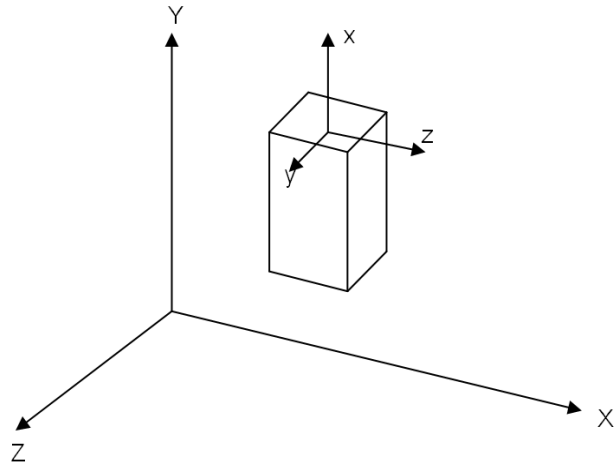


**Figure 3.11.** Local coordinates of vertical member in +Y direction.

$$\mathbf{B} = \begin{bmatrix}
 0 & 1 & 0 & 0 & 0 & 0 & 0 & 0 & 0 & 0 & 0 & 0 \\
 \sin\gamma & 0 & \cos\gamma & 0 & 0 & 0 & 0 & 0 & 0 & 0 & 0 & 0 \\
 \cos\gamma & 0 & -\sin\gamma & 0 & 0 & 0 & 0 & 0 & 0 & 0 & 0 & 0 \\
 0 & 0 & 0 & 0 & 1 & 0 & 0 & 0 & 0 & 0 & 0 & 0 \\
 0 & 0 & 0 & \sin\gamma & 0 & \cos\gamma & 0 & 0 & 0 & 0 & 0 & 0 \\
 0 & 0 & 0 & \cos\gamma & 0 & -\sin\gamma & 0 & 0 & 0 & 0 & 0 & 0 \\
 0 & 0 & 0 & 0 & 0 & 0 & 0 & 1 & 0 & 0 & 0 & 0 \\
 0 & 0 & 0 & 0 & 0 & 0 & \sin\gamma & 0 & \cos\gamma & 0 & 0 & 0 \\
 0 & 0 & 0 & 0 & 0 & 0 & \cos\gamma & 0 & -\sin\gamma & 0 & 0 & 0 \\
 0 & 0 & 0 & 0 & 0 & 0 & 0 & 0 & 0 & 0 & 1 & 0 \\
 0 & 0 & 0 & 0 & 0 & 0 & 0 & 0 & 0 & \sin\gamma & 0 & \cos\gamma \\
 0 & 0 & 0 & 0 & 0 & 0 & 0 & 0 & 0 & \cos\gamma & 0 & -\sin\gamma
 \end{bmatrix} \quad (3.24)$$



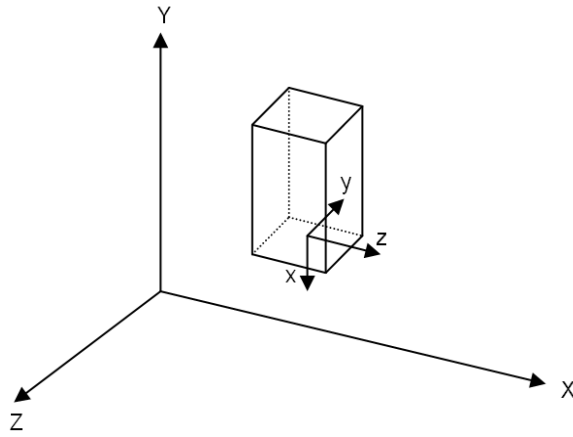


**Figure 3.12.** Local coordinates of vertical member in -Y direction.

$$B = \begin{bmatrix}
 0 & -1 & 0 & 0 & 0 & 0 & 0 & 0 & 0 & 0 & 0 & 0 \\
 \sin \gamma & 0 & -\cos \gamma & 0 & 0 & 0 & 0 & 0 & 0 & 0 & 0 & 0 \\
 \cos \gamma & 0 & \sin \gamma & 0 & 0 & 0 & 0 & 0 & 0 & 0 & 0 & 0 \\
 0 & 0 & 0 & 0 & -1 & 0 & 0 & 0 & 0 & 0 & 0 & 0 \\
 0 & 0 & 0 & \sin \gamma & 0 & -\cos \gamma & 0 & 0 & 0 & 0 & 0 & 0 \\
 0 & 0 & 0 & \cos \gamma & 0 & \sin \gamma & 0 & 0 & 0 & 0 & 0 & 0 \\
 0 & 0 & 0 & 0 & 0 & 0 & 0 & -1 & 0 & 0 & 0 & 0 \\
 0 & 0 & 0 & 0 & 0 & 0 & \sin \gamma & 0 & -\cos \gamma & 0 & 0 & 0 \\
 0 & 0 & 0 & 0 & 0 & 0 & \cos \gamma & 0 & \sin \gamma & 0 & 0 & 0 \\
 0 & 0 & 0 & 0 & 0 & 0 & 0 & 0 & 0 & 0 & -1 & 0 \\
 0 & 0 & 0 & 0 & 0 & 0 & 0 & 0 & 0 & \sin \gamma & 0 & -\cos \gamma \\
 0 & 0 & 0 & 0 & 0 & 0 & 0 & 0 & 0 & \cos \gamma & 0 & \sin \gamma
 \end{bmatrix} \quad (3.25)$$

### 3.2.3 Relationship between External Loads and Member End Forces

The relationship between member end forces and member end deformations at joint  $i$  is given as  $F_i = k_i u_i$ . This equation can be generalized as  $U = B D$  for the whole frame when all the members are included in the above expression. In this equation, dimension of vectors  $F$  and  $u$  is  $6*m$  where,  $m$  is total number of members in the space frame. Stiffness matrix  $k$  in that equation is obtained by collecting the local stiffness matrices of frame members. This matrix has dimension of  $(6*m \times 6*m)$ . When this equation is expanded to include all the members in the frame, it follows that

$U = B D$  . In this expression, the dimension of matrix  $B$  is  $(6*m \times 6*m)$  and the dimension of the displacement matrix  $D$  is also  $(6*m \times 1)$ .

When an elastic frame is subjected to external loads, frame joints are displaced and frame members are deflected. In this case, work done by the external loads acting on frame joints is equal to the strain energy stored in frame members on due to the law of conservation of energy. It follows that:

$$\frac{1}{2} P^T D = \frac{1}{2} F^T U \quad (3.26)$$

where;  $P$  is the external load vector,  $D$  is the joint displacements vector,  $F$  is the vector of member end forces, and  $U$  is the vector of member end displacement. Remembering from Equation (3.27) that  $U = B D$  , it follows that

$$\frac{1}{2} P^T D = \frac{1}{2} F^T B D \Rightarrow P^T = F^T B \quad (3.27)$$

Transpose of Equation (3.28) yields;

$$P = B^T F \quad (3.28)$$

This equation represents the relationship between the external load vector and member end forces.  $B^T$  in this equation is the transpose of the displacement transformation matrix  $B$  .

### 3.2.4 Overall Stiffness Matrix

The external load vector  $P$  can be related to joint displacement vector  $D$  using the relationships  $U = B D$  and  $F_i = k_i u_i$  . When these expressions are substituted in Equation (3.29);

$$P = B^T k B D = K D \quad (3.29)$$

is obtained. Here,  $K$  is called overall stiffness matrix of the structure in global coordinate system. This matrix is constructed by carrying out triple matrix multiplication shown in Equation (3.29). It is apparent that the overall stiffness matrix can be obtained by collecting the contributions of each member to this matrix.

$$K_S = \sum_{i=1}^m K_i = \sum_{i=1}^m B_i^T k_i B_i \quad (3.30)$$

where,  $m$  is the number of members in space frame. Overall stiffness matrix of a structure is diagonally symmetric. Therefore, it is sufficient for structure to build the half of this matrix.

### 3.2.5 Member End Conditions

In some cases, beams of steel frames are connected to columns with hinge connections where bending moment transfer is not possible. In such a case, value of the bending moment is equal to zero at that joint. Therefore, end displacements and end forces should be recalculated by equating bending moment to the zero at the hinged joint. Consequently, member stiffness matrix for a member having a hinge connection at one end is not same as the one which is rigidly connected to columns. In general, there can be 4 types of members in a steel frame. These members depending on the end conditions are tabulated in Table 3.1 and described in the following.

**Table 3.1.** Hinge condition types.

Type	Member End Types
Type 1	Both ends are moment resisting
Type 2	First end is hinged
Type 3	Far end is hinged
Type 4	Both ends are hinged

#### 3.2.5.1. Type 1: Frame member both ends are moment resisting

Stiffness and transformation matrices for that condition were given in Equations (3.3) and (3.21).

### 3.2.5.2. Type 2: Frame member having a hinge connection at its first end

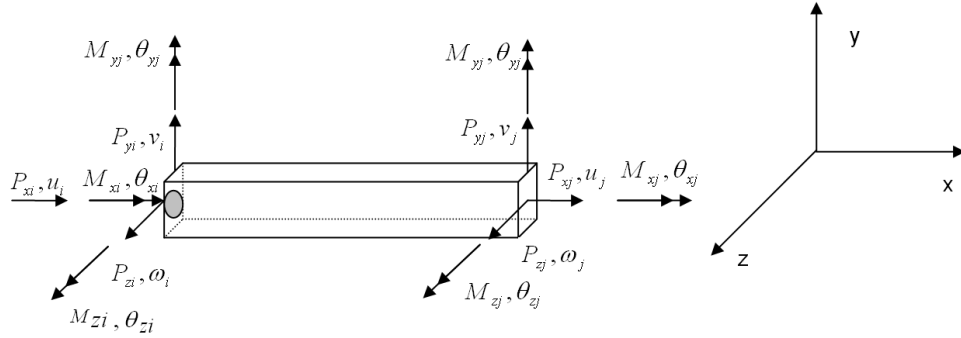


**Figure 3.13.** 3-D frame member having a hinge connection at its first end.

It is clear from Figure 3.13. that when first end of a frame member is hinged the bending moment about z axis becomes zero at that joint  $M_{zi} = 0$ . This condition yields the following Equation (3.31).

$$\frac{6EI_z}{L^2}v_i + \frac{4EI_z}{L}\theta_{zi} - \frac{6EI_z}{L^2}v_j + \frac{2EI_z}{L}\theta_{zj} = 0 \rightarrow \theta_{zi} = -\frac{3}{2L}v_i + \frac{3}{2L}v_j - \frac{\theta_{zj}}{2} \quad (3.31)$$

In Equation (3.31), if  $\theta_{zi}$  equality is substituted in to stiffness equations following equations are obtained.

$$P_{xi} = \frac{EA}{L}u_i - \frac{EA}{L}u_j$$

$$P_{yi} = \frac{12EI_z}{L^3}v_i + \frac{6EI_z}{L^2}\left(-\frac{3}{2L}v_i + \frac{3}{2L}v_j - \frac{\theta_{zj}}{2}\right) - \frac{12EI_z}{L^3}v_j + \frac{6EI_z}{L^2}\theta_{zj}$$

$$P_{zi} = \frac{3EI_z}{L^3}v_i - \frac{3EI_z}{L^3}v_j + \frac{3EI_z}{L^2}\theta_{zj}$$

$$P_{zi} = \frac{12EI_y}{L^3}\omega_i - \frac{6EI_y}{L^2}\theta_{yi} - \frac{12EI_y}{L^3}\omega_j - \frac{6EI_y}{L^2}\theta_{yj} \quad (3.32)$$

$$M_{xi} = \frac{GJ}{L}\theta_{xi} - \frac{GJ}{L}\theta_{ji}$$

$$M_{yi} = -\frac{6EI_y}{L^2}\omega_i + \frac{4EI_y}{L}\theta_{yi} + \frac{6EI_y}{L^2}\omega_j + \frac{2EI_y}{L}\theta_{yj}$$

$$P_{xj} = -\frac{EA}{L}u_i + \frac{EA}{L}u_j$$

$$P_{yj} = -\frac{12EI_z}{L^3}v_i - \frac{6EI_z}{L^2}\left(-\frac{3}{2L}v_i + \frac{3}{2L}v_j - \frac{\theta_{zj}}{2}\right) + \frac{12EI_z}{L^3}v_j - \frac{6EI_z}{L^2}\theta_{zj}$$

After simplification, the relationships between end forces and displacements are obtained as follows.

$$P_{yj} = -\frac{3EI_z}{L^3}v_i + \frac{3EI_z}{L^3}v_j - \frac{3EI_z}{L^2}\theta_{zj}$$

$$P_{zj} = -\frac{12EI_y}{L^3}\omega_i + \frac{6EI_y}{L^2}\theta_{yi} + \frac{12EI_y}{L^3}\omega_j + \frac{6EI_y}{L^2}\theta_{yj}$$

$$M_{xj} = -\frac{GJ}{L}\theta_{xi} + \frac{GJ}{L}\theta_{ji} \tag{3.33}$$

$$M_{yj} = -\frac{6EI_y}{L^2}\omega_i + \frac{2EI_y}{L}\theta_{yi} + \frac{6EI_y}{L^2}\omega_j + \frac{4EI_y}{L}\theta_{yj}$$

$$M_{zj} = \frac{6EI_z}{L^2}v_i + \frac{2EI_z}{L}\left(-\frac{3}{2L}v_i + \frac{3}{2L}v_j - \frac{\theta_{zj}}{2}\right) - \frac{6EI_z}{L^2}v_j + \frac{4EI_z}{L}\theta_{zj}$$

$$M_{zj} = \frac{3EI_z}{L^2}v_i - \frac{3EI_z}{L^2}v_j + \frac{3EI_z}{L}\theta_{zj}$$

When these are expressed in a matrix form, following stiffness matrix is obtained for a frame member having a hinge at its first end.

$$k = \begin{bmatrix} \frac{EA}{L} & 0 & 0 & 0 & 0 & 0 & -\frac{EA}{L} & 0 & 0 & 0 & 0 & 0 \\ 0 & \frac{12EI_z}{L^3} & 0 & 0 & 0 & \frac{6EI_z}{L^2} & 0 & -\frac{12EI_z}{L^3} & 0 & 0 & 0 & \frac{6EI_z}{L^2} \\ 0 & 0 & \frac{12EI_y}{L^3} & 0 & -\frac{6EI_y}{L^2} & 0 & 0 & 0 & -\frac{12EI_y}{L^3} & 0 & -\frac{6EI_y}{L^2} & 0 \\ 0 & 0 & 0 & \frac{GJ}{L} & 0 & 0 & 0 & 0 & 0 & -\frac{GJ}{L} & 0 & 0 \\ 0 & 0 & -\frac{6EI_y}{L^2} & 0 & \frac{4EI_y}{L} & 0 & 0 & 0 & \frac{6EI_y}{L^2} & 0 & \frac{2EI_y}{L} & 0 \\ 0 & 0 & 0 & 0 & 0 & 0 & 0 & 0 & 0 & 0 & 0 & 0 \\ -\frac{EA}{L} & 0 & 0 & 0 & 0 & 0 & \frac{EA}{L} & 0 & 0 & 0 & 0 & 0 \\ 0 & -\frac{12EI_z}{L^3} & 0 & 0 & 0 & -\frac{6EI_z}{L^2} & 0 & \frac{12EI_z}{L^3} & 0 & 0 & 0 & -\frac{6EI_z}{L^2} \\ 0 & 0 & -\frac{12EI_y}{L^3} & 0 & \frac{6EI_y}{L^2} & 0 & 0 & 0 & \frac{12EI_y}{L^3} & 0 & \frac{6EI_y}{L^2} & 0 \\ 0 & 0 & 0 & -\frac{GJ}{L} & 0 & 0 & 0 & 0 & 0 & \frac{GJ}{L} & 0 & 0 \\ 0 & 0 & -\frac{6EI_y}{L^2} & 0 & \frac{2EI_y}{L} & 0 & 0 & 0 & \frac{6EI_y}{L^2} & 0 & \frac{4EI_y}{L} & 0 \\ 0 & \frac{3EI_z}{L^2} & 0 & 0 & 0 & 0 & 0 & -\frac{3EI_z}{L^2} & 0 & 0 & 0 & \frac{3EI_z}{L} \end{bmatrix} \quad (3.34)$$

Displacement transformation matrix of a frame member having a hinge at its first end is given in the Equation (3.35). Only difference between this matrix and displacement transformation matrix for Type 1 given in Equation (3.21) is that all terms in line parallel to  $\theta_{zi}$  be equal to zero. Since  $\theta_{zi}$  term, representing rotation on hinged joint is eliminated from stiffness equations. Transformation matrix for that case becomes in the following.

$$B = \begin{bmatrix} b_{11} & b_{12} & b_{13} & 0 & 0 & 0 & 0 & 0 & 0 & 0 & 0 & 0 \\ b_{21} & b_{22} & b_{23} & 0 & 0 & 0 & 0 & 0 & 0 & 0 & 0 & 0 \\ b_{31} & b_{32} & b_{33} & 0 & 0 & 0 & 0 & 0 & 0 & 0 & 0 & 0 \\ 0 & 0 & 0 & b_{11} & b_{12} & b_{13} & 0 & 0 & 0 & 0 & 0 & 0 \\ 0 & 0 & 0 & b_{21} & b_{22} & b_{23} & 0 & 0 & 0 & 0 & 0 & 0 \\ 0 & 0 & 0 & 0 & 0 & 0 & 0 & 0 & 0 & 0 & 0 & 0 \\ 0 & 0 & 0 & 0 & 0 & 0 & b_{11} & b_{12} & b_{13} & 0 & 0 & 0 \\ 0 & 0 & 0 & 0 & 0 & 0 & b_{21} & b_{22} & b_{23} & 0 & 0 & 0 \\ 0 & 0 & 0 & 0 & 0 & 0 & b_{31} & b_{32} & b_{33} & 0 & 0 & 0 \\ 0 & 0 & 0 & 0 & 0 & 0 & 0 & 0 & 0 & b_{11} & b_{12} & b_{13} \\ 0 & 0 & 0 & 0 & 0 & 0 & 0 & 0 & 0 & b_{21} & b_{22} & b_{23} \\ 0 & 0 & 0 & 0 & 0 & 0 & 0 & 0 & 0 & b_{31} & b_{32} & b_{33} \end{bmatrix} \quad (3.35)$$

where,  $b_{i,j}$ ,  $i=1,2,3$ ,  $j=1,2,3$  terms are given in Equation (3.22). Transformation matrix of vertical member in +Y direction is given in the following.

$$B = \begin{bmatrix} 0 & 1 & 0 & 0 & 0 & 0 & 0 & 0 & 0 & 0 & 0 & 0 \\ \sin \gamma & 0 & \cos \gamma & 0 & 0 & 0 & 0 & 0 & 0 & 0 & 0 & 0 \\ \cos \gamma & 0 & -\sin \gamma & 0 & 0 & 0 & 0 & 0 & 0 & 0 & 0 & 0 \\ 0 & 0 & 0 & 0 & 1 & 0 & 0 & 0 & 0 & 0 & 0 & 0 \\ 0 & 0 & 0 & \sin \gamma & 0 & \cos \gamma & 0 & 0 & 0 & 0 & 0 & 0 \\ 0 & 0 & 0 & 0 & 0 & 0 & 0 & 0 & 0 & 0 & 0 & 0 \\ 0 & 0 & 0 & 0 & 0 & 0 & 0 & 1 & 0 & 0 & 0 & 0 \\ 0 & 0 & 0 & 0 & 0 & 0 & \sin \gamma & 0 & \cos \gamma & 0 & 0 & 0 \\ 0 & 0 & 0 & 0 & 0 & 0 & \cos \gamma & 0 & -\sin \gamma & 0 & 0 & 0 \\ 0 & 0 & 0 & 0 & 0 & 0 & 0 & 0 & 0 & 0 & 1 & 0 \\ 0 & 0 & 0 & 0 & 0 & 0 & 0 & 0 & 0 & \sin \gamma & 0 & \cos \gamma \\ 0 & 0 & 0 & 0 & 0 & 0 & 0 & 0 & 0 & \cos \gamma & 0 & -\sin \gamma \end{bmatrix} \quad (3.36)$$

Similarly, transformation matrix of vertical member in -Y direction is given in the following.

$$B = \begin{bmatrix} 0 & -1 & 0 & 0 & 0 & 0 & 0 & 0 & 0 & 0 & 0 & 0 \\ \sin \gamma & 0 & -\cos \gamma & 0 & 0 & 0 & 0 & 0 & 0 & 0 & 0 & 0 \\ \cos \gamma & 0 & \sin \gamma & 0 & 0 & 0 & 0 & 0 & 0 & 0 & 0 & 0 \\ 0 & 0 & 0 & 0 & -1 & 0 & 0 & 0 & 0 & 0 & 0 & 0 \\ 0 & 0 & 0 & \sin \gamma & 0 & -\cos \gamma & 0 & 0 & 0 & 0 & 0 & 0 \\ 0 & 0 & 0 & 0 & 0 & 0 & 0 & 0 & 0 & 0 & 0 & 0 \\ 0 & 0 & 0 & 0 & 0 & 0 & 0 & -1 & 0 & 0 & 0 & 0 \\ 0 & 0 & 0 & 0 & 0 & 0 & \sin \gamma & 0 & -\cos \gamma & 0 & 0 & 0 \\ 0 & 0 & 0 & 0 & 0 & 0 & \cos \gamma & 0 & \sin \gamma & 0 & 0 & 0 \\ 0 & 0 & 0 & 0 & 0 & 0 & 0 & 0 & 0 & 0 & -1 & 0 \\ 0 & 0 & 0 & 0 & 0 & 0 & 0 & 0 & 0 & \sin \gamma & 0 & -\cos \gamma \\ 0 & 0 & 0 & 0 & 0 & 0 & 0 & 0 & 0 & \cos \gamma & 0 & \sin \gamma \end{bmatrix} \quad (3.37)$$

### 3.2.5.3. Type 3: Frame member having a hinge connection at its second end

When second end of a frame member is hinged, as shown in Figure 3.14., bending moment about z axis will be zero at that joint  $M_{zj} = 0$ . From this equation rotation about z axis of that end of frame member  $\theta_{zj}$  is obtained as follows.

$$\frac{6EI_z}{L^2} v_i + \frac{2EI_z}{L} \theta_{zi} - \frac{6EI_z}{L^2} v_j + \frac{4EI_z}{L} \theta_{zj} = 0 \rightarrow \theta_{zj} = -\frac{3}{2L} v_i - \frac{\theta_{zi}}{2} + \frac{3}{2L} v_j \quad (3.38)$$

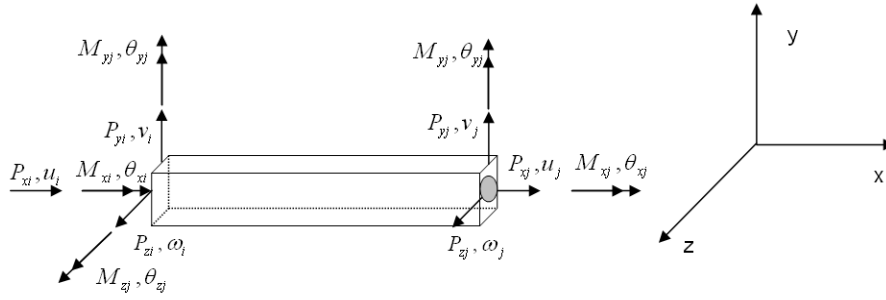


**Figure 3.14.** 3-D frame member having a hinge connection at its second end.

Substituting  $\theta_{zj}$  in Equation (3.1), following equations are obtained

$$P_{xi} = \frac{EA}{L} u_i - \frac{EA}{L} u_j$$

$$P_{yi} = \frac{12EI_z}{L^3} z v_i + \frac{6EI_z}{L^2} z \theta_{zi} - \frac{12EI_z}{L^3} z v_j + \frac{6EI_z}{L^2} z \left( -\frac{3}{2L} v_i + \frac{3}{2L} v_j - \frac{\theta_{zj}}{2} \right)$$

$$P_{yi} = \frac{3EI_z}{L^3} z v_i + \frac{3EI_z}{L^2} z \theta_{zi} - \frac{3EI_z}{L^3} z v_j$$

$$P_{zi} = \frac{12EI_y}{L^3} \omega_i - \frac{6EI_y}{L^2} \theta_{yi} - \frac{12EI_y}{L^3} \omega_j - \frac{6EI_y}{L^2} \theta_{yj} \quad (3.39)$$

$$M_{xi} = \frac{GJ}{L} \theta_{xi} - \frac{GJ}{L} \theta_{ji}$$

$$M_{yi} = -\frac{6EI_y}{L^2} \omega_i + \frac{4EI_y}{L} \theta_{yi} + \frac{6EI_y}{L^2} \omega_j + \frac{2EI_y}{L} \theta_{yj}$$

$$M_{zi} = \frac{6EI_z}{L^2} z v_i + \frac{4EI_z}{L} z \theta_{zi} - \frac{6EI_z}{L^2} z v_j + \frac{2EI_z}{L} z \left( -\frac{3}{2L} v_i + \frac{3}{2L} v_j - \frac{\theta_{zj}}{2} \right)$$

$$M_{zi} = \frac{3EI_z}{L^2} z v_i + \frac{3EI_z}{L} z \theta_{zi} - \frac{3EI_z}{L^2} z v_j$$



After simplification, the relationships between end forces and displacements are obtained.

$$\begin{aligned}
 P_{xj} &= -\frac{EA}{L}u_i + \frac{EA}{L}u_j \\
 P_{yj} &= -\frac{12EI_z}{L^3}v_i - \frac{6EI_z}{L^2}\theta_{zj} + \frac{12EI_z}{L^3}v_j - \frac{6EI_z}{L^2}\left(-\frac{3}{2L}v_i + \frac{3}{2L}v_j - \frac{\theta_{zj}}{2}\right) \\
 P_{yj} &= -\frac{3EI_z}{L^3}v_i - \frac{3EI_z}{L^2}\theta_{zj} + \frac{3EI_z}{L^3}v_j
 \end{aligned} \tag{3.40}$$

$$P_{zj} = -\frac{12EI_y}{L^3}\omega_i + \frac{6EI_y}{L^2}\theta_{yj} + \frac{12EI_y}{L^3}\omega_j + \frac{6EI_y}{L^2}\theta_{yj}$$

$$M_{xj} = -\frac{GJ}{L}\theta_{xi} + \frac{GJ}{L}\theta_{ji}$$

$$M_{yj} = -\frac{6EI_y}{L^2}\omega_i + \frac{2EI_y}{L}\theta_{yj} + \frac{6EI_y}{L^2}\omega_j + \frac{4EI_y}{L}\theta_{yj}$$

When they are written in matrix form, following equation system is obtained

$$\begin{bmatrix}
 \frac{EA}{L} & 0 & 0 & 0 & 0 & 0 & -\frac{EA}{L} & 0 & 0 & 0 & 0 & 0 \\
 0 & \frac{12EI_z}{L^3} & 0 & 0 & 0 & \frac{6EI_z}{L^2} & 0 & -\frac{12EI_z}{L^3} & 0 & 0 & 0 & \frac{6EI_z}{L^2} \\
 0 & 0 & \frac{12EI_y}{L^3} & 0 & -\frac{6EI_y}{L^2} & 0 & 0 & 0 & -\frac{12EI_y}{L^3} & 0 & -\frac{6EI_y}{L^2} & 0 \\
 0 & 0 & 0 & \frac{GJ}{L} & 0 & 0 & 0 & 0 & 0 & -\frac{GJ}{L} & 0 & 0 \\
 0 & 0 & -\frac{6EI_y}{L^2} & 0 & \frac{4EI_y}{L} & 0 & 0 & 0 & \frac{6EI_y}{L^2} & 0 & \frac{2EI_y}{L} & 0 \\
 0 & \frac{3EI_z}{L^2} & 0 & 0 & 0 & \frac{3EI_z}{L} & 0 & -\frac{3EI_z}{L^2} & 0 & 0 & 0 & 0 \\
 -\frac{EA}{L} & 0 & 0 & 0 & 0 & 0 & \frac{EA}{L} & 0 & 0 & 0 & 0 & 0 \\
 0 & -\frac{12EI_z}{L^3} & 0 & 0 & 0 & -\frac{6EI_z}{L^2} & 0 & \frac{12EI_z}{L^3} & 0 & 0 & 0 & -\frac{6EI_z}{L^2} \\
 0 & 0 & -\frac{12EI_y}{L^3} & 0 & \frac{6EI_y}{L^2} & 0 & 0 & 0 & \frac{12EI_y}{L^3} & 0 & \frac{6EI_y}{L^2} & 0 \\
 0 & 0 & 0 & -\frac{GJ}{L} & 0 & 0 & 0 & 0 & 0 & \frac{GJ}{L} & 0 & 0 \\
 0 & 0 & -\frac{6EI_y}{L^2} & 0 & \frac{2EI_y}{L} & 0 & 0 & 0 & \frac{6EI_y}{L^2} & 0 & \frac{4EI_y}{L} & 0 \\
 0 & 0 & 0 & 0 & 0 & 0 & 0 & 0 & 0 & 0 & \frac{L}{L} & 0
 \end{bmatrix} \tag{3.41}$$

Displacement transformation matrix for a frame member having a hinge connection at its second end is given in Equation (3.41). Difference between this matrix and transformation matrix given in Equation (3.21) is that all terms, corresponding to  $\theta_{zj}$ ,

term is equal to zero. Because,  $\theta_j$  is eliminated from the equation system given in Equations (3.40).

Therefore, displacement transformation matrix changes to the following form.

$$\mathbf{B} = \begin{bmatrix} b_{11} & b_{12} & b_{13} & 0 & 0 & 0 & 0 & 0 & 0 & 0 & 0 & 0 \\ b_{21} & b_{22} & b_{23} & 0 & 0 & 0 & 0 & 0 & 0 & 0 & 0 & 0 \\ b_{31} & b_{32} & b_{33} & 0 & 0 & 0 & 0 & 0 & 0 & 0 & 0 & 0 \\ 0 & 0 & 0 & b_{11} & b_{12} & b_{13} & 0 & 0 & 0 & 0 & 0 & 0 \\ 0 & 0 & 0 & b_{21} & b_{22} & b_{23} & 0 & 0 & 0 & 0 & 0 & 0 \\ 0 & 0 & 0 & b_{31} & b_{32} & b_{33} & 0 & 0 & 0 & 0 & 0 & 0 \\ 0 & 0 & 0 & 0 & 0 & 0 & b_{11} & b_{12} & b_{13} & 0 & 0 & 0 \\ 0 & 0 & 0 & 0 & 0 & 0 & b_{21} & b_{22} & b_{23} & 0 & 0 & 0 \\ 0 & 0 & 0 & 0 & 0 & 0 & b_{31} & b_{32} & b_{33} & 0 & 0 & 0 \\ 0 & 0 & 0 & 0 & 0 & 0 & 0 & 0 & 0 & b_{11} & b_{12} & b_{13} \\ 0 & 0 & 0 & 0 & 0 & 0 & 0 & 0 & 0 & b_{21} & b_{22} & b_{23} \\ 0 & 0 & 0 & 0 & 0 & 0 & 0 & 0 & 0 & 0 & 0 & 0 \end{bmatrix} \quad (3.42)$$

For a frame member along the +Y axis displacement transformation matrix has the following form.

$$\mathbf{B} = \begin{bmatrix} 0 & 1 & 0 & 0 & 0 & 0 & 0 & 0 & 0 & 0 & 0 & 0 \\ \sin \gamma & 0 & \cos \gamma & 0 & 0 & 0 & 0 & 0 & 0 & 0 & 0 & 0 \\ \cos \gamma & 0 & -\sin \gamma & 0 & 0 & 0 & 0 & 0 & 0 & 0 & 0 & 0 \\ 0 & 0 & 0 & 0 & 1 & 0 & 0 & 0 & 0 & 0 & 0 & 0 \\ 0 & 0 & 0 & \sin \gamma & 0 & \cos \gamma & 0 & 0 & 0 & 0 & 0 & 0 \\ 0 & 0 & 0 & \cos \gamma & 0 & -\sin \gamma & 0 & 0 & 0 & 0 & 0 & 0 \\ 0 & 0 & 0 & 0 & 0 & 0 & 0 & 1 & 0 & 0 & 0 & 0 \\ 0 & 0 & 0 & 0 & 0 & 0 & \sin \gamma & 0 & \cos \gamma & 0 & 0 & 0 \\ 0 & 0 & 0 & 0 & 0 & 0 & \cos \gamma & 0 & -\sin \gamma & 0 & 0 & 0 \\ 0 & 0 & 0 & 0 & 0 & 0 & 0 & 0 & 0 & 0 & 1 & 0 \\ 0 & 0 & 0 & 0 & 0 & 0 & 0 & 0 & 0 & \sin \gamma & 0 & \cos \gamma \\ 0 & 0 & 0 & 0 & 0 & 0 & 0 & 0 & 0 & 0 & 0 & 0 \end{bmatrix} \quad (3.43)$$

If the frame member is along the -Y axis displacement transformation becomes.

$$\mathbf{K} = \begin{bmatrix}
0 & -1 & 0 & 0 & 0 & 0 & 0 & 0 & 0 & 0 & 0 & 0 \\
\sin \gamma & 0 & -\cos \gamma & 0 & 0 & 0 & 0 & 0 & 0 & 0 & 0 & 0 \\
\cos \gamma & 0 & \sin \gamma & 0 & 0 & 0 & 0 & 0 & 0 & 0 & 0 & 0 \\
0 & 0 & 0 & 0 & -1 & 0 & 0 & 0 & 0 & 0 & 0 & 0 \\
0 & 0 & 0 & \sin \gamma & 0 & -\cos \gamma & 0 & 0 & 0 & 0 & 0 & 0 \\
0 & 0 & 0 & \cos \gamma & 0 & \sin \gamma & 0 & 0 & 0 & 0 & 0 & 0 \\
0 & 0 & 0 & 0 & 0 & 0 & 0 & -1 & 0 & 0 & 0 & 0 \\
0 & 0 & 0 & 0 & 0 & 0 & \sin \gamma & 0 & -\cos \gamma & 0 & 0 & 0 \\
0 & 0 & 0 & 0 & 0 & 0 & \cos \gamma & 0 & \sin \gamma & 0 & 0 & 0 \\
0 & 0 & 0 & 0 & 0 & 0 & 0 & 0 & 0 & 0 & -1 & 0 \\
0 & 0 & 0 & 0 & 0 & 0 & 0 & 0 & 0 & \sin \gamma & 0 & -\cos \gamma \\
0 & 0 & 0 & 0 & 0 & 0 & 0 & 0 & 0 & 0 & 0 & 0
\end{bmatrix} \quad (3.44)$$

#### 3.2.5.4. Type 4: Frame member having a hinge connections at both ends

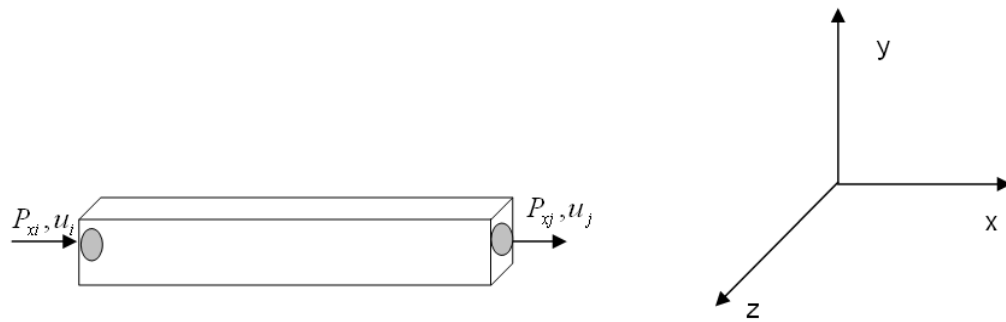


**Figure 3.15.** 3-D frame member having a hinge connections at both ends.

When both ends of a frame member are hinged, member becomes an axial member. It only transfers axial forces. In this case,  $v_i, v_j, w_i, w_j, M_{xi}, M_{xj}, M_{yi}, M_{yj}, M_{zi}, M_{zj}$  terms become equal to zero. Thus, relationships between end forces and joint displacements are reduced to those given in the following Equation (3.45).

$$P_{xi} = \frac{EA}{L} u_i - \frac{EA}{L} u_j \quad , \quad P_{xj} = -\frac{EA}{L} u_i + \frac{EA}{L} u_j \quad (3.45)$$

when these equations are written in matrix form, the following stiffness matrix is obtained.

$$[k] = \begin{bmatrix} \frac{EA}{L} & 0 & 0 & 0 & 0 & 0 & -\frac{EA}{L} & 0 & 0 & 0 & 0 & 0 \\ 0 & 0 & 0 & 0 & 0 & 0 & 0 & 0 & 0 & 0 & 0 & 0 \\ 0 & 0 & 0 & 0 & 0 & 0 & 0 & 0 & 0 & 0 & 0 & 0 \\ 0 & 0 & 0 & 0 & 0 & 0 & 0 & 0 & 0 & 0 & 0 & 0 \\ 0 & 0 & 0 & 0 & 0 & 0 & 0 & 0 & 0 & 0 & 0 & 0 \\ 0 & 0 & 0 & 0 & 0 & 0 & 0 & 0 & 0 & 0 & 0 & 0 \\ -\frac{EA}{L} & 0 & 0 & 0 & 0 & 0 & \frac{EA}{L} & 0 & 0 & 0 & 0 & 0 \\ 0 & 0 & 0 & 0 & 0 & 0 & 0 & 0 & 0 & 0 & 0 & 0 \\ 0 & 0 & 0 & 0 & 0 & 0 & 0 & 0 & 0 & 0 & 0 & 0 \\ 0 & 0 & 0 & 0 & 0 & 0 & 0 & 0 & 0 & 0 & 0 & 0 \\ 0 & 0 & 0 & 0 & 0 & 0 & 0 & 0 & 0 & 0 & 0 & 0 \\ 0 & 0 & 0 & 0 & 0 & 0 & 0 & 0 & 0 & 0 & 0 & 0 \end{bmatrix} \quad (3.46)$$

The displacement transformation matrix for this case is given in Equation (3.43). In this displacement transformation matrix all terms corresponding to  $v_i, v_j, w_i, w_j, \theta_{xi}, \theta_{xj}, \theta_{yi}, \theta_{yj}, \theta_{zi}, \theta_{zj}$  are equal to zero. Consequently the displacement transformation takes the following form.

$$B = \begin{bmatrix} b_{11} & b_{12} & b_{13} & 0 & 0 & 0 & 0 & 0 & 0 & 0 & 0 & 0 \\ 0 & 0 & 0 & 0 & 0 & 0 & 0 & 0 & 0 & 0 & 0 & 0 \\ 0 & 0 & 0 & 0 & 0 & 0 & 0 & 0 & 0 & 0 & 0 & 0 \\ 0 & 0 & 0 & 0 & 0 & 0 & 0 & 0 & 0 & 0 & 0 & 0 \\ 0 & 0 & 0 & 0 & 0 & 0 & 0 & 0 & 0 & 0 & 0 & 0 \\ 0 & 0 & 0 & 0 & 0 & 0 & 0 & 0 & 0 & 0 & 0 & 0 \\ 0 & 0 & 0 & 0 & 0 & 0 & b_{11} & b_{12} & b_{13} & 0 & 0 & 0 \\ 0 & 0 & 0 & 0 & 0 & 0 & 0 & 0 & 0 & 0 & 0 & 0 \\ 0 & 0 & 0 & 0 & 0 & 0 & 0 & 0 & 0 & 0 & 0 & 0 \\ 0 & 0 & 0 & 0 & 0 & 0 & 0 & 0 & 0 & 0 & 0 & 0 \\ 0 & 0 & 0 & 0 & 0 & 0 & 0 & 0 & 0 & 0 & 0 & 0 \\ 0 & 0 & 0 & 0 & 0 & 0 & 0 & 0 & 0 & 0 & 0 & 0 \end{bmatrix} \quad (3.47)$$

When the member along the +Y axis displacement transformation matrix becomes.

$$B = \begin{bmatrix} 0 & 1 & 0 & 0 & 0 & 0 & 0 & 0 & 0 & 0 & 0 & 0 \\ 0 & 0 & 0 & 0 & 0 & 0 & 0 & 0 & 0 & 0 & 0 & 0 \\ 0 & 0 & 0 & 0 & 0 & 0 & 0 & 0 & 0 & 0 & 0 & 0 \\ 0 & 0 & 0 & 0 & 0 & 0 & 0 & 0 & 0 & 0 & 0 & 0 \\ 0 & 0 & 0 & 0 & 0 & 0 & 0 & 0 & 0 & 0 & 0 & 0 \\ 0 & 0 & 0 & 0 & 0 & 0 & 0 & 0 & 0 & 0 & 0 & 0 \\ 0 & 0 & 0 & 0 & 0 & 0 & 0 & 1 & 0 & 0 & 0 & 0 \\ 0 & 0 & 0 & 0 & 0 & 0 & 0 & 0 & 0 & 0 & 0 & 0 \\ 0 & 0 & 0 & 0 & 0 & 0 & 0 & 0 & 0 & 0 & 0 & 0 \\ 0 & 0 & 0 & 0 & 0 & 0 & 0 & 0 & 0 & 0 & 0 & 0 \\ 0 & 0 & 0 & 0 & 0 & 0 & 0 & 0 & 0 & 0 & 0 & 0 \\ 0 & 0 & 0 & 0 & 0 & 0 & 0 & 0 & 0 & 0 & 0 & 0 \end{bmatrix} \quad (3.48)$$

For a frame member along  $-Y$  axis displacement transformation matrix has following form.

$$B = \begin{bmatrix} 0 & -1 & 0 & 0 & 0 & 0 & 0 & 0 & 0 & 0 & 0 & 0 \\ 0 & 0 & 0 & 0 & 0 & 0 & 0 & 0 & 0 & 0 & 0 & 0 \\ 0 & 0 & 0 & 0 & 0 & 0 & 0 & 0 & 0 & 0 & 0 & 0 \\ 0 & 0 & 0 & 0 & 0 & 0 & 0 & 0 & 0 & 0 & 0 & 0 \\ 0 & 0 & 0 & 0 & 0 & 0 & 0 & 0 & 0 & 0 & 0 & 0 \\ 0 & 0 & 0 & 0 & 0 & 0 & 0 & 0 & 0 & 0 & 0 & 0 \\ 0 & 0 & 0 & 0 & 0 & 0 & 0 & -1 & 0 & 0 & 0 & 0 \\ 0 & 0 & 0 & 0 & 0 & 0 & 0 & 0 & 0 & 0 & 0 & 0 \\ 0 & 0 & 0 & 0 & 0 & 0 & 0 & 0 & 0 & 0 & 0 & 0 \\ 0 & 0 & 0 & 0 & 0 & 0 & 0 & 0 & 0 & 0 & 0 & 0 \\ 0 & 0 & 0 & 0 & 0 & 0 & 0 & 0 & 0 & 0 & 0 & 0 \\ 0 & 0 & 0 & 0 & 0 & 0 & 0 & 0 & 0 & 0 & 0 & 0 \end{bmatrix} \quad (3.49)$$

### 3.3 Theory of Thin-Walled Open Members Including Warping Effect

Cold-formed thin-walled open steel sections are generally subjected to in-plane and out-of-plane loads. Due to this general loading condition, high levels of torsional moments develop in thin-walled members in addition to other internal actions. These may arise from eccentrically applied loads with respect to their shear centre or in some cases due to bending of members in the transverse direction. In most of cases, the lateral displacements of these beams are completely restrained while the rotations are elastically restrained at the loading points by slabs or other structural elements. The simple beam theory becomes inadequate to predict the behavior of such thin-walled beams [105]. This is due to the fact that the larger axial warping deformations take place in the cross-section because of torsional moments, as a result of which the plane section no longer remains

plane. It becomes necessary in this case to consider the stresses developed in the section due to flexural twist in addition to stresses due to other internal actions. Computation of these stresses requires more complex theory than the simple beam theory. The most rigorous theory in this regard is due to Vlasov [106, 107]. Vlasov's theory is based on the assumption that the outline of a section of a thin-walled beam remains unchanged under an action of external loading. In Figure 3.16., the meaning of this assumption is illustrated.

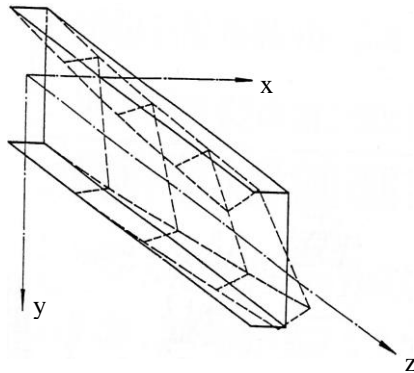


**Figure 3.16.** Clarification of Vlasov's Theory.

The simplicity of this approach is that it includes additional terms similar to simple bending expressions to accommodate the effect of warping restraint. This additional term contains bi-moment acting on section, sectorial co-ordinate and warping constant of the section. Hence, use of Vlasov's theorems makes it necessary to compute the sectorial properties of the cross-section in addition to section properties [107, 108].

### 3.3.1. Twisting Moment and Bimoment

The theory of St. Venant is perfectly valid only for a beam of circular solid cross section. The application of the theory can be accepted only when additional stresses caused by the warping of a beam can be ignored. When bending on the beam element due to torsion acts round the minor axis of a component rectangle, its effect becomes very important. Distortion due to twisting moment applied at the unrestrained end of an I-beam is illustrated in Figure 3.17.

The web and each flange are rotated by an angle  $\phi$  round their respective centers of gravity and each flange is deflected by an amount of  $\Delta$ . The first distortion is caused by a St. Venant's Twist where the second is caused by a bending twist. Because of the considerable rigidity of these flanges the twisting component producing deflection  $\Delta$  may

be several times greater than the component producing a rotation angle  $\phi$ . This twisting moment causing bending of rectangular components of beam round their respective minor axes of symmetry is called flexural twist ( $T_w$ ).

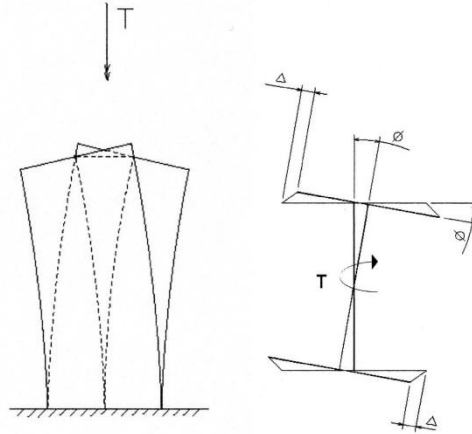


**Figure 3.17.** I-section beam distorted by twisting moment.

A flexural twist does not include the twisting moment causing the warping of each component of the beam. This component is very small for a thin-walled beam so it can be neglected. In sum, twisting moment acting on a thin-walled beam is composed of flexural and pure twisting moments and may be written as:

$$T = T_w + T_v \quad (3.50)$$

A flexural twist causes a pair or pairs of bending moments. Such a pair of bending moments is called Bimoment ( $M_w$ ).

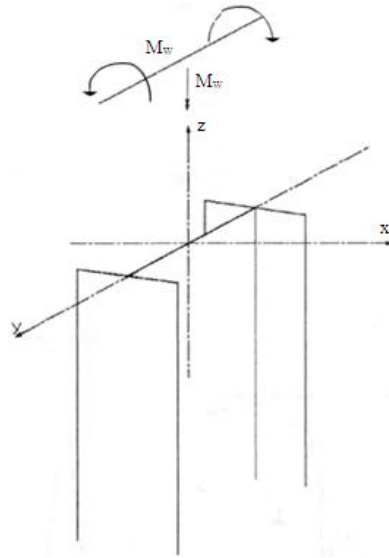


**Figure 3.18.** Physical interpretation of bimoment.

A bending moment is defined as a pair of forces. Bimoment is a pair of equal but opposite bending moments acting in two parallel planes. The numerical value of a bimoment is given by the product of the distance of these parallel planes times the moment on one of them.

### 3.3.2. Cross-Sectional Properties of a Thin-Walled Section

Considering a thin-walled section as in Figure 3.19, sectorial coordinate of a section is defined as the center line of an outline of a cross section of a thin-walled beam. Sectorial coordinate is denoted as  $\omega_{DOS}$  and called as, sectorial coordinate of S with respect to the pole D and origin O.



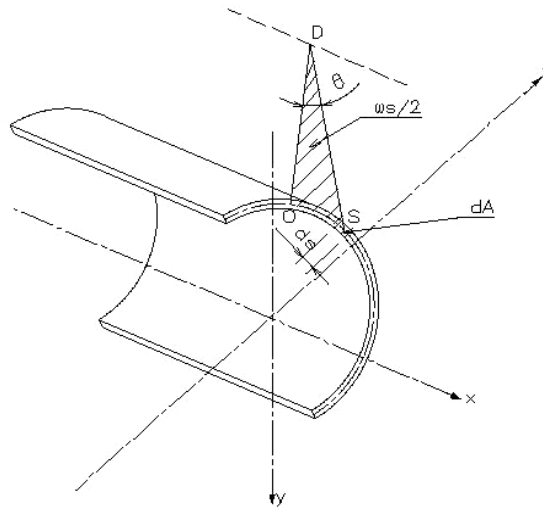


**Figure 3.19.** Sectorial co-ordinate on a thin-walled section.

First subscript of  $\omega_{DOS}$  denotes a point called a pole of the sectorial coordinates from which lines radiate to every point on the center line of the outline, where the second subscript denotes a point of intersection of initial radius of the sectorial coordinate with the centerline of the outline of the section and third subscript refers to a particular point S on the center line of an outline and its unit is area unit. The sectorial coordinate has a sign and if the angle ODS is measured from the radius DO in a counterclockwise direction, the sign of sectorial coordinate is negative and the sign is positive when the angle is measured in a clockwise direction.

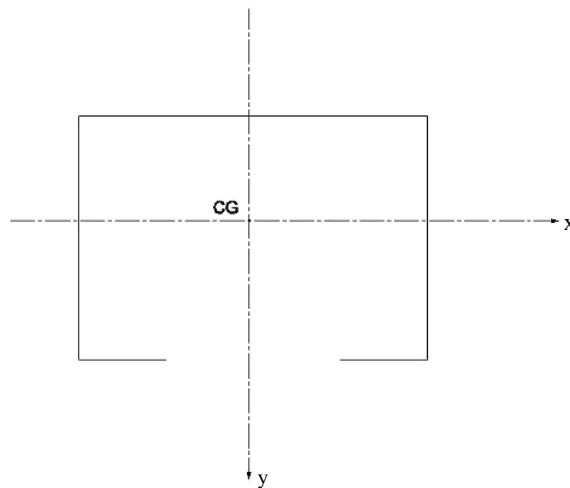


**Figure 3.20.** Thin-walled structure and a rectangular coordinate system's origin on its centroid.

In Figure 3.20., a thin-walled structure's cross section with a rectangular cross section passing through its centroid is demonstrated. Linear coordinates of this section can be used to find the following properties of a section.

$$\begin{aligned}
 &\text{A statical moment about xx axis } S_x = \int_A y dA \\
 &\text{A statical moment about yy axis } S_y = \int_A x dA \\
 &\text{A product moment of inertia about xy axis } I_{xy} = \int_A xy dA \\
 &\text{A moment of inertia about xx axis } I_{xx} = \int_A y^2 dA \\
 &\text{A moment of inertia about yy axis } I_{yy} = \int_A x^2 dA
 \end{aligned} \tag{3.51}$$

For the analysis of internal stresses due to bi-moment and flexural twist some additional properties are needed. These additional properties can be found by the help of a sectorial coordinate and a linear coordinate.

The sectorial statical moment of a section from a pole D and initial radius DO:

$$S_{w_{DO}} = \int_A w dA \tag{3.52}$$

The sectorial linear statical moment of a section about xx axis:

$$S_{wx_{DO}} = \int_A y w dA \tag{3.53}$$

The sectorial linear statical moment of a section about yy axis:

$$S_{wy_{DO}} = \int_A x w dA \tag{3.54}$$

The sectorial moment of inertia of a section for a pole D on initial radius DO:

$$I_w = \int_A w^2 dA \tag{3.55}$$

The origin of the principal linear coordinates is called as center of gravity of a section and denoted as C.G. In the same way pole of the sectorial coordinates is called the shear center. A principal sectorial moment of inertia is found from Equation (3.55) using the principal sectorial coordinates.

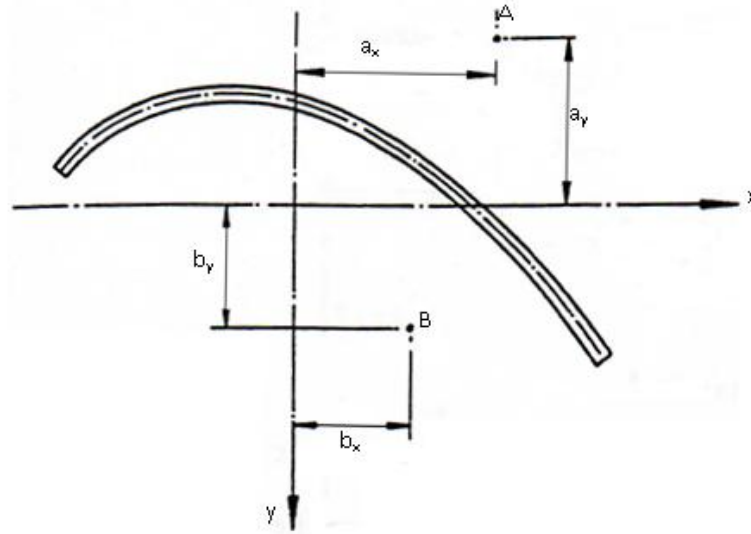


**Figure 3.21.** The cross-section of a thin-walled beam.

The method of finding a position of the principal pole (shear centre) resembles that of finding of the principal radius. An arbitrarily placed initial pole B and an initial radius are assumed as shown in Figure 3.21. Using the sectorial co-ordinates of the shear centre of this system the Cartesian co-ordinates of the shear centre A can be found from Equations (3.56) and (3.57).

$$a_x = b_x + \frac{I_{yy}Swx_{BO} - I_{xy}Swy_{BO}}{I_{xx}I_{yy} - I_{xy}^2} \quad (3.56)$$

and

$$a_y = b_y - \frac{I_{xx}Swy_{BO} - I_{xy}Swx_{BO}}{I_{xx}I_{yy} - I_{xy}^2} \quad (3.57)$$

where;

$$I_{xy} = \int_A xy dA$$

$a_x$  and  $a_y$  are the linear co-ordinates of principal pole A,  $b_x$  and  $b_y$  are the linear co-ordinates of arbitrarily placed pole B,  $I_{xx}$  and  $I_{yy}$  are the moment of inertia of a given section about its respective principal axes  $xx$  and  $yy$ ,  $Swx_{BO}$  and  $Swy_{BO}$  represent sectorial static moments of a section calculated from pole B shown in Figure 3.21.

The above formulas are valid only if the given axis  $xx$  and  $yy$  do not coincide with the principal axes of a section ( $I_{xy} \neq 0$ ), but they pass through the centre of gravity. In the case where the axes  $xx$  and  $yy$  are identical ( $I_{xy} = 0$ ) Equations (3.58) and (3.59) must be used.

$$a_x = b_x + \frac{S_{wx_{BO}}}{I_{xx}} \quad (3.58)$$

and

$$a_y = b_y - \frac{S_{wy_{BO}}}{I_{yy}} \quad (3.59)$$

### 3.3.3. Stresses Due to Bi-moment and Flexural Twist

A thin-walled beam in Figure 3.16 is under the action of external forces. Based on the Vlasov's [90] theory, thin-walled beam theory is valid as long as the cross section of the beam retains the same outline before and after the application of these forces. This assumption refers only to distortions of the outline in planes perpendicular to a longitudinal axis of beam, also strains in these planes are neglected.

Beam's longitudinal distortion, including warping can even be large and in the plane perpendicular to the longitudinal axis, rotations and translations are permitted for the cross section as long as the shape of its outline remains unchanged.

Thin-walled beam theory is valid under the assumption of no excessive deformations. Compared to other dimensions thickness is very small, so normal stress can be taken uniform over thickness. The material of the thin-walled beam has a linear elastic behavior characterized by the longitudinal modulus of elasticity ( $E$ ), the modulus of rigidity ( $G$ ), and Poisson's ratio ( $\nu$ ). Because of these assumptions in thin-walled beam theory there will be a few percents of error is introduced in analysis, which is acceptable from the analysis point of view.

The stress in a longitudinal fiber of a thin-walled beam due to a bi-moment is equal to a product of this bi-moment multiplied by the principal sectorial coordinate of this fiber and divided by the principal sectorial moment of inertia of its cross section. Equation (3.60) expresses this statement where  $\sigma_B(s)$  is longitudinal stress of fiber caused by bi-moment  $M_\omega$ :

$$\sigma_B(s) = M_\omega \frac{\omega(s)}{I_\omega} \quad (3.60)$$

Shear stress in a fiber of a thin-walled beam caused by a flexural twist is equal to the product of this flexural twist multiplied by the sectorial statical moment of this point and divided by the wall thickness at this point and the principal sectorial moment of inertia.

Equation (3.61) expresses this statement where  $\tau_\omega(s)$  is the shear stress due to a flexural twist a fiber and  $t_s$  is thickness of the wall at the section at point  $s$ , and  $s$  is a variable representing a coordinate measured along the center line of an outline of the section.

$$\tau_\omega(s) = T_\omega \frac{S_\omega(s)}{t_s I_\omega} = T_\omega \frac{\int_a^s \omega(s) dA}{t_s I_\omega} \quad (3.61)$$

The stresses introduced by Equations (3.60) and (3.61) can added algebraically to other stresses caused by axial, shear forces and bending moments about the principal axes of a section. Stress equations for a thin-walled beam are given as:

$$\sigma_s = \frac{P}{A} + M_{xx} \frac{y(s)}{I_{xx}} + M_{yy} \frac{x(s)}{I_{yy}} + M_\omega \frac{\omega(s)}{I_\omega} \quad (3.62)$$

$$\tau(s) = Q_y \frac{S_x(s)}{t_s I_{xx}} + Q_x \frac{S_y(s)}{t_s I_{yy}} \pm T_v \frac{t(s)}{I_s} + T_\omega \frac{S_\omega(s)}{t_s I_\omega} \quad (3.63)$$

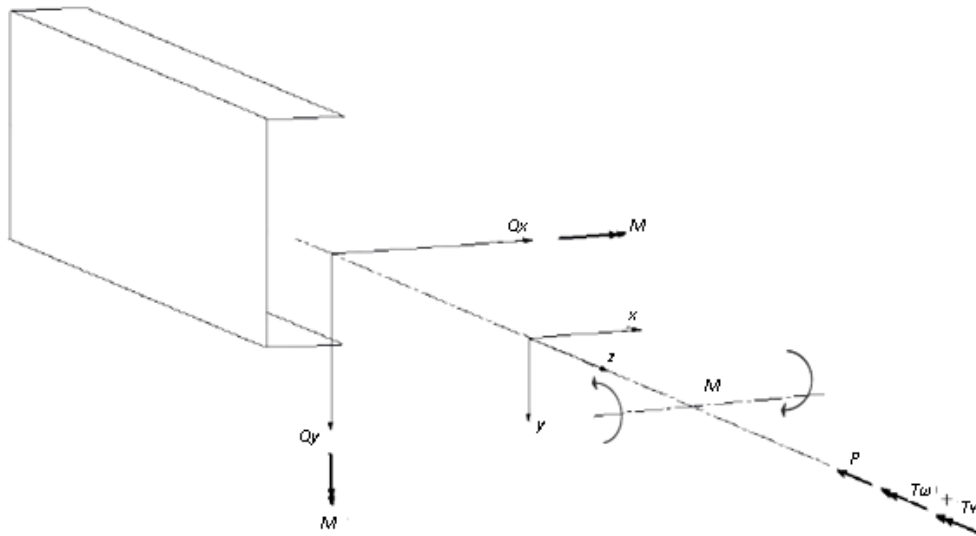


**Figure 3.22.** The sign convention of internal forces on a thin-walled beam.

For the Equations (3.62) and (3.63) the moments of inertia are calculated with respect to the principal axes and so for the moments are also taken about principal axes. Shear forces  $Q_x$  and  $Q_y$  are also acting along their respective principal axes.

Equations (3.60) to (3.61) are valid only for the elastic range. When the beam is in the plastic or elasto-plastic range their value and distribution will change. Even in the plastic stage, stresses due to bi-moment and flexural twist will not disappear, only their magnitude and distribution will change.

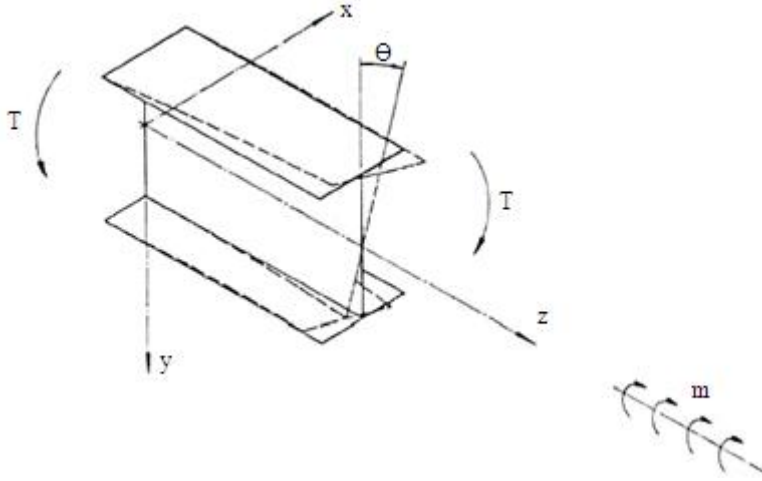


**Figure 3.23.** Thin-walled section subjected to torsion

The solution of the problem shown in Figure 3.23 can be obtained by the differential equation formulating the relation between the angle of twist of a beam and the external load. In Equation (3.50) if the definitions of  $T_v = GJ \frac{d\theta}{dz}$  and  $T_\omega = -EI_\omega \frac{d^3\theta}{dz^3}$  are used  $T$  can be expressed as;

$$T = GJ \frac{d\theta}{dz} - EI_\omega \frac{d^3\theta}{dz^3} \quad (3.64)$$

In case of distributed torque along the beam;

$$t = \frac{dT}{dz} = GJ \frac{d^2\theta}{dz^2} - EI_\omega \frac{d^4\theta}{dz^4} \quad (3.65)$$

Dividing both sides by  $EI_\omega$  ;

$$\frac{d^4\theta}{dz^4} - \frac{GJ}{EI_\omega} \frac{d^2\theta}{dz^2} = - \frac{t}{EI_\omega} \quad (3.66)$$

If  $k^2 = \frac{GJ}{EI_\omega}$  is taken;

$$\frac{d^4\theta}{dz^4} - k^2 \frac{d^2\theta}{dz^2} = -\frac{t}{EI_\omega} \quad (3.67)$$

where  $\theta$  is the angle of twist of a beam over distance  $z$ ,  $t$  is the distributed torque per unit length at the point given by co-ordinate  $z$ ,  $I_\omega$  is the principal sectorial moment of inertia of a section at point  $z$ . In the formulation of  $k$ ,  $G$  denotes shear modulus,  $J$  denotes torsional moment of inertia (torsional constant),  $E$  denotes Young's modulus. The definition of  $J$  and  $I_\omega$  can be given as  $J = \sum_{i=1}^n \frac{b_i t_i^3}{3}$  and  $I_\omega = \int_A w^2 dA$ .  $b_i$ ,  $t_i$  and  $n$  are the length of a single element, the mean thickness of a single element, and the number of elements in a thin-walled section, respectively.

Solving the differential Equation (3.67), one can find in turn, values of the internal bi-moment and flexural twist as represented in Equations (3.68) and (3.69).

$$M_\omega = -EI_\omega \frac{d^2\theta}{dz^2} \quad (3.68)$$

$$T_\omega = \frac{d(M_\omega)}{dz} = -EI_\omega \frac{d^3\theta}{dz^3} \quad (3.69)$$

Finally, the value of an internal St. Venant twist can be found from ;

$$T_v(z) = T(z) - T_\omega(z) \quad (3.70)$$

### 3.3.4. Torsional Stiffness Matrix

The total torque acting on a member is a vector that is in the longitudinal direction of a member [88]. In Figure 3.24, for example  $M_{xi}$  and  $M_{xj}$  are applied The *St. Venant* torques, and  $\theta_{xi}$  and  $\theta_{xj}$  are the resulting displacement parameters. The *St Venant* torque is a vector that acts in the same direction as these end-torsional moments. However, warping torque  $T_w$  vector does not act in the same direction. For thin-walled members the warping torque can be represented in terms of the pair of bending moments, and these moments can be represented as a vector that acts in the direction of Y axis (Figure 3.25.). These moments ( $M_{wi}$  and  $M_{wj}$ ) are called as bi moment. General definition of a bi moment is a pair equal but opposite bending moments acting in two parallel planes. The resulting displacement parameters of the warping torque ( $\theta_{wi}$  and  $\theta_{wj}$ ) can be

represented as vector which are the first derivative of the resulting displacement parameters of the *St Venant* torque ( $\theta_{xi}$  and  $\theta_{xj}$ ). Relationship between the resulting displacement parameters ( $\theta_{xi}, \theta_{xj}, \theta_{wi}$  and  $\theta_{wj}$ ) and torsional moments ( $M_{xi}, M_{xj}, M_{wi}$  and  $M_{wj}$ ) can be represented by using equilibrium equations which yields to the following form.

$$\begin{bmatrix} \mathbf{S}_{1,1} & \dots & \mathbf{S}_{1,2} \\ \dots & \dots & \dots \\ \mathbf{S}_{2,1} & \dots & \mathbf{S}_{2,2} \end{bmatrix} \begin{bmatrix} \theta_{xi} \\ \theta_{wi} \\ \theta_{xj} \\ \theta_{wj} \end{bmatrix} = \begin{bmatrix} M_{xi} \\ M_{wi} \\ M_{xj} \\ M_{wj} \end{bmatrix} \quad (3.71)$$

where,  $\mathbf{S}_{ij}$  is the torsional stiffness matrix. Terms of this matrix are calculated in the following

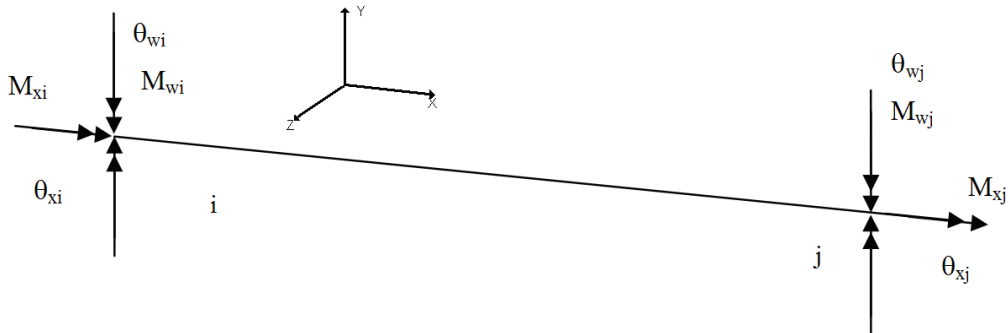


**Figure 3.24.** Beam element subjected to the torsion.



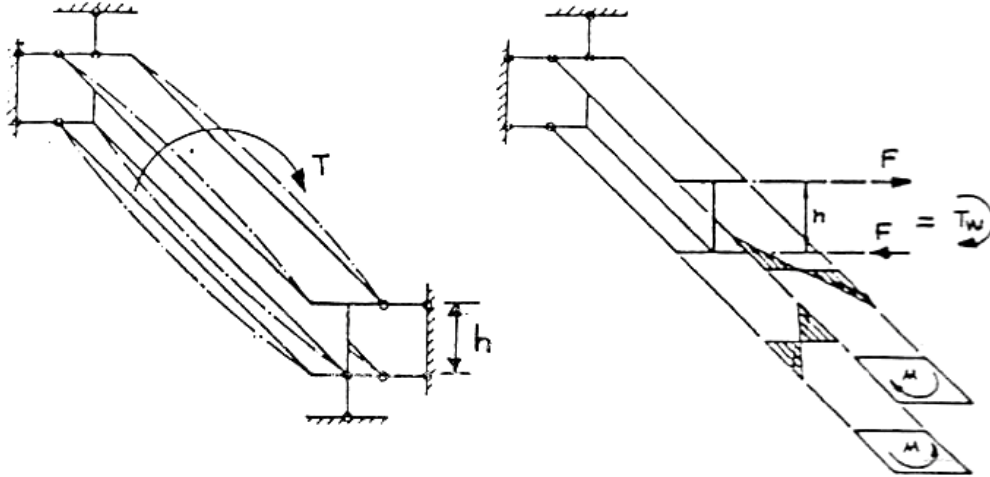


**Figure 3.25.** Twisting torque acting on beam element.

If the torque is constant along the beam then  $t$  becomes zero in Equation (3.67).

$$\frac{d^4\theta}{dz^4} - k^2 \frac{d^2\theta}{dz^2} = 0 \quad (3.72)$$

Solution of the differential equation given in (3.72) is obtained as,

$$\theta = A \sinh kz + B \cosh kz + Cz + D \quad (3.73)$$

where A, B, C and D are integration constants that are determined using the boundary conditions of the beam element.

Let us consider a beam with the boundary conditions which is subjected to the torsional moment shown in the Figure 3.25. The terms of the torsional stiffness matrix of this beam element are obtained by applying the following boundary conditions to Equation (3.67) as carried out in the following.

First boundary condition ( $\theta_{xi} = 1$ ;  $\theta_{xj} = 0$ ;  $\theta_{wi} = 0$ ;  $\theta_{wj} = 0$ ); After applying these boundary conditions and solving the linear system of equations obtained, end moments are obtained as in the following:

$$M_{xi} = -M_{xj} = -GJ \cdot \sqrt{\frac{GJ}{EI_w}} \frac{\sinh(\alpha l)}{2 \cosh(\alpha l) - \alpha l \cosh(\alpha l) - 2} \quad (3.74)$$

and

$$M_{wi} = -M_{wj} = -GJ \cdot \frac{\cosh(\alpha l) - 1}{2 \cosh(\alpha l) - \alpha l \cosh(\alpha l) - 2} \quad (3.75)$$

Second boundary conditions ( $\theta_{xi} = 0$ ;  $\theta_{xj} = 0$ ;  $\theta_{wi} = 1$ ;  $\theta_{wj} = 0$ ) yield to the following end moments are obtained:

$$M_{wi} = -M_{wj} = -GJ \cdot \frac{\cosh(\alpha l) - 1}{2 \cosh(\alpha l) - \alpha l \cosh(\alpha l) - 2} \quad (3.76)$$

$$M_{wi} = \frac{GJ}{\alpha} \cdot \frac{\sinh(\alpha l) - \alpha l \cosh(\alpha l)}{2 \cosh(\alpha l) - \alpha l \cosh(\alpha l) - 2} \quad (3.77)$$

$$M_{wj} = \frac{GJ}{\alpha} \cdot \frac{\alpha l - \sinh(\alpha l)}{2 \cosh(\alpha l) - \alpha l \cosh(\alpha l) - 2} \quad (3.78)$$

If Equations (3.74), (3.75), (3.76), (3.77), and (3.78) are written in matrix form, the torsional stiffness matrix of the beam element is obtained which takes into account the effect of cross sectional warping.

$$\begin{bmatrix} -T_1 & -T_2 & T_1 & -T_2 \\ -T_2 & T_3 & T_2 & T_4 \\ T_1 & T_2 & -T_1 & T_2 \\ -T_2 & T_4 & T_2 & T_3 \end{bmatrix} \cdot \begin{bmatrix} \theta_{xi} \\ \theta_{wi} \\ \theta_{xj} \\ \theta_{wj} \end{bmatrix} = \begin{bmatrix} M_{xi} \\ M_{wi} \\ M_{xj} \\ M_{wj} \end{bmatrix} \quad (3.79)$$

where;

$$T_1 = GJ \frac{\alpha \sinh(\alpha l)}{2 \cosh(\alpha l) - \alpha l \cosh(\alpha l) - 2} \quad (3.80)$$

$$T_2 = GJ \frac{\cosh(\alpha l) - 1}{2 \cosh(\alpha l) - \alpha l \cosh(\alpha l) - 2} \quad (3.81)$$

$$T_3 = \frac{GJ}{\alpha} \cdot \frac{\sinh(\alpha l) - \alpha l \cosh(\alpha l)}{2 \cosh(\alpha l) - \alpha l \cosh(\alpha l) - 2} \quad (3.82)$$

$$T_4 = \frac{GJ}{\alpha} \cdot \frac{\alpha l - \sinh(\alpha l)}{2 \cosh(\alpha l) - \alpha l \cosh(\alpha l) - 2} \quad (3.83)$$

These terms are added to the local stiffness matrix of the three dimensional beam element which has twelve rows and twelve columns as shown in Equation (3.3). This brings the total number of degrees of freedom to seven at a joint of space frame. These degrees of freedoms are the usual three translations along X, Y, and Z axes, three rotations about

the global axes and additional warping deformation. Consequently, the member stiffness matrix in local coordinate system has fourteen rows and fourteen columns which are shown in Equation (3.84). Three dimensional steel structures are analyzed includes warping effect by using this stiffness matrix. At the end of the analysis, in addition to the member end forces and end moments, bi-moments are also obtained.

$$k = \begin{bmatrix} \frac{EA}{L} & 0 & 0 & 0 & 0 & 0 & 0 & -\frac{EA}{L} & 0 & 0 & 0 & 0 & 0 & 0 \\ 0 & \frac{12EI_z}{L^3} & 0 & 0 & 0 & 0 & \frac{6EI_z}{L^2} & 0 & -\frac{12EI_z}{L^3} & 0 & 0 & 0 & 0 & \frac{6EI_z}{L^2} \\ 0 & 0 & \frac{12EI_y}{L^3} & 0 & 0 & -\frac{6EI_y}{L^2} & 0 & 0 & 0 & -\frac{12EI_y}{L^3} & 0 & 0 & -\frac{6EI_y}{L^2} & 0 \\ 0 & 0 & 0 & -T_1 & -T_2 & 0 & 0 & 0 & 0 & 0 & T_1 & -T_2 & 0 & 0 \\ 0 & 0 & 0 & -T_2 & T_3 & 0 & 0 & 0 & 0 & 0 & 0 & T_2 & T_4 & 0 & 0 \\ 0 & 0 & \frac{6EI_y}{L^2} & 0 & 0 & \frac{4EI_y}{L} & 0 & 0 & 0 & \frac{6EI_y}{L^2} & 0 & 0 & \frac{2EI_y}{L} & 0 & 0 \\ 0 & \frac{6EI_z}{L^2} & 0 & 0 & 0 & 0 & \frac{4EI_z}{L} & 0 & -\frac{6EI_z}{L^2} & 0 & 0 & 0 & 0 & \frac{2EI_z}{L} & 0 \\ -\frac{EA}{L} & 0 & 0 & 0 & 0 & 0 & 0 & \frac{EA}{L} & 0 & 0 & 0 & 0 & 0 & 0 & 0 \\ 0 & -\frac{12EI_z}{L^3} & 0 & 0 & 0 & 0 & -\frac{6EI_z}{L^2} & 0 & \frac{12EI_z}{L^3} & 0 & 0 & 0 & 0 & -\frac{6EI_z}{L^2} & 0 \\ 0 & 0 & -\frac{12EI_y}{L^3} & 0 & 0 & \frac{6EI_y}{L^2} & 0 & 0 & 0 & \frac{12EI_y}{L^3} & 0 & 0 & \frac{6EI_y}{L^2} & 0 & 0 \\ 0 & 0 & 0 & T_1 & T_2 & 0 & 0 & 0 & 0 & 0 & -T_1 & T_2 & 0 & 0 & 0 \\ 0 & 0 & 0 & -T_2 & T_4 & 0 & 0 & 0 & 0 & 0 & 0 & T_2 & T_3 & 0 & 0 \\ 0 & 0 & -\frac{6EI_y}{L^2} & 0 & 0 & \frac{2EI_y}{L} & 0 & 0 & 0 & \frac{6EI_y}{L^2} & 0 & 0 & \frac{4EI_y}{L} & 0 & 0 \\ 0 & \frac{6EI_z}{L^2} & 0 & 0 & 0 & 0 & \frac{2EI_z}{L} & 0 & -\frac{6EI_z}{L^2} & 0 & 0 & 0 & 0 & \frac{4EI_z}{L} & 0 \end{bmatrix} \quad (3.84)$$



## CHAPTER 4

### GEOMETRIC NONLINEARITY AND STABILITY FUNCTIONS

#### 4.1. Geometric Nonlinearity

A variety of classifications may be used to describe the deformational response of structures; for example, small or large, elastic or inelastic, etc. In general, deformations of structures under the external loads are small, and hence the application of the equilibrium equations on the undeformed shape of the structure does not introduce large errors. However, when structure consists of slender members, the deformations become large and small deflection theory is no longer valid. The equilibrium equations are required to be written in such structures on the deformed shape of its elements. In other words, the deflected shape of the structure should be taken into account. When this is considered in the displacement computations, the relationship between the external loads and displacements become nonlinear.

Geometric nonlinearity is required to be considered in the analysis of a structure, if its deflections are large compared with its initial dimensions. In structures with large displacements, although the material behaves linear elastic, the response of the structure becomes nonlinear [109]. Under certain types of loading, namely, even when small deformations are presumed, nonlinear behavior can be predicted. Changes in stiffness and loads occur as the structure deforms. When geometric nonlinearity occurs in a structure, the effect of axial forces to member stiffness must be taken into account. This is called second-order analysis of structures which is also known as P-Delta analysis. The Second-order analysis when accounting for P-Delta combines two effects to reach a solution:

- Large displacement theory - the resulting forces and moments take full account of the effects due to the deformed shape of both the structure and its members,
- The effect of element axial loads on structure stiffness. Tensile loads straighten the geometry of an element thereby stiffening it. Compressive loads accentuate deformation thereby reducing the stiffness of the element.

P-Delta is a non-linear effect that occurs in every structure where elements are subject to axial load. It is associated with the magnitude of the applied axial load ( $P$ ) and a displacement ( $\delta$ ) as shown in Figure 4.1.

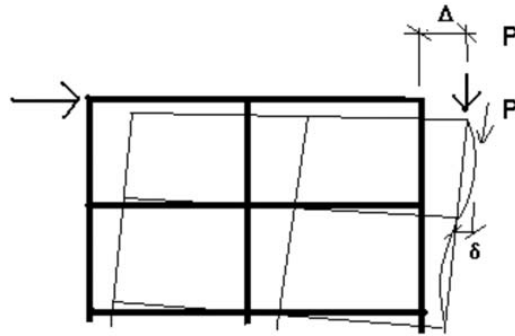


**Figure 4.1.** P-Delta effects.

There are two P-Delta effects:

- P-“BIG” delta ( $P-\Delta$ ) - a structure effect
- P-“little” delta ( $P-\delta$ ) - a member effect

The magnitude of the P-Delta effect is related to the magnitude of axial load  $P$ , stiffness/slenderness of the structure as a whole and the slenderness of individual elements. The axial forces in a member have a significant effect on its flexural bending that cause nonlinearity in the behavior of structures. This is called geometric nonlinearity. The developments occurred in the computational structures technology and the design methods have yielded ever more slender and more flexible structures which make it necessary to consider the geometric nonlinearity namely the P-Delta effects in their analysis if more accurate and realistic structural responses under the external loads are desired to be obtained. Noticing the fact that cold-formed steel sections are quite slender elements, the prediction of the structural response of frames made of such members also necessitates the consideration of the geometric nonlinearity in their analysis.

Structural elements subjected to both axial forces and bending moments are called beam-columns. Such members are exposed to the interaction of these effects. The lateral deflection of a member causes additional bending moment when an axial force is applied. This changes the flexural stiffness of the member. Similarly, the presence of bending moments also affects the axial stiffness of the member due to shortening of the member caused by the bending deformations. If the deformations are small, the interaction between bending and axial forces can be ignored. In such a case, the force-deformation relationship for a beam-column is the same as Equation (3.2). However, if the deformations are large, the stiffness matrix  $\mathbf{k}$  is affected by the interaction between bending and axial forces, and it is not linear anymore [110]. The nonlinear stiffness matrix can be derived by using stability functions.

## 4.2. Stability Functions

The stability functions are the modification factors from  $s_1$  to  $s_9$ . These functions can be defined with respect to member length, cross-sectional properties, axial force, and the end moments. The effect of axial force on torsional stiffness and the effect of torsional moment on axial stiffness are neglected [110].

where;

$s_1$  : stability function for the effect of flexure on axial stiffness,

$s_2$  : stability function for the effect of axial force on flexural stiffness against rotation of near end about z-axis,

$s_3$  : stability function for the effect of axial force on flexural stiffness against rotation of far end about z-axis,

$s_4$  : stability function for the effect of axial force on flexural stiffness against rotation of near end about y-axis,

$s_5$  : stability function for the effect of axial force on flexural stiffness against rotation of far end about y-axis,

$s_6$  : stability function for the effect of axial force on flexural stiffness (about z-axis) against translation in y-direction,

$s_7$  : stability function for the effect of axial force on shear stiffness in y-direction against translation in y-direction,

$s_8$  : stability function for the effect of axial force on flexural stiffness (about y-axis) against translation in z-direction,

$s_9$  : stability function for the effect of axial force on shear stiffness in z-direction against translation in z-direction.

### 4.2.1. Effect of Flexure on Axial Stiffness

The axial stiffness of the beam in the absence of end moments is given by  $EA/L$ , and the axial deformation due to axial loading  $P$  is given by  $PL/(EA)$ . However, the end moments produce an additional axial deformation in the beam. In order to include the effect of flexure on axial deformation, the axial stiffness of the beam-column must be modified.

For this purpose, the modified axial stiffness can be illustrated as  $s_1(EA/L)$ . An expression for  $s_1$  is derived as follows [110].

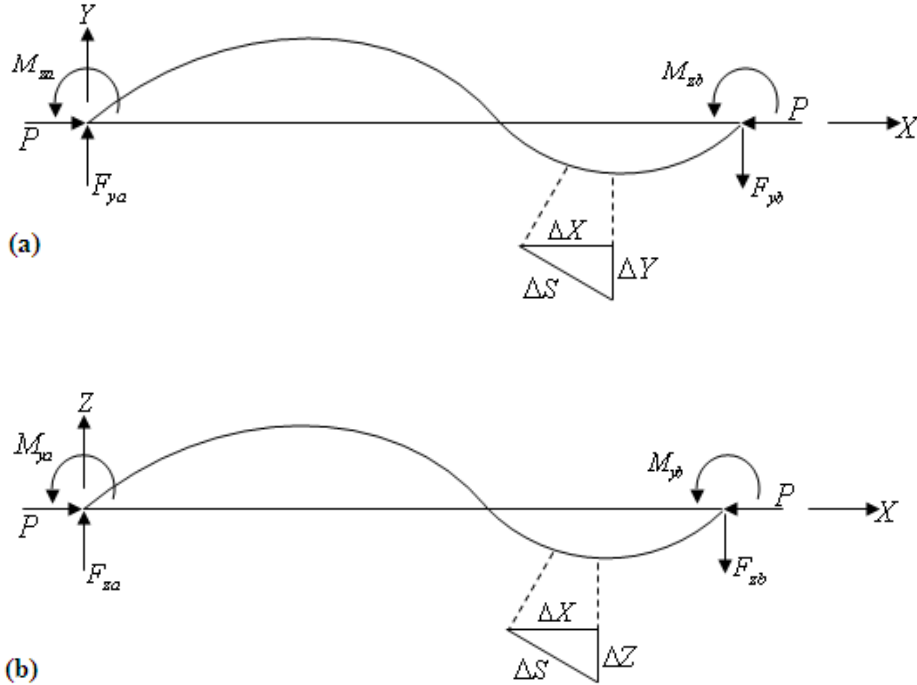


**Figure 4.2.** Effect of Flexure on Axial Stiffness: (a) Bending in X-Y plane; (b) Bending in X-Z plane.

From Figure 4.2. (a) and (b);

$$ds^2 = dx^2 + dy^2 + dz^2 \quad (4.1)$$

by rearranging this equation,

$$\frac{ds^2}{dx^2} = 1 + \frac{dy^2}{dx^2} + \frac{dz^2}{dx^2} \quad (4.2)$$

Shortening due to bending can approximately be defined as,

$$d\delta_b = ds - dx \quad (4.3)$$

dividing equation (4.3) by  $dx$ ,



$$\frac{d\delta_b}{dx} = \frac{ds}{dx} - 1 \quad (4.4)$$

Neglecting higher order terms,

$$\frac{d\delta_b}{dx} = \frac{1}{2} \left[ \left( \frac{dy}{dx} \right)^2 + \left( \frac{dz}{dx} \right)^2 \right] \quad (4.5)$$

Therefore, the shortening of the beam-column due to bending is,

$$\delta_b = \int_0^L \frac{d\delta_b}{dx} dx \quad (4.6)$$

$$\delta_b = \frac{1}{2} \int_0^L \left[ \left( \frac{dy}{dx} \right)^2 + \left( \frac{dz}{dx} \right)^2 \right] dx \quad (4.7)$$

Total shortening of the beam-column is expressed,

$\delta_t$  = shortening due to axial load ( $\delta_a$ ) + shortening due to bending ( $\delta_b$ )

$$\delta_t = \frac{PL}{EA} + \frac{1}{2} \int_0^L \left[ \left( \frac{dy}{dx} \right)^2 + \left( \frac{dz}{dx} \right)^2 \right] dx \quad (4.8)$$

$$\delta_t = \frac{PL}{EA} + \left\{ 1 + \frac{EA}{2PL} \int_0^L \left[ \left( \frac{dy}{dx} \right)^2 + \left( \frac{dz}{dx} \right)^2 \right] dx \right\} \quad (4.9)$$

$$\delta_t = \frac{P}{s_1 \left( \frac{EA}{L} \right)} \quad (4.10)$$

$$\text{and } s_1 = \frac{1}{1 + \frac{EA}{2PL} \int_0^L \left[ \left( \frac{dy}{dx} \right)^2 + \left( \frac{dz}{dx} \right)^2 \right] dx} \quad (4.11)$$

The curvature  $\left( \frac{d^2 y}{dx^2} \right)$  can be defined from Figure 4.2 (a),

$$\left(\frac{d^2y}{dx^2}\right) = \frac{1}{EI_z} \left[ -M_{za} + \frac{x}{L}(M_{za} + M_{zb}) - Py \right] \quad (4.12)$$

$$\text{Let } \alpha^2 = \frac{P}{EI_z} \quad (4.13)$$

Substituting equation (4.13) in equation (4.12) and rearranging the terms,

$$\left(\frac{d^2y}{dx^2}\right) + \alpha^2 y = \frac{\alpha^2}{PL} M_{za} + M_{zb} - \frac{\alpha^2}{P} M_{za} \quad (4.14)$$

The solution for equation (4.14) is given by the summation of complementary function and particular integral;

$$y = A \sin \alpha x + B \cos \alpha x + \left\{ \frac{x}{PL} (M_{za} + M_{zb}) - \frac{M_{za}}{P} \right\} \quad (4.15)$$

Substituting the boundary conditions  $y=0$  at  $x=0$  and  $x=L$ ,

$$\left. \begin{aligned} A &= -\frac{1}{P} \operatorname{cosec} \alpha L \left( M_{za} \cos \alpha L + M_{zb} \right) \\ \text{and} \\ B &= \frac{M_{za}}{P} \end{aligned} \right\} \quad (4.16)$$

The slope of beam in the X-Y plane is given by,

$$\frac{dy}{dx} = A\alpha \cos \alpha x - B\alpha \sin \alpha x + \frac{1}{PL} M_{za} + M_{zb} \quad (4.17)$$

Similarly, the equation of the beam-column for bending in the X-Z plane is

$$z = C \sin \beta x + D \cos \beta x + \left\{ \frac{x}{PL} M_{ya} + M_{yb} - \frac{M_{ya}}{P} \right\} \quad (4.18)$$

$$\text{where } \beta^2 = \frac{P}{EI_y} \quad (4.19)$$

Substituting the boundary conditions  $z=0$  at  $x=0$  and  $x=L$ ,

$$\left. \begin{aligned}
C &= -\frac{1}{P} \operatorname{cosec} \beta L \left[ M_{ya} \cos \beta L + M_{yb} \right] \\
\text{and} \\
D &= \frac{M_{ya}}{P}
\end{aligned} \right\} \quad (4.20)$$

The slope of the beam in the X-Z plane is given by,

$$\frac{dz}{dx} = C \beta \cos \beta x - D \beta \sin \beta x + \frac{1}{PL} M_{ya} + M_{yb} \quad (4.21)$$

Now the integrals in equation (4.11) can be evaluated. The final result of the integration is;

$$\begin{aligned}
\int_0^L \left( \frac{dy}{dx} \right)^2 dx &= \frac{1}{2P^2L} [\alpha L M_{za}^2 + M_{zb}^2 \cot \alpha L + \alpha L \operatorname{cosec}^2 \alpha L \\
&\quad - 2 M_{za} + M_{zb}^2 + 2\alpha L M_{za} M_{zb} \operatorname{cosec} \alpha L \quad 1 + \alpha L \cot \alpha L ] \\
(4.22)
\end{aligned}$$

$$\begin{aligned}
\text{where; } H_z &= [\alpha L M_{za}^2 + M_{zb}^2 \cot \alpha L + \alpha L \operatorname{cosec}^2 \alpha L \\
&\quad - 2 M_{za} + M_{zb}^2 + 2\alpha L M_{za} M_{zb} \operatorname{cosec} \alpha L \quad 1 + \alpha L \cot \alpha L ] \\
&= \frac{1}{2P^2L} H_z \quad (4.23)
\end{aligned}$$

and

$$\begin{aligned}
\int_0^L \left( \frac{dz}{dx} \right)^2 dx &= \frac{1}{2P^2L} [\beta L M_{ya}^2 + M_{yb}^2 \cot \beta L + \beta L \operatorname{cosec}^2 \beta L \\
&\quad - 2 M_{ya} + M_{yb}^2 + 2\beta L M_{ya} M_{yb} \operatorname{cosec} \beta L \quad 1 + \beta L \cot \beta L ] \\
(4.24)
\end{aligned}$$

$$\begin{aligned}
\text{where; } H_y &= [\beta L M_{ya}^2 + M_{yb}^2 \cot \beta L + \beta L \operatorname{cosec}^2 \beta L \\
&\quad - 2 M_{ya} + M_{yb}^2 + 2\beta L M_{ya} M_{yb} \operatorname{cosec} \beta L \quad 1 + \beta L \cot \beta L ] \\
&= \frac{1}{2P^2L} H_y \quad (4.25)
\end{aligned}$$

Therefore, equation (4.11) becomes,

$$s_1 = \frac{1}{1 + \frac{EA}{4P^3L^2} [H_y + H_z]} \quad (4.26)$$

A similar approach can be used to derive an expression for  $s_1$  for a beam-column with axial tensile force  $P$ . The final expression is as follows:

$$s_1 = \frac{1}{1 + \frac{EA}{4P^3L^2} [H_y' + H_z']} \quad (4.27)$$

$$\text{where; } H_y' = \left[ \begin{array}{l} \beta L M_{ya}^2 + M_{yb}^2 \coth \beta L + \beta L \operatorname{cosech}^2 \beta L \\ -2 M_{ya} + M_{yb}^2 + 2\beta L M_{ya} M_{yb} \operatorname{cosech} \beta L \quad 1 + \beta L \coth \beta L \end{array} \right] \quad (4.28)$$

and

$$H_z' = \left[ \begin{array}{l} \alpha L M_{za}^2 + M_{zb}^2 \coth \alpha L + \alpha L \operatorname{cosech}^2 \alpha L \\ -2 M_{za} + M_{zb}^2 + 2\alpha L M_{za} M_{zb} \operatorname{cosech} \alpha L \quad 1 + \alpha L \coth \alpha L \end{array} \right] \quad (4.29)$$

## 4.2.2. Effect of Axial Force on Flexural Stiffness

### 4.2.2.1. Bending in X-Y Plane

From Figure 4.2 (a), the differential equation of the beam-column bending in the X-Y plane is given by Equation (4.14) for which the solution is given by equation (4.15). The constants  $A$  and  $B$  are obtained from Equation (4.16). The end slopes of the beam-column are obtained by substituting  $x=0$  and  $x=L$  in equation (4.17);

$$\left( \frac{dy}{dx} \right)_{x=0} = \theta_{za} = A\alpha + \frac{1}{PL} M_{za} + M_{zb} \quad (4.30)$$

$$\left( \frac{dy}{dx} \right)_{x=L} = \theta_{zb} = A\alpha \cos \alpha L - B\alpha \sin \alpha L + \frac{1}{PL} [M_{ya} + M_{yb}] \quad (4.31)$$

Equations (4.30) and (4.31) can be rearranged and rewritten in matrix form as;

$$\begin{Bmatrix} M_{za} \\ M_{zb} \end{Bmatrix} = \begin{Bmatrix} s_2 \left( \frac{4EI_z}{L} \right) & s_3 \left( \frac{2EI_z}{L} \right) \\ s_3 \left( \frac{2EI_z}{L} \right) & s_2 \left( \frac{4EI_z}{L} \right) \end{Bmatrix} \begin{Bmatrix} \theta_{za} \\ \theta_{zb} \end{Bmatrix} \quad (4.32)$$

when  $P$  is compressive, the  $s_2$  and  $s_3$  functions take the following form;

$$s_2 = \frac{1}{4} \alpha L \frac{\sin \alpha L - \alpha L \cos \alpha L}{2 - 2 \cos \alpha L - \alpha L \sin \alpha L} \quad (4.33)$$

$$s_3 = \frac{1}{2} \alpha L \frac{\alpha L - \sin \alpha L}{2 - 2 \cos \alpha L - \alpha L \sin \alpha L} \quad (4.34)$$

For members subject to axial tensile force  $P$  and bending in the  $X$ - $Y$  plane,  $P$  is replaced by  $-P$  in equation (4.12). Solving the resulting differential equation, equation (4.32) can again be obtained as;

$$s_2 = \frac{1}{4} \alpha L \frac{\alpha L \cosh \alpha L - \sinh \alpha L}{2 - 2 \cosh \alpha L + \alpha L \sinh \alpha L} \quad (4.35)$$

$$s_3 = \frac{1}{2} \alpha L \frac{\sinh \alpha L - \alpha L}{2 - 2 \cosh \alpha L + \alpha L \sinh \alpha L} \quad (4.36)$$

#### 4.2.2.2. Bending in $X$ - $Z$ Plane

From Figure 4.2(b), and following the same procedure previously mentioned, the stability functions for bending in  $X$ - $Z$  plane can be derived. The relationship between end moments and end slopes is given by;

$$\begin{Bmatrix} M_{ya} \\ M_{yb} \end{Bmatrix} = \begin{Bmatrix} s_4 \left( \frac{4EI_y}{L} \right) & s_5 \left( \frac{2EI_y}{L} \right) \\ s_5 \left( \frac{2EI_y}{L} \right) & s_4 \left( \frac{4EI_y}{L} \right) \end{Bmatrix} \begin{Bmatrix} \theta_{ya} \\ \theta_{yb} \end{Bmatrix} \quad (4.37)$$

where;

$$s_4 = \frac{1}{4} \beta L \frac{\sin \beta L - \beta L \cos \beta L}{2 - 2 \cos \beta L - \beta L \sin \beta L} \quad \text{for compressive } P \quad (4.38)$$

$$s_4 = \frac{1}{4} \beta L \frac{\beta L \cosh \beta L - \sinh \beta L}{2 - 2 \cosh \beta L + \beta L \sinh \beta L} \quad \text{for tensile } P \quad (4.39)$$

and

$$s_5 = \frac{1}{2} \beta L \frac{\beta L - \sin \beta L}{2 - 2 \cos \beta L - \beta L \sin \beta L} \quad \text{for compressive } P \quad (4.40)$$

$$s_5 = \frac{1}{2} \beta L \frac{\sinh \beta L - \beta L}{2 - 2 \cosh \beta L + \alpha L \sinh \beta L} \quad \text{for tensile } P \quad (4.41)$$

#### 4.2.2.3. Effect of Axial Force on Stiffness Against Translation

If both of the ends of a beam-column are restrained against rotation, but one end is translated through a distance  $\Delta$  relative to the other, the flexural and shear stiffnesses of the beam against this translation are affected by the axial force  $P$ .

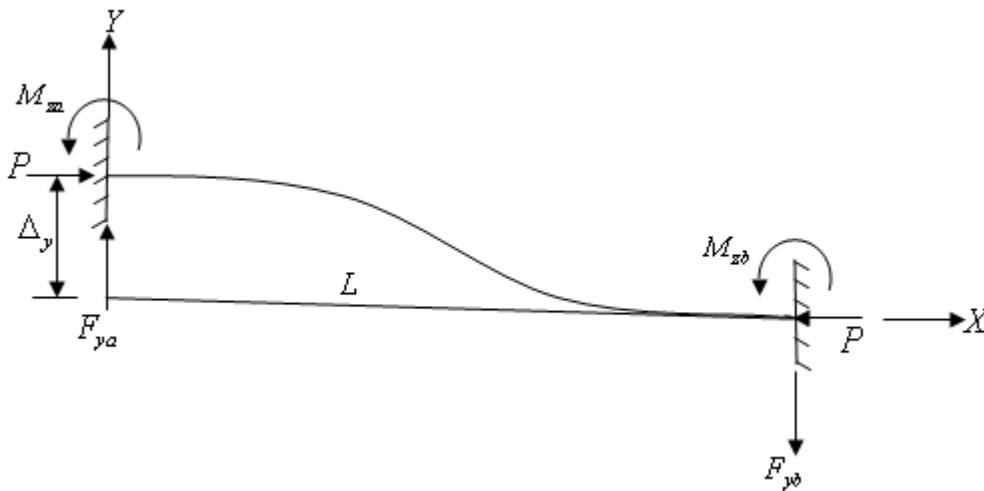


**Figure 4.3.** Effect of Axial Force on Stiffness Against Translation.

#### 4.2.2.3.1. Translation in X-Y Plane

From Figure 4.3 and using the slope-deflection equation;

$$M_{za} = s_2 \left( \frac{4EI_z}{L} \right) \frac{\Delta_y}{L} + s_3 \left( \frac{2EI_z}{L} \right) \frac{\Delta_y}{L} \quad (4.42)$$

$$= \left( \frac{6EI_z}{L^2} \right) \Delta_y \left\{ \frac{2}{3} s_2 + \frac{1}{3} s_3 \right\} \quad (4.43)$$

$$= s_6 \left( \frac{6EI_z}{L^2} \right) \Delta_y \quad (4.44)$$

where;

$$s_6 = \frac{2}{3} s_2 + \frac{1}{3} s_3 \quad (4.45)$$

Substituting the values of  $s_2$  and  $s_3$  from equations (4.33) and (4.34) when the axial force is compressive, and from equations (4.35) and (4.36) when the axial force is tensile, the expressions for  $s_6$  can be obtained as;

When  $P$  is compressive;

$$s_6 = \frac{1}{6} \frac{\alpha^2 L^2 (1 - \cos \alpha L)}{(2 - 2 \cos \alpha L - \alpha L \sin \alpha L)} \quad (4.46)$$

When  $P$  is tensile;

$$s_6 = \frac{1}{6} \frac{\alpha^2 L^2 (\cosh \alpha L - 1)}{(2 - 2 \cosh \alpha L - \alpha L \sinh \alpha L)} \quad (4.47)$$

Once again from Figure 4.2.,

$$F_{ya} = \frac{\sum M}{L} \quad (4.48)$$

where;

$$\sum M = M_{za} + M_{zb} - P \Delta_y \quad (4.49)$$

and

$$M_{za} = s_2 \left( \frac{4EI_z}{L} \right) \frac{\Delta_y}{L} + s_3 \left( \frac{2EI_z}{L} \right) \frac{\Delta_y}{L} \quad (4.50)$$

$$M_{zb} = s_3 \left( \frac{2EI_z}{L} \right) \frac{\Delta_y}{L} + s_2 \left( \frac{4EI_z}{L} \right) \frac{\Delta_y}{L} \quad (4.51)$$

Thus,

$$F_{ya} = \left[ s_2 \left( \frac{8EI_z}{L^3} \right) + s_3 \left( \frac{4EI_z}{L^3} \right) - \frac{P}{L} \right] \Delta_y \quad (4.52)$$

If  $\alpha^2 = \frac{P}{EI_z}$  is taken;

$$F_{ya} = \frac{12EI_z}{L^3} \left\{ \frac{2}{3} s_2 + \frac{1}{3} s_3 - \frac{\alpha^2 L^2}{12} \right\} = s_7 \left( \frac{12EI_z}{L^3} \right) \quad (4.53)$$

where;

$$s_7 = \frac{2}{3} s_2 + \frac{1}{3} s_3 - \frac{\alpha^2 L^2}{12} \quad (4.54)$$

Substituting for  $s_2$  and  $s_3$  from equations (4.35) and (4.36) when axial force is compressive;

$$s_7 = \frac{1}{6} \frac{\alpha^2 L^2 (1 - \cos \alpha L)}{2 - 2 \cos \alpha L - \alpha L \sin \alpha L} - \frac{\alpha^2 L^2}{12} \quad (4.55)$$

When the axial force  $P$  is tensile,  $P$  is replaced by  $-P$  in equation (4.49) and values of  $s_2$  and  $s_3$  are obtained from equations (4.35) and (4.36);

$$s_7 = \frac{1}{6} \frac{\alpha^2 L^2 (\cosh \alpha L - 1)}{2 - 2 \cosh \alpha L + \alpha L \sinh \alpha L} + \frac{\alpha^2 L^2}{12} \quad (4.56)$$



#### 4.2.2.3.2. Translation in X-Z Plane

Proceeding as in the previous section,  $s_8$  can be given;

$$s_8 = \frac{2}{3}s_4 + \frac{1}{3}s_5 \quad (4.57)$$

Substituting the values of  $s_4$  and  $s_5$  from equations (4.38) and (4.40) when the axial force is compressive, and from equations (4.39) and (4.41) when the axial force is tensile, the expressions for  $s_8$  is shown as;

$$s_8 = \frac{1}{6} \frac{\beta^2 L^2 (1 - \cos \beta L)}{2 - 2 \cos \beta L - \beta L \sin \beta L} \quad (4.58)$$

When  $P$  is tensile;

$$s_8 = \frac{1}{6} \frac{\beta^2 L^2 \cosh \beta L - 1}{2 - 2 \cosh \beta L + \beta L \sinh \beta L} \quad (4.59)$$

Proceeding as in the previous section,  $s_9$  can be derived;

$$s_9 = \frac{2}{3}s_4 + \frac{1}{3}s_5 - \frac{\beta^2 L^2}{12} \quad \text{when the axial force } P \text{ is compressive} \quad (4.60)$$

$$s_9 = \frac{2}{3}s_4 + \frac{1}{3}s_5 + \frac{\beta^2 L^2}{12} \quad \text{when the axial force } P \text{ is tensile} \quad (4.61)$$

Substituting the values of  $s_4$  and  $s_5$  from equations (4.38) and (4.40) when the axial force is compressive, and from equations (4.39) and (4.41) when the axial force is tensile, the expressions for  $s_9$  is shown as;

When  $P$  is compressive;

$$s_9 = \frac{1}{6} \frac{\beta^2 L^2 (1 - \cos \beta L)}{2 - 2 \cos \beta L - \beta L \sin \beta L} - \frac{\beta^2 L^2}{12} \quad (4.62)$$

When  $P$  is tensile;

$$s_9 = \frac{1}{6} \frac{\beta^2 L^2 \cosh \beta L - 1}{2 - 2 \cosh \beta L + \beta L \sinh \beta L} + \frac{\beta^2 L^2}{12} \quad (4.63)$$

The nonlinear stiffness matrix of a three dimensional steel structure, including warping effect, using the stability functions  $s_1$  through  $s_9$  is shown below in Figure 4.4.

$$K = \begin{bmatrix} s_1 \frac{EA}{L} & 0 & 0 & 0 & 0 & 0 & 0 & s_1 \frac{-EA}{L} & 0 & 0 & 0 & 0 & 0 & 0 \\ 0 & s_7 \frac{12EI_z}{L^3} & 0 & 0 & 0 & 0 & s_6 \frac{6EI_z}{L^2} & 0 & s_7 \frac{-12EI_z}{L^3} & 0 & 0 & 0 & 0 & s_6 \frac{6EI_z}{L^2} \\ 0 & 0 & s_9 \frac{12EI_y}{L^3} & 0 & 0 & s_8 \frac{-6EI_y}{L^2} & 0 & 0 & 0 & s_9 \frac{-12EI_y}{L^3} & 0 & 0 & s_8 \frac{-6EI_y}{L^2} & 0 \\ 0 & 0 & 0 & -T_1 & -T_2 & 0 & 0 & 0 & 0 & 0 & T_1 & -T_2 & 0 & 0 \\ 0 & 0 & 0 & -T_2 & T_3 & 0 & 0 & 0 & 0 & 0 & T_2 & T_4 & 0 & 0 \\ 0 & 0 & s_8 \frac{-6EI_y}{L^2} & 0 & 0 & s_4 \frac{4EI_y}{L} & 0 & 0 & 0 & s_8 \frac{6EI_y}{L^2} & 0 & 0 & s_5 \frac{2EI_y}{L} & 0 \\ 0 & s_6 \frac{6EI_z}{L^2} & 0 & 0 & 0 & 0 & s_2 \frac{4EI_z}{L} & 0 & s_6 \frac{-6EI_z}{L^2} & 0 & 0 & 0 & 0 & s_3 \frac{2EI_z}{L} \\ s_1 \frac{-EA}{L} & 0 & 0 & 0 & 0 & 0 & 0 & s_1 \frac{EA}{L} & 0 & 0 & 0 & 0 & 0 & 0 \\ 0 & s_7 \frac{-12EI_z}{L^3} & 0 & 0 & 0 & 0 & s_6 \frac{-6EI_z}{L^2} & 0 & s_7 \frac{12EI_z}{L^3} & 0 & 0 & 0 & 0 & s_6 \frac{-6EI_z}{L^2} \\ 0 & 0 & s_9 \frac{-12EI_y}{L^3} & 0 & 0 & s_8 \frac{6EI_y}{L^2} & 0 & 0 & 0 & s_9 \frac{12EI_y}{L^3} & 0 & 0 & s_8 \frac{6EI_y}{L^2} & 0 \\ 0 & 0 & 0 & T_1 & T_2 & 0 & 0 & 0 & 0 & 0 & -T_1 & T_2 & 0 & 0 \\ 0 & 0 & 0 & -T_2 & T_4 & 0 & 0 & 0 & 0 & 0 & T_2 & T_3 & 0 & 0 \\ 0 & 0 & s_8 \frac{-6EI_y}{L^2} & 0 & 0 & s_5 \frac{2EI_y}{L} & 0 & 0 & 0 & s_8 \frac{6EI_y}{L^2} & 0 & 0 & s_4 \frac{4EI_y}{L} & 0 \\ 0 & s_6 \frac{6EI_z}{L^2} & 0 & 0 & 0 & 0 & s_3 \frac{2EI_z}{L} & 0 & s_6 \frac{-6EI_z}{L^2} & 0 & 0 & 0 & 0 & s_2 \frac{4EI_z}{L} \end{bmatrix}$$

**Figure 4.4.** Nonlinear stiffness matrix of a three-dimensional steel element.

### 4.3. Analysis of 3-D Frames Including Geometric Nonlinearity

The nonlinear response of a structure is obtained through successive linear elastic analysis as shown in the flow chart of Figure 4.5. Initially the axial forces are presumed to be zero. With zero values of axial forces, stability functions become equal to 1. Linear elastic analysis of the structure is carried out and axial forces in members are determined. With these values of axial forces the stability functions are calculated and structural analysis is repeated. This process is continued until the convergence is obtained in the axial force values of members. The joint displacements and member forces obtained at this final iteration yields the accurate response of the structure to external loads where the geometric nonlinearity of its members in local coordinate system is taken into account.

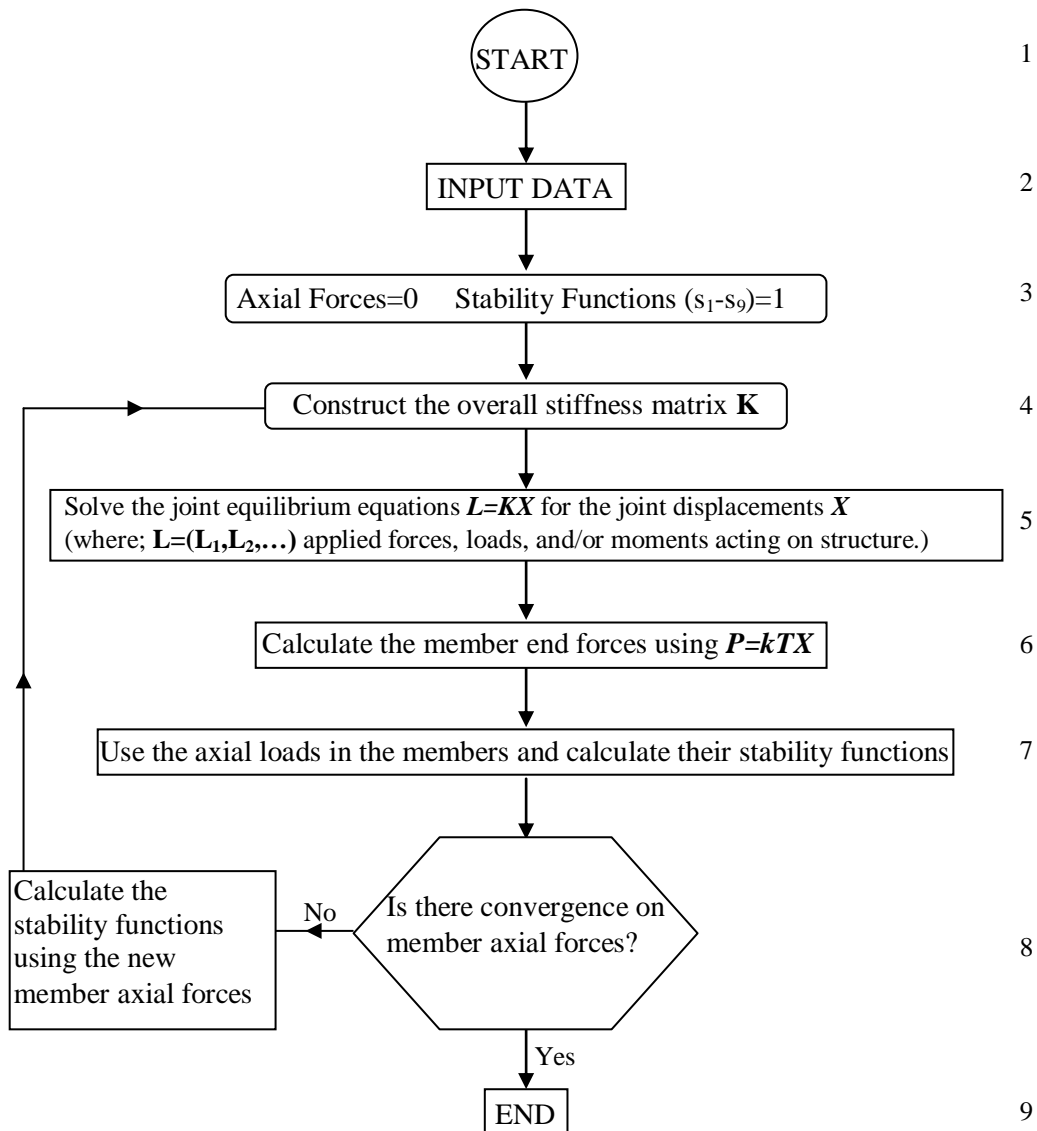


**Figure 4.5.** Nonlinear response of a structure obtained through successive elastic linear analysis.

## 4.4. Numerical Examples

### 4.4.1. Example 1

8-member, 4m x 4m one bay, three dimensional steel frame consisting of W150x13.5 cross-section for all frame members is chosen as a first numerical example to demonstrate the effect of geometric nonlinearity. The loading and geometric properties of the frame are shown in Figure 4.6. Consideration of geometric nonlinearity in the response of cold-formed steel structures is a necessity if realistic results are desired to be obtained in their design. The commercial structural analysis program SAP2000 v14 [111] which has the facility of carrying out P-Delta analysis has been used to check the results those obtained with proposed algorithm in this study. It is apparent from Table 4.1 that the joint displacements calculated by carrying out nonlinear analysis in this work are almost same as the ones obtained by SAP2000 v14.

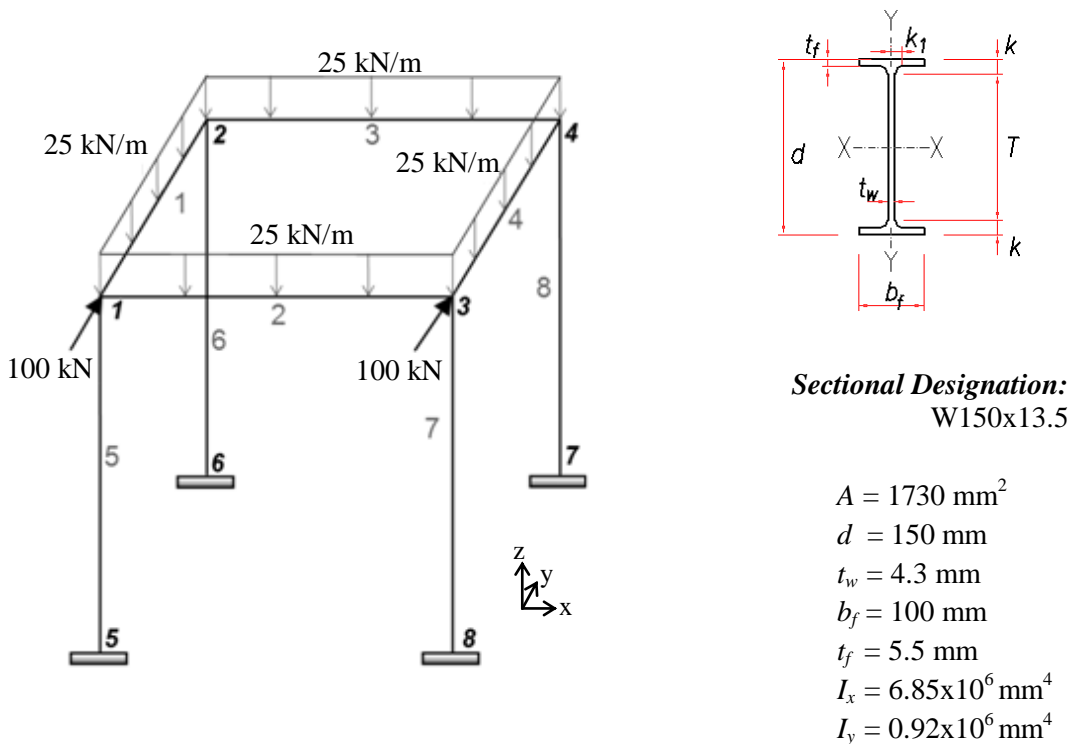


**Figure 4.6.** 8-member three dimensional steel frame.

**Table 4.1.** Joint displacements obtained by the nonlinear analysis using SAP2000 v14 and nonlinear analysis by the routine developed in this study for 8-members three dimensional steel frame.

Joint Displacements						
# of joint	Joint displacements obtained by carrying out the nonlinear analysis explained in this study			Joint displacements obtained by carrying out the nonlinear analysis using SAP2000 v14		
	X-DISP (m)	Y-DISP (m)	Z-DISP (m)	X-DISP (m)	Y-DISP (m)	Z-DISP (m)
1	0.14392E-04	0.32517E+00	-0.58206E-03	0.1459E-04	0.3320E+00	-0.600E-03
2	0.13080E-04	0.32476E+00	-0.16912E-02	0.1322E-04	0.3314E+00	-0.170E-02
3	0.14392E-04	0.32517E+00	-0.58206E-03	0.1459E-04	0.3320E+00	-0.600E-03
4	0.13080E-04	0.32476E+00	-0.16912E-02	0.1322E-04	0.3314E+00	-0.170E-02

#### 4.4.2. Example 2

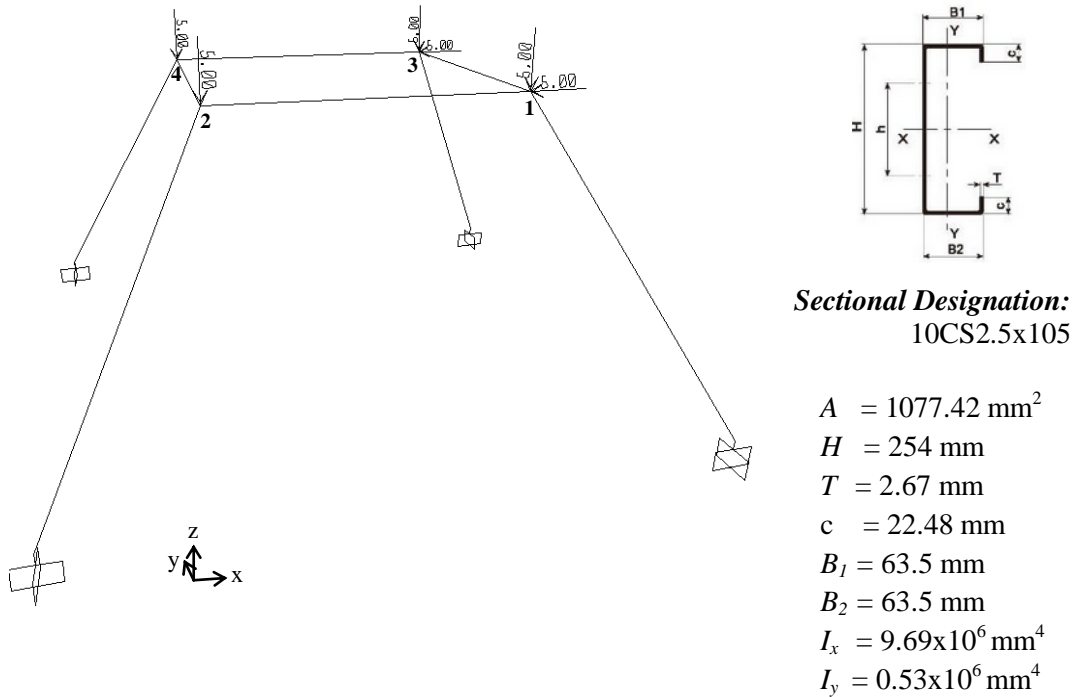


**Figure 4.7.** 8-member, 3D steel frame with crosswise columns.

In order to reflect the effect of geometric nonlinearity in a clearer manner, a 3D steel frame with crosswise columns is selected as a second numerical example. This frame has 5 kN concentrated loading on each joint and 5 kN horizontal loads on two joints as shown in Figure 4.7. The cold-formed 10CS2.5x105 cross-section, which is taken from AISI Design Manual 2007 Excerpts-Gross Section Property Tables [112], is assigned to all frame members. The frame has 4m x 4m top area and 8m x 8m basement area. Similar to first example, the joint displacements calculated by carrying out nonlinear analysis in this work are almost same as the ones obtained by SAP2000 v14 [111] as tabulated in Table 4.2.

**Table 4.2.** Joint displacements obtained by the nonlinear analysis using SAP2000 v14 and nonlinear analysis by the routine developed in this study for 8-member, 3D steel frame with crosswise columns.

Joint Displacements						
Joint displacements obtained by carrying out the nonlinear analysis proposed in this study				Joint displacements obtained by carrying out the nonlinear analysis using SAP2000 v14		
# of joint	X-DISP (m)	Y-DISP (m)	Z-DISP (m)	X-DISP (m)	Y-DISP (m)	Z-DISP (m)
1	-0.12323E-01	0.24354E-05	-0.62881E-02	-0.1240E-01	0.2439E-05	-0.630E-02
2	-0.12234E-01	0.41895E-04	0.58946E-02	-0.1230E-01	0.4180E-04	0.590E-02
3	-0.12323E-01	-0.24354E-05	-0.62881E-02	-0.1240E-01	-0.2439E-05	-0.630E-02
4	-0.12234E-01	-0.41895E-04	0.58946E-02	-0.1230E-01	-0.4180E-04	0.590E-02





## CHAPTER 5

### OPTIMUM DESIGN OF COLD-FORMED THIN-WALLED OPEN SECTIONS

#### 5.1. Definitions

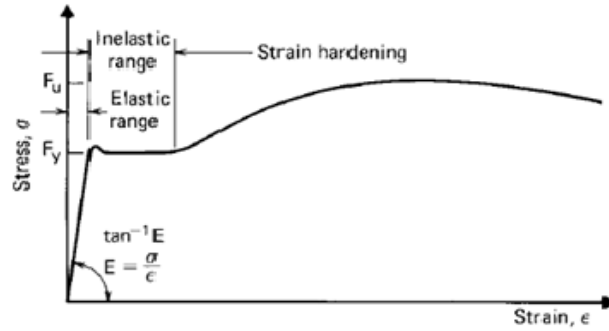
Cold-formed steel products are just what the name connotes; products that are made by bending a flat sheet of steel at room temperature into a shape that will support more load than the flat sheet itself.

It is a fact that material properties play an important role in the performance of structural members. Designers should be familiar with the mechanical properties of the steel sheets, strip, plates, or flat bars generally used in cold-formed steel construction in designing this type of steel structural members. Besides, since mechanical properties are greatly affected by temperature, special attention must be given by the designer for extreme conditions that is temperature below  $-34^{\circ}\text{C}$  and above  $93^{\circ}\text{C}$ . Sixteen steels are specified in the current edition of the North American Specification [113] for structural applications. These steels are identified in ASTM standards for sheet material as SS or, in the case of high-strength, low-alloy steels, as HSLAS or HSLAS-F steels [2, 117].

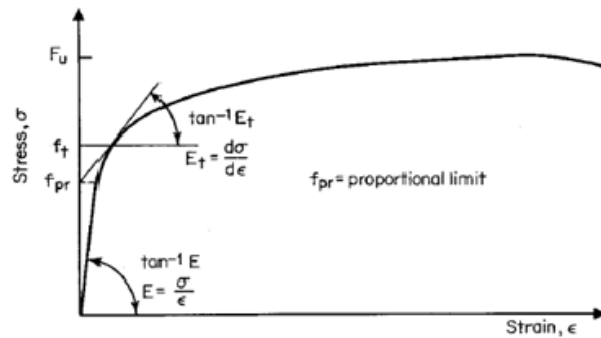
##### 5.1.1. Yield Point, Tensile Strength, and Stress-Strain

The strength of cold-formed steel structural members depends on the yield point or yield strength, except in connections and in those cases where elastic local buckling or overall buckling is critical.

There are two general types of stress–strain curves, as shown in Figure 5.1. One is of the sharp-yielding type (Figure 5.1. (a)) and the other is of the gradual-yielding type (Figure 5.1. (b)). Steels produced by hot rolling are usually sharp-yielding. For this type of steel, the yield point is defined by the level at which the stress–strain curve becomes horizontal. Steels that are cold-formed or cold-worked show gradual-yielding. For gradual-yielding steel, the stress–strain curve is rounded out at the “knee” and the yield strength is determined by either the offset method or the strain-under-load method.



(a)



(b)

**Figure 5.1.** Stress–strain curves of carbon steel sheet or strip (a) Sharp-yielding; (b) Gradual-yielding.

## 5.1.2. Modulus of Elasticity, Tangent Modulus, and Shear Modulus

### 5.1.2.1. Modulus of Elasticity, $E$

The strength of members that fail by buckling depends not only on the yield point but also on the modulus of elasticity  $E$  and the tangent modulus  $E_t$ . The modulus of elasticity is defined by the slope of the initial straight portion of the stress–strain curve. The values of  $E$  on the basis of the standard methods usually range from 200 to 208 GPa. A value of 203 GPa is recommended by AISI (American Iron and Steel Institute) in its specification for design purposes [113]. This value is slightly higher than 200 GPa currently used in the AISC (American Institute of Steel Construction) specification [114].

### 5.1.2.2. Tangent Modulus, $E_t$

The tangent modulus is defined by the slope of the stress–strain curve at any point, as shown in Figure 5.1.(b). For sharp yielding,  $E_t=E$  up to the yield point, but with gradual yielding,  $E_t=E$  only up to the proportional limit. Once the stress exceeds the proportional limit, the tangent modulus  $E_t$  becomes progressively smaller than the initial modulus of elasticity. For this reason, for moderate slenderness the sharp-yielding steels have larger buckling strengths than gradual-yielding steels. Various buckling provisions of the AISI specification [113] have been written for gradual-yielding steels whose proportional limit is usually not lower than about 70% of the specified minimum yield point.

### 5.1.2.3. Shear Modulus, $G$

By definition, shear modulus,  $G$ , is the ratio between the shear stress and the shear strain. It is the slope of the straight line portion of the shear stress–strain curve. Based on the theory of elasticity, the shear modulus can be computed by the following equation,

$$G = \frac{E}{2*(1 + \mu)} \quad (5.1)$$

where  $E$  is the tensile modulus of elasticity and  $\mu$  is the Poisson's ratio. By using  $E=203$  GPa and  $\mu=0.3$  for steel in the elastic range, the value of shear modulus,  $G$ , is taken as 78 GPa in the AISI Specification. This  $G$  value is used for computing the torsional buckling stress for the design of beams, columns, and wall studs.

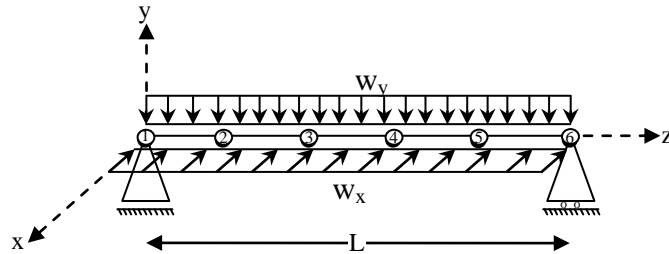
## 5.2. Optimum Design of Cold-Formed Thin-Walled Beams with Open Steel Sections

The calculations of geometrical properties of a thin-walled beam with a complex cross-section are tiresome and tough as described comprehensively in Chapter 3.3.2. The proposed algorithm in this study supplies a facility for an automatic evaluation of open cross-sectional properties of thin-walled beams. The geometrical data which need to be entered to perform the analysis have been brought to the minimum; i.e. the coordinates of joints, the elements connecting them and their thickness [115]. So, the determination of the torsional and flexural properties of thin-walled beams with arbitrary open cross-sections is easily reified.

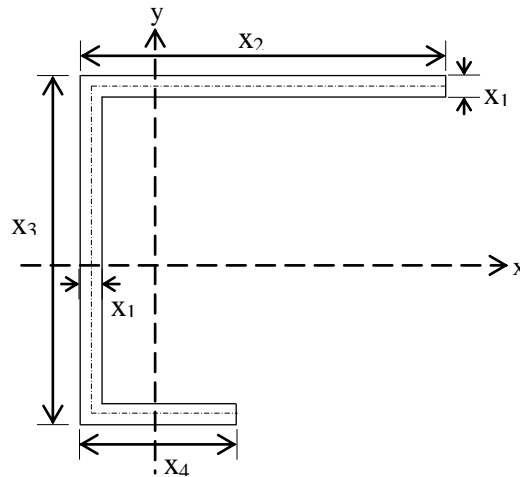
The optimum design problem of a cold-formed thin-walled open cross-section shown in Figure 5.2. can be formulated as given in the following. Consider that this section is used in a simply supported beam which is laterally supported and is subjected to general loading. The design variables can be selected as the cross-sectional dimensions of the section as shown in Figure 5.2. If the objective function is taken as the weight of the beam to be minimized then;

$$W = [x_1 * (x_2 + x_3 + x_4)] * l * \rho \quad (5.2)$$

where,  $l$  is the span of the beam and  $\rho$  is the density of steel.



a) Simply supported thin-walled steel beam.



b) Thin-walled cross-section.

**Figure 5.2.** Thin-walled steel beam with unsymmetrical channel shape.

Consider the simply supported beam shown in Figure 5.2. (a) subjected to general loading. Assume that the beam is made of thin-walled open section shown in Figure 5.2. (b). The optimum design problem of the simply supported beam considered necessities selection of the dimensions of thin plates used in the upper and lower flanges as well as web of the thin-walled section shown in Figure 5.2. (b) such that maximum displacement and stress occur in the beam under the general loading are less than their upper bounds and the weight of the beam is minimum. The mathematical model of this problem can be expressed as

$$\text{Min } W = f(x_i), \quad i = 1, \dots, n \quad (5.3)$$

Subjected to;

$$g_j(x_i) = \frac{\delta_j}{\delta_{ju}} - 1 \leq 0, \quad j = 1, \dots, p \quad (5.4)$$

$$g_s(x_i) = \frac{\sigma_s^{\max}}{\sigma_y} - 1 \leq 0, \quad s = 1, \dots, r \quad (5.5)$$

$$g_k(x_i) = \frac{x_k}{x_1} - u_k \leq 0, \quad k = 1, \dots, m \quad (5.6)$$

$$x_{li} \leq x_i \leq x_{ui} \quad (5.7)$$

where  $f(x_i)$  represents the weight of the beam which is taken as objective function.  $x_i$  is the  $i^{\text{th}}$  design variable.  $x_{li}$  and  $x_{ui}$  are the lower and upper bounds imposed on the design variable  $i$ .  $n$  is the total number of variables.  $g_j(x_i)$  is the displacement constraint. The simply supported beam modeled as three dimensional structure as shown in Figure 5.2. (a) in order to be able to consider general loading conditions that may act along any axis. Beam is subdivided into number of elements and joint displacements are computed using matrix displacement analysis which takes into account the effect of warping.  $\delta_j$  is the displacement of joint  $j$  which is required to be restricted and  $\delta_{ju}$  is its upper bound.  $p$  is the total number of restricted displacements in the design problem.  $g_s(x_i)$  represents normal stress constraints.  $\sigma_s^{\max}$  is the maximum normal stress occurs in the beam. This stress is obtained by calculating the normal stresses for each element using Equations (3.62) and (3.63) and selecting the largest one.  $\sigma_y$  is the yield stress of the steel.  $r$  is the total number of elements considered along the beam.  $g_k(x_i)$  is the local buckling constraints that is to be imposed on the web of the thin-walled section to prevent web buckling. Among the design variables  $x_1$  represents the thickness of the steel plate out of which thin-walled section is formed. Steel plates are produced within a certain thickness in practice. Hence in the optimum design, the algorithm should select appropriate values from a discrete set. Similar tables can be presented for the flange, width and web depths which consist of list of practically preferable values. Therefore the optimum design problem turns out to be a discrete programming problem. The design algorithm is expected to select appropriate values for the design variables such that the design constraints are satisfied and the weight of the beam is minimum. This is a combinatorial

optimum design problem and recent meta-heuristic techniques are shown to be quite effective in finding the solution of such problems [116].

### 5.3. Optimum Design of Steel Frames of Cold-Formed Thin-Walled Open Sections to AISI-LRFD

The members of steel frames made of cold-formed thin-walled open sections are subjected bending moments in addition to axial forces. Structural members are subject to combined compressive axial load and bending, this type of member is usually referred to as a beam-column [117]. In the case of individual member made of cold-formed thin-walled steel section the bending may result from eccentric loading as shown in Figure 5.3. (a), transverse loads as shown in Figure 5.3 (b), or applied moments as shown in Figure 5.3. (c). Such members are often found in framed structures, trusses, and exterior wall studs. In steel structures, beams are usually supported by columns through framing angles or brackets on the sides of the columns. The reactions of beams can be considered as eccentric loading, which produces bending moments. The structural behavior of beam-columns depends on the shape and dimensions of the cross section, the location of the applied eccentric load, the column length, and the condition of bracing, and so on.

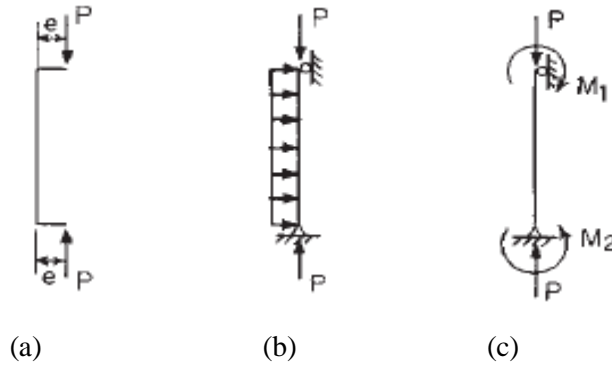


**Figure 5.3.** Beam-columns; (a) subject to eccentric loads, (b) subject to axial and transverse loads, (c) subject to axial loads and end moments.

#### 5.3.1. Discrete Optimum Design Process

The optimum design problem of steel frames made of cold-formed thin-walled open sections necessitates consideration of satisfaction of the design limitations defined by the provisions of AISI-LRFD [113]. In this study, it is assumed that cold-formed steel beam-column members will be made of standard C-sections with lips. The optimum design problem of such frames requires selection of appropriate C-sections from the available list of steel C-sections for its members. This selection should be carried out in such way that the beam-column members of the frame should satisfy the serviceability and strength

requirements specified by the code of practice while the economy is observed in the overall or material cost of the beam-column. When the design constraints are implemented from AISI-LRFD [113] the following discrete programming problem is obtained.

### 5.3.1.1. Objective Function

The objective function is taken as the minimum weight of the steel structure which is expressed as in the following.

$$\min W = \sum_{i=1}^{ng} m_i \sum_{j=1}^{s_i} l_j \quad (5.8)$$

where  $m_i$  in Equation (5.8) gives the unit weight of the C-section with lip selected from AISI Design Manual 2007 Excerpts-Gross Section Property Tables [112] for the beam-column members belonging to group  $i$ ,  $s_i$  is the total number of members in group  $i$ , and  $ng$  is the total number of groups.  $l_j$  is the length of the beam-column member  $j$ .

### 5.3.1.2. Strength Constraints

The following are the design provisions adapted from Section C5.2 of the 2007 edition of the North American (AISI) specification for the strength capacity of beam-columns [113].

#### 5.3.1.2.1. Effective Slenderness Ratio

The maximum allowable slenderness ratio of compression members has been preferably limited to 200.

$$\frac{K_x * L_x}{r_x} \text{ or } \frac{K_y * L_y}{r_y} < 200 \quad (5.9)$$

where,

$K_x$  = effective length factor for buckling about  $x$  axis

$L_x$  = unbraced length for bending about  $x$  axis

$K_y$  = effective length factor for buckling about  $y$  axis

$L_y$  = unbraced length for bending about  $y$  axis

$r_x, r_y$  = radius of gyration of cross section about  $x$  and  $y$  axes

The governed slenderness ratio is selected as the maximum of those about x and y axis as mentioned in Equation (5.9).

### 5.3.1.2.2. Computation of Nominal Axial Strength, $P_n$

#### 5.3.1.2.2.1. Nominal Buckling Stress, $F_n$

##### 5.3.1.2.2.1.1. Elastic Flexural Buckling Stress

The elastic flexural buckling stress  $F_e$ , was calculated as follows:

$$F_e = \frac{\pi^2 E}{(KL/r)^2} \quad (5.10)$$

where,

$E$  = modulus of elasticity of steel

$K$  = effective length factor

$L$  = laterally unbraced length of member

$r$  = radius of gyration of full, unreduced cross section about axis of buckling

##### 5.3.1.2.2.1.2. Elastic Flexural-Torsional Buckling Stress

For single symmetric sections subject to flexural-torsional buckling,  $F_e$  is taken as

$$F_e = \frac{1}{2\beta} \left[ (\sigma_{ex} + \sigma_t) - \sqrt{(\sigma_{ex} + \sigma_t)^2 - 4\beta\sigma_{ex}\sigma_t} \right] \quad (5.11)$$

where,

$$\beta = 1 - \frac{x_0}{r_0} \quad (5.12)$$

here,  $x_0$  and  $r_0$  are directly calculated by the equations given in Part I of the AISI Design Manual [113].

$$\sigma_{ex} = \frac{\pi^2 E}{(K_x L_x / r_x)^2} \quad (5.13)$$



here,  $\sigma_{ex}$  is the effective slenderness ratio about  $x$  axis as described in Equation (5.13).

$$\sigma_t = \frac{1}{Ar_0^2} \left[ GJ + \frac{\pi^2 EC_w}{(K_t L_t)^2} \right] \quad (5.14)$$

here,  $G$  is shear modulus,  $J$  is Saint-Venant torsion constant of cross-section,  $C_w$  is torsional warping constant of cross-section,  $K_t$  is effective length factors for twisting,  $L_t$  is unbraced length of member for twisting.

$F_e$ , is taken as the smaller of those calculated in Equations (5.10) and (5.11).

Afterwards the nominal buckling stress is calculated as follows,

For  $\lambda_c \leq 1.5$ ;

$$F_n = 0.658^{\lambda_c^2} F_y \quad (5.15)$$

For  $\lambda_c > 1.5$ ;

$$F_n = \left( \frac{0.877}{\lambda_c^2} \right) F_y \quad (5.16)$$

where,

$$\lambda_c = \sqrt{\frac{F_y}{F_e}} \quad (5.17)$$

here,  $F_y$  is the yield stress and  $F_e$  is the least of the applicable elastic flexural and elastic flexural-torsional buckling stress determined by Equations (5.10) and/or (5.11).

#### 5.3.1.2.2.2. Nominal Load, $P_n$ , Based On Flexural Buckling

The nominal axial strength [compressive resistance],  $P_n$ , is calculated in accordance with Equation (5.18).

$$P_n = A_e F_n \quad (5.18)$$

where,  $A_e$  is the effective area calculated at stress  $F_n$ . Effective area  $A_e$  can be computed according to Section B4 of the 2007 edition of the North American Specification [113].

### 5.3.1.2.2.3. Nominal Load, $P_n$ , Based On Distortional Buckling

The nominal load  $P_n$  for distortional buckling can be computed according to Section C4.2(b) of the AISI [113].

For  $\lambda_d \leq 0.561$

$$P_n = P_y \quad (5.19)$$

For  $\lambda_d > 0.561$

$$P_n = \left( 1 - 0.25 \left( \frac{P_{crd}}{P_y} \right)^{0.6} \right) \left( \frac{P_{crd}}{P_y} \right)^{0.6} P_y \quad (5.20)$$

where,

$$\lambda_d = \sqrt{P_y / P_{crd}}$$

$P_n$  = Nominal axial strength

$P_y = A_g F_y$  (where,  $A_g$  is the gross area of the cross-section and  $F_y$  is the yield stress)

$P_{crd} = A_g F_d$  (where,  $F_d$  is the elastic distortional buckling stress calculated according to Section C4.2(a), (b) or (c) of the AISI [113])

$P_n$ , is taken as the smaller of those calculated in Equations (5.18) and (5.19 or 5.20).

### 5.3.1.2.3. Computation of Allowable Strength, $M_n$

#### 5.3.1.2.3.1. Nominal Section Strength, $M_n$

The nominal section strength for initiation of yielding is calculated by using Equation (5.21):

$$M_n = S_e F_y \quad (5.21)$$

where,

$F_y$  = design yield stress.

$S_e$  = elastic section modulus of effective section calculated with extreme compression or tension fiber at  $F_y$ .

### 5.3.1.2.3.2. Distortional Buckling Strength, $M_n$

The nominal load  $P_n$  for distortional buckling can be computed according to Section C4.2(b) of the AISI [113].

For  $\lambda_d \leq 0.673$

$$M_n = M_y \quad (5.22)$$

For  $\lambda_d > 0.673$

$$M_n = \left( 1 - 0.22 \left( \frac{M_{crd}}{M_y} \right)^{0.5} \right) \left( \frac{M_{crd}}{M_y} \right)^{0.5} M_y \quad (5.23)$$

where,

$$\lambda_d = \sqrt{M_y / M_{crd}}$$

$M_y = S_{fy} F_y$  (where,  $S_{fy}$  is the elastic section modulus of full unreduced section relative to extreme fiber in first yield)

$M_{crd} = S_f F_d$  (where,  $S_f$  is the elastic section modulus of full unreduced section relative to extreme compression fiber and  $F_d$  is the elastic distortional buckling stress calculated according to Section C4.2(a), (b) or (c) of the AISI [113])

$M_n$ , is taken as the smaller of those calculated in Equations (5.21) and (5.22 or 5.23).

### 5.3.1.2.4. Checking Combined Tension Axial Load and Bending

For axially loaded tension members, the nominal tensile strength,  $T_n$ , is the value obtained in accordance with the Equation (5.24).

$$T_n = A_g F_y \quad (5.24)$$

where,

$T_n$  = nominal tensile strength

$A_g$  = gross area of the cross-section

$F_y$  = design yield stress

When cold-formed steel members are subject to concurrent bending and tensile axial load, the member shall satisfy the interaction equations given below which are prescribed in Section C5.1 of the North American Specification for the LRFD methods [113].

The required strengths (factored tension and moments)  $T$ ,  $M_x$ , and  $M_y$  shall satisfy the following interaction equations:

$$\frac{M_{ux}}{\phi_b M_{nxt}} + \frac{M_{uy}}{\phi_b M_{nyt}} + \frac{T_u}{\phi_t T_n} \leq 1.0 \quad (5.25)$$

$$\frac{M_{ux}}{\phi_b M_{nx}} + \frac{M_{uy}}{\phi_b M_{ny}} - \frac{T_u}{\phi_t T_n} \leq 1.0$$

where,

$M_{ux}$ ,  $M_{uy}$  = the required flexural strengths [factored moments] with respect to centroidal axes.

$\phi_b$  = for flexural strength [moment resistance] equals 0.90 or 0.95 (LRFD).

$M_{nxt}, M_{nyt}$  =  $S_{ft} F_y$  (where,  $S_{ft}$  is the section modulus of full unreduced section relative to extreme tension fiber about appropriate axis and  $F_y$  is the design yield stress).

$T_u$  = required tensile axial strength [factored tension].

$\phi_t$  = 0.95 (LRFD).

$T_n$  = nominal tensile axial strength [resistance].

$M_{nx}, M_{ny}$  = nominal flexural strengths [moment resistances] about centroidal axes.

### 5.3.1.2.5. Checking Combined Compressive Axial Load and Bending (Beam-Columns)

The following are the design provisions adapted from Section C5.2 of the 2007 edition of the North American specification [113] for the design of beam-columns.

For  $\frac{P_u}{\phi_c P_n} > 0.15$ ,

$$\frac{P_u}{\phi_c P_n} + \frac{C_{mx} M_{ux}}{\phi_b M_{nx} \alpha_x} + \frac{C_{my} M_{uy}}{\phi_b M_{ny} \alpha_y} \leq 1.0 \quad (5.26)$$

$$\frac{P_u}{\phi_c P_{no}} + \frac{M_{ux}}{\phi_b M_{nx}} + \frac{M_{uy}}{\phi_b M_{ny}} \leq 1.0$$

For  $\frac{P_u}{\phi_c P_n} \leq 0.15$ ,

$$\frac{P_u}{\phi_c P_n} + \frac{M_{ux}}{\phi_b M_{nx}} + \frac{M_{uy}}{\phi_b M_{ny}} \leq 1.0 \quad (5.27)$$

where,

$P_u$  = required compressive axial strength [factored compressive force].

$\phi_c = 0.85$  (LRFD).

$M_{ux}$ ,  $M_{uy}$  = the required flexural strengths [factored moments] with respect to centroidal axes of effective section.

$\phi_b$  = for flexural strength [moment resistance] equals 0.90 or 0.95 (LRFD).

$M_{nx}$ ,  $M_{ny}$  = the nominal flexural strengths [moment resistances] about centroidal axes.

and

$$\alpha_x = 1 - \frac{P_u}{P_{E_x}} > 0.0 \quad (5.28)$$

$$\alpha_y = 1 - \frac{P_u}{P_{E_y}} > 0.0$$

where,

$$P_{E_x} = \frac{\pi^2 EI_x}{(K_x L_x)^2} \quad (5.29)$$

$$P_{E_y} = \frac{\pi^2 EI_y}{(K_y L_y)^2}$$

where,

$I_x$  = moment of inertia of full unreduced cross section about  $x$  axis.

$K_x$  = effective length factor for buckling about  $x$  axis.

$L_x$  = unbraced length for bending about  $x$  axis.

$I_y$  = moment of inertia of full unreduced cross section about  $y$  axis.

$K_y$  = effective length factor for buckling about  $y$  axis.

$L_y$  = unbraced length for bending about  $y$  axis.

$P_{no}$  = nominal axial strength [resistance] determined in accordance with Section C4 of AISI [113], with  $F_n = F_y$ .

$C_{mx}, C_{my}$  = coefficients taken as 0.85 or 1.0.

### 5.3.1.3. Deflection and Drift Constraints

The deflection, top-storey drift and inter-storey drift constraints functions are given in the following Equations (5.30), (5.31) and (5.32), respectively [118].

$$g_d(x) = \frac{\delta_{jl}}{L / Ratio} - 1.0 \leq 0 \quad j = 1, 2, \dots, n_{sm} \quad l = 1, 2, \dots, n_{lc} \quad (5.30)$$

$$g_{td} = \frac{\Delta_{jl}^{top}}{H / Ratio} - 1.0 \leq 0 \quad j = 1, 2, \dots, n_{jtop} \quad l = 1, 2, \dots, n_{lc} \quad (5.31)$$

$$g_{id} = \frac{\Delta_{jl}^{oh}}{h_{sx} / Ratio} - 1.0 \leq 0 \quad j = 1, 2, \dots, n_{st} \quad l = 1, 2, \dots, n_{lc} \quad (5.32)$$

where,  $\delta_{jl}$  is the maximum deflection of  $j^{th}$  member under the  $l^{th}$  load case,  $L$  is the length of member,  $n_{sm}$  is the total number of members where deflections limitations are to be imposed,  $n_{lc}$  is the number of load cases,  $H$  is the height of the frame,  $n_{top}$  is the number of joints on the top storey,  $\Delta_{jl}^{top}$  is the top storey displacement of the  $j^{th}$  joint under  $l^{th}$  load case,  $n_{st}$  is the number of storey,  $n_{lc}$  is the number of load cases and  $\Delta_{jl}^{oh}$  is the storey drift of the  $j^{th}$  storey under  $l^{th}$  load case,  $h_{sx}$  is the storey height and  $Ratio$  is limitation ratio for lateral displacements described in ASCE Ad Hoc Committee report [120] .

### 5.3.1.4. Serviceability Constraints

The accepted range of drift limits by first-order analysis is  $1/750$  to  $1/250$  times the building height  $H$  with a recommended value of  $H/400$  [120]. The typical limits on the inter-storey drift are  $1/500$  to  $1/200$  times the storey height. The deflection limits recommended for general use which is repeated in Table 5.1.

**Table 5.1.** Displacement limitations for steel frames.

Item	Deflection Limit
Floor girder deflection for service live load	$L/360$
Roof girder deflection	$L/240$
Lateral drift for service wind load	$H/400$
Inter storey drift for service wind load	$H/300$

### 5.3.1.5. Geometric Constraints

Geometric limitations as shown in Figure 5.4. are included in the design problem as in the Equations (5.33) and (5.34); where  $n_{ccj}$  is the number of column-to-column geometric constraints defined in the problem,  $m_i^a$  is the unit weight of  $C$ -section selected for above storey,  $m_i^b$  is the unit weight of  $C$ -section selected for below storey,  $D_i^a$  is the depth of  $C$ -section selected for above storey,  $D_i^b$  is the depth of  $C$ -section selected for below storey,  $n_{ji}$  is the number of joints where beams are connected to the web of a column,  $n_{j2}$  is the number of joints where beams connected to the flange of a column,  $D^{ci}$  is the depth of  $C$ -section selected for the column at joint  $i$ ,  $t_b^{ci}$  is the flange thickness of  $C$ -section selected for the column at joint  $i$ ,  $B_f^{ci}$  is the flange width of  $C$ -section selected for the column at joint  $i$  and  $B_f^{bi}$  is the flange width of  $C$ -section selected for the beam at joint  $i$ .

$$g_{cc} \quad x = \sum_{i=1}^{n_{ccj}} \left( \frac{D_i^a}{D_i^b} - 1.0 \right) + \sum_{i=1}^{n_{ccj}} \left( \frac{m_i^a}{m_i^b} - 1.0 \right) \leq 0 \quad (5.33)$$

$$g_{bc} \quad x = \sum_{i=1}^{n_{js}} \left( \frac{B_i^{bi}}{D^{ci} - 2t_b^{ci}} - 1.0 \right) \leq 0 \quad \text{or} \quad \sum_{i=1}^{n_{j2}} \left( \frac{B_f^{bi}}{B_f^{ci}} - 1.0 \right) \leq 0 \quad (5.34)$$

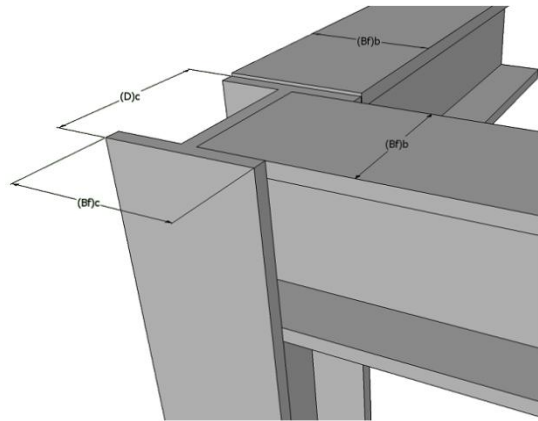


**Figure 5.4.** Geometric constraints for a typical beam-column.



## CHAPTER 6

### ARTIFICIAL BEE COLONY OPTIMIZATION

#### 6.1. Introduction

In the artificial bee colony algorithm, all bees are categorized in three main groups. These are employed bees, onlooker bees and scout bees. The first group of bees is the *employed bees* that locate food source, evaluate its amount of nectar and keep the location of better sources in their memory. These bees when fly back to hive they share this information to other bees in the dancing area by dancing. The dancing time represents the amount of nectar in the food source. The second group is the *onlooker bees* who observe the dance and may decide to fly to the food source if they find it is worthwhile to visit the food source. Therefore, foods sources reach in the amount of nectar attract more onlooker bees (Figure 6.1. (courtesy of researchgate.net)).

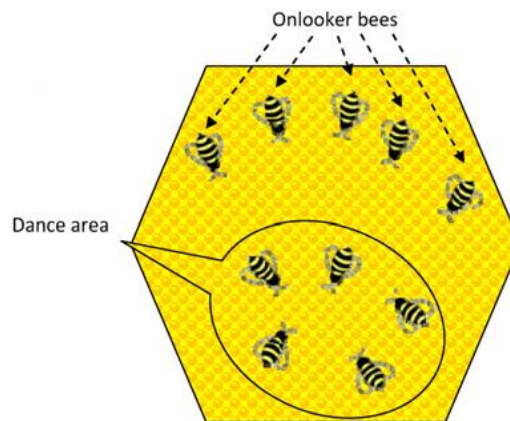


**Figure 6.1.** Sharing the fitness of solutions between employed bees and onlooker bees.

The third group is *scout bees* that explore new food sources in the vicinity of the hive randomly. The employed bee whose food source has been abandoned by the bees becomes a scout bee. A typical bee colony model is shown in Figure 6.2. (courtesy of researchgate.net). Each employed bee in the colony goes to one food source and this food source is selected only by one employed bee. Therefore, number of employed bees in the artificial bee colony algorithm is equal to number of food sources. By the time the food source is exhausted, onlooker and employed bees of this food source are replaced by scout bees. Then, these bees start finding new food sources by making random search. For structural design problems, all available designs are represented as food sources which are used by bee swarms in the artificial bee colony algorithm. Amount of each food source represents weight of structure [118].

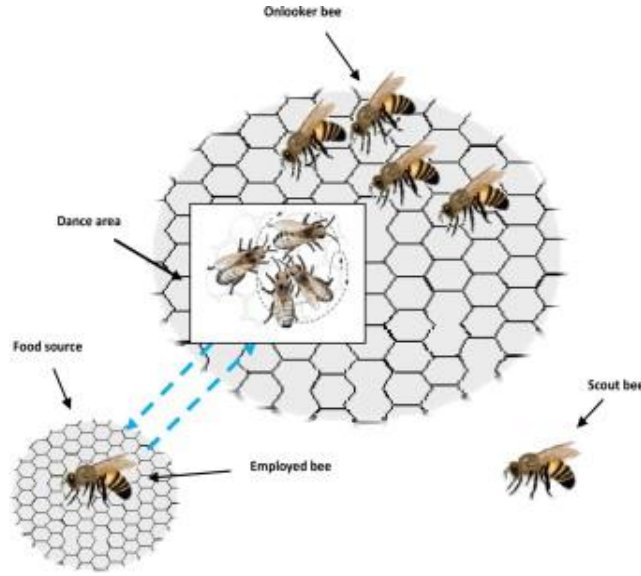


**Figure 6.2.** A Bee Colony Model.

## 6.2. Mathematical Formulation of Structural Optimization Problem

The design of steel structures requires the selection of members from a standard steel pipe section table such that the structure satisfies the strength and serviceability requirements specified by a chosen code of practice, while the economy is observed in the overall or material cost of the structure. For a steel structure which consists of  $N_m$  members grouped into  $N_d$  design variables, this problem can be formulated as follows [119].

### 6.2.1. Objective Function

Find a vector of integer values  $\mathbf{I}$  (Equation 6.1) representing the sequence numbers of standard sections in a given section table

$$\mathbf{I}^T = [I_1, I_2, \dots, I_{N_d}] \quad (6.1)$$

to generate a vector of cross-sectional areas  $\mathbf{A}$  for  $N_m$  members of the truss

$$\mathbf{A}^T = [A_1, A_2, \dots, A_{N_m}] \quad (6.2)$$

such that  $\mathbf{A}$  minimizes the objective function

$$W = \sum_{m=1}^{N_m} \rho_m L_m A_m \quad (6.3)$$

where  $W$  refers to the weight of the frame or a steel section;  $\rho_m, A_m, L_m$  are cross-sectional area, length and unit weight of the  $m$ -th member, respectively.

### 6.2.2. Design Constraints

The structural behavior and performance limitations of steel structure can be formulated as follows:

$$g_s = \frac{\sigma_s}{(\sigma_s)_{all}} - 1 \leq 0 \quad ; \quad s = 1, \dots, N_s \quad (6.4)$$

$$g_d = \frac{d_d}{(d_d)_{all}} - 1 \leq 0 \quad ; \quad d = 1, \dots, N_d \quad (6.5)$$

$$g_v = \frac{\lambda_v}{(\lambda_v)_{all}} - 1 \leq 0 \quad ; \quad v = 1, \dots, N_v \quad (6.6)$$

In Equations (6.4) – (6.6), the functions  $g_s$ ,  $g_d$  and  $g_v$  are referred to as constraints being bounds on strength, deflection, and , geometric constraints, respectively;  $\sigma_s$  and  $(\sigma_s)_{all}$  are the computed and allowable axial stresses for the  $s$ -th member, respectively; and  $d_d$ , and  $(d_d)_{all}$ , are the deflections computed the displacement of the  $d$ -th joint and its permissible value; finally,  $\lambda_v$  and  $(\lambda_v)_{all}$  are the geometric constraint and its upper limit for  $v$ -th member, respectively.

### 6.3. Steps of Artificial Bee Colony Algorithm

Steps of artificial bee colony algorithm for optimum design of structural engineering problems are defined as:

**Step1:** Search parameters of artificial bee colony algorithm are defined in this step. These are number of employed bees ( $NEB$ ), number of onlooker bees ( $NOB$ ), number of cycles and control parameter adjusting the food source (limit). In the algorithm, number of onlooker bees is equal to number of employed bees.

**Step2:** After defining search parameters, all foragers in the colony search food source randomly. This means  $NEB+NOB$  frame designs are generated randomly. Generated steel structure designs are evaluated and penalized in accordance with their weights and constraints violations. Penalized weight of each steel structure design is calculated by following function.

$$W_p = W \cdot (1 + C)^\varepsilon \quad (6.7)$$

where,  $W$  is the value of objective function of optimization problem.  $W_p$  is the penalized weight of structure,  $C$  is the total constraint violation value calculated from the sum of the values of constraints violation functions of objective function,  $\varepsilon$  is penalty coefficient taken as 2.0.

$$C = \sum g_s + \sum g_d + \sum g_v \quad (6.8)$$

where,  $g_s$ ,  $g_d$ , and  $g_v$ , are the constraints violation functions for strength, deflection and geometric constraints functions. In general form, constraints violation functions can be expressed as:

$$C_i = \begin{cases} 0 & \text{if } g_i(x_j) \leq 0 \quad i=1, \dots, NC \\ g_i(x_j) & \text{if } g_i(x_j) > 0 \quad j=1, \dots, NG \end{cases} \quad (6.9)$$

where,  $g_i(x)$  is  $i^{\text{th}}$  constraints function,  $x$  is the vector of design variables,  $NC$  is the number of constraint functions and  $NG$  is the total number of member groups in the optimization problem.

**Step3:** After evaluation process, bees having the best steel structure designs become employed bees. Then, employed bees start to generate a new steel structure designs by using the old one as follows:

$$v_{ij} = x_{ij} + \phi_{ij} \cdot (x_{ij} - x_{kj}), \quad i, k = 1, 2, \dots, NEB, \quad j = 1, 2, \dots, NG \quad (6.10)$$

where,  $i$  represents employed bee number index,  $k$  and  $j$  are randomly chosen indexes. Although  $k$  is generated randomly, it is not equal to  $i$ .  $\phi_{ij}$  is a uniformly distributed random number between  $[-1, 1]$ . This parameter adjusts size of neighborhood steel structure design region. Then, new steel structure designs generated from employed bees are evaluated and their penalized weights are calculated by using aforementioned process. After evaluation process, penalized weights of new steel structure designs and old steel structure designs are compared. If penalized weight of the new steel structure design is better than the old one, the old steel structure design is replaced with the new one. This process is called *greedy selection*.

**Step 4:** After finding new steel structure designs and replacements, all employed bees return their hive and start their waggle dance. Waggle dance of employed bees are related to penalized weight of structural design. The remainders of the bees (onlooker bees) watch the waggle dance and make a decision. This decision process of each onlooker bee depends on its probability value associated with steel structure design. Probability of  $i^{\text{th}}$

steel structure design is calculated according to  $i^{th}$  onlooker bee by using following function;

$$P_i = \frac{(W_p)_i}{\sum_{i=1}^{NOB} (W_p)_i} \quad (6.11)$$

Then onlooker bees generate new steel structure designs by using Equation (6.11) and make greedy selection the same as the case of employed bees.

**Step 5:** If steel structure design cannot be replaced with the old steel structure design, this steel structure design is abandoned and the employed bee associated with that fame design becomes a scout bee. Scout bees generate new steel structure designs by using random selection process the same as step 2.

**Step 6:** The steps 3 and 5 are repeated until a pre-assigned maximum iteration number is reached.

The flowchart shown in Figure 6.3. demonstrates the artificial bee colony (ABC) algorithm for a maximum cycle number (MCN) of iterations.

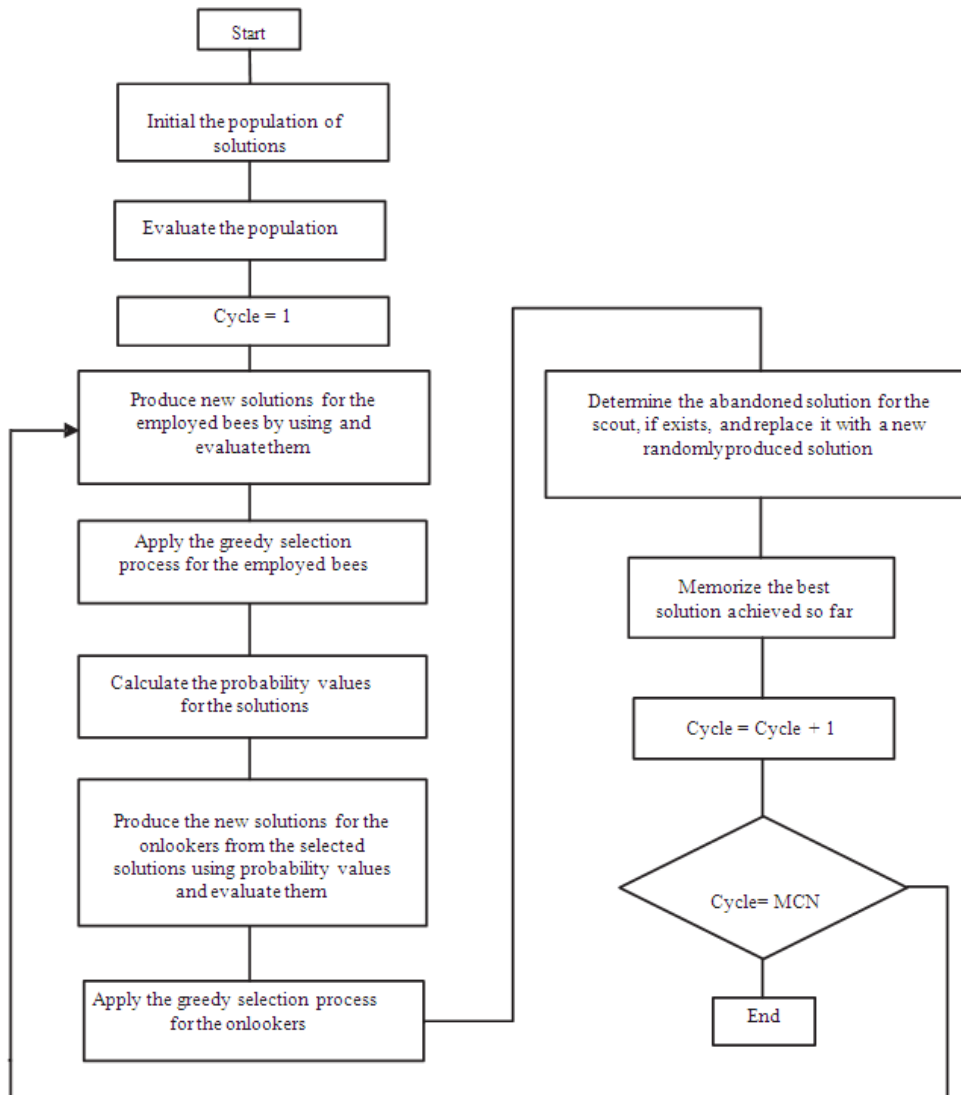


**Figure 6.3.** Flowchart of the Artificial Bee Colony (ABC) algorithm.

#### 6.4. Optimum Design Algorithm

The optimum design algorithm developed for steel frames made of cold-formed thin-walled steel sections is based on artificial bee colony method. In the case of single span beams, it treats the geometric dimensions of cold-formed thin-walled section as design variables. In the optimum design, artificial bee colony algorithm initiates the design process by first selecting values randomly for the geometric dimensions of thin steel plates which make the cold-formed thin-walled section from the design pool. Once the dimensions are decided, the geometry of a cold-formed thin-walled steel section then becomes available. Artificial bee colony algorithm is then proceeds to apply its steps that are listed above until the convergence is obtained.

In the case of steel frames, the sequence number of the C-sections selected for each member group from the available list is treated as design variable. Artificial bee colony algorithm randomly selects sequence numbers for the C-sections for the frame member groups. Selection these numbers makes the sectional designations and cross sectional properties of C-sections available for the algorithm. The design algorithm consists of the following steps for both cases;

1. Select the values of artificial bee colony parameters. These parameters are the bee colony size, the maximum cycle number and the value for limit by which if there is no improvement in the amount of nectar from a food source after a predefined iteration (limit), this food source is discarded by its employed bee. These values are decided after carrying out several trials in the design examples.
2. Generate a solution (population) matrix. Select randomly dimensions for a steel section in the case of single span beam and sequence numbers of C-sections from the discrete list for each group in the case of frames.
3. Generate the geometrical data such as member incidences, joint coordinates automatically using the values selected.
4. Carry out the successive linear elastic analysis to obtain nonlinear response of a steel member or the frame until the convergence is reached in the axial force values of members. In the case of steel frames the loss of stability at any stage of this nonlinear analysis is checked. If the loss of stability occurs then this selected design vector is taken out from solution matrix and replaced by a new design vector that is selected randomly again. This replacement process is repeated until a design vector is determined that does not have instability problem. This vector is then checked whether it satisfies the design constraints. If it does not it is once more discarded. However, if it is slightly infeasible it is considered for the solution matrix.
5. Calculate the objective function value for the newly selected design vector. If this value is better than the worst vector in the solution matrix, it is then included in the solution matrix while the worst one is taken out of this matrix. The solution matrix is then sorted in descending order by the objective function value.
6. Repeat steps 2 and 6 are until the pre-selected maximum number of iterations is reached. The maximum number of iterations is selected large enough such that within this number of design cycles no further improvement is observed in the objective function.





## CHAPTER 7

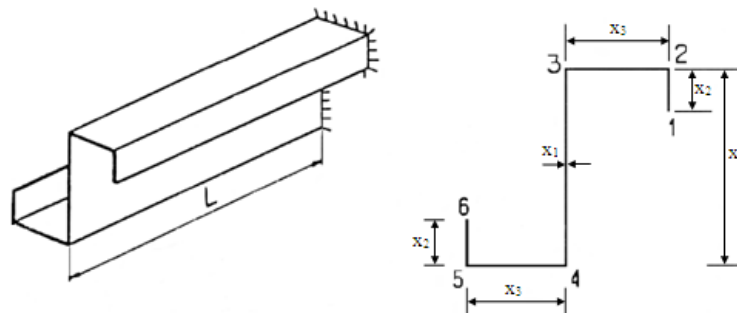
### DESIGN EXAMPLES

#### 7.1. Introduction

In this chapter, the design algorithm developed is used to determine the optimum designs of number of cold-formed thin-walled open sections and steel frames having these sections, subjected to various external loading. The modulus of elasticity and shear modulus of steel are taken as  $E=203.000$  GPa and  $G=78.000$  GPa respectively in the design examples considered as recommended in Chapter 5 for cold-formed steel sections.

One of the advantages of the artificial bee colony (ABC) algorithm is that it requires pre-determination of only three parameters. These are the bee colony size, the maximum cycle number (MCN), and the limit. In the first six design examples considered in this chapter the bee colony size is taken as 30 and the maximum cycle number (MCN) is chosen as 1000. With these selections the total objective function evaluations become is 30000. The value of the limit which is used to abandon the food source is selected as 30. For the last two design examples, bee colony size, the maximum cycle number (MCN), and the limit value are selected as 50, 2000, and 250, respectively. The maximum number of iterations is limited to 5000 for first six design examples and 75000 for last two design examples. Each design example has been re-designed 5 times; each run starting from a random population with different seed values in order to investigate the variance of optimum results. Among these, the best optimum designs are presented here.

#### 7.2. A Thin-Walled Z-Lip Cantilever Beam



(a) Z-lip cantilever beam.

(b) Design variables.

**Figure 7.1.** A thin-walled Z-lip cantilever beam; (a) Z-lip cantilever beam, (b) Design variables.

In the first design example, a thin-walled Z-lip cantilever beam shown in Figure 7.1 (a) is designed by the optimum design algorithm developed for thin-walled beams with arbitrary open sections.  $L$  is the length of the beam and taken as 1.5 m. The design variables  $x_1$ ,  $x_2$ ,  $x_3$ , and  $x_4$  that are the geometric dimensions of thin plates are shown in Figure 7.1 (b). A design pool is prepared that contains separate values for each design variable. First column of the pool contains values from 1 mm to 3 mm with the increment of 0.25 mm for  $x_1$  which represents the thickness ( $t$ ) of the section. The second column of the pool has values starting from 15 mm to 30 mm with the increment of 0.25 mm for  $x_2$  which represents the depth ( $d$ ) of the section. The third column of the pool contains values from 30 mm to 90 mm with the increment of 0.25 mm for  $x_3$  which represents flange width ( $b$ ) of the section, and finally the last column has values from 85 mm to 305 mm with the increment of 0.25 mm for  $x_4$  which represents the depth ( $h$ ) of the section. The beam is subjected to 25N equipment load through its x-axis as shown in Figure 7.2. and 250 N through its y-axis as well as 180 Nm moment through its x-axis at its free end (Joint 2). Besides, the beam is subjected to two different distributed loading; *i*) 250 N/m and *ii*) 200N/m with 0.05 m eccentricity to all over the beam. The latter distributed loading causes 10Nm distributed torque throughout the beam along x-axis. The details of loading to which beam is subjected is presented in Figure 7.2. The yield stress of steel is taken as  $345\text{N/mm}^2$  (50 ksi) [113] which is considered the upper bound for the normal stresses in the beam. The deflection is limited to  $length/360$  which is 4.167 mm as recommended in the ASCE Ad Hoc Committee report [120] for the lateral displacements and deflection of beams in steel frames.

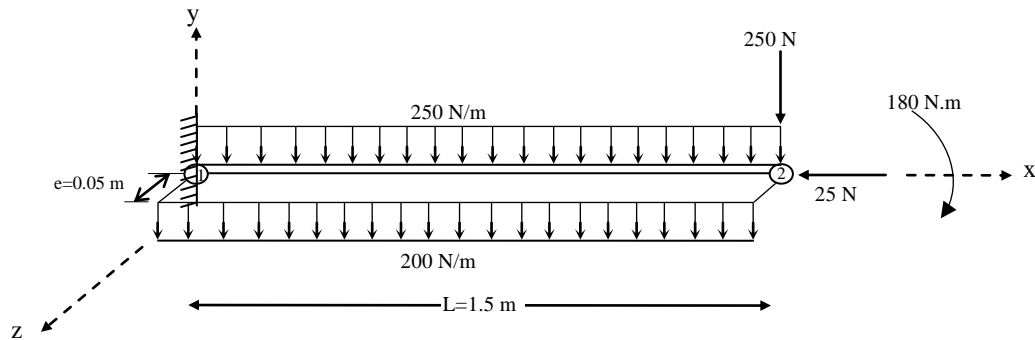


**Figure 7.2.** Loading of thin-walled Z-lip cantilever beam.

Additionally, the following geometric limits are applied as size constraints [117] to the cold-formed thin-walled Z-section in order to control local buckling of thin walls;  $50 < h/t < 200$ ,  $25 < b/t < 100$ ,  $6.25 < d/t < 50$ ,  $2 < h/b < 8$ .

The optimum design problem of the above thin-walled section is solved by the design algorithm developed. The design constraints are taken as those explained in Chapter 5.2. that are not taken from AISI-LRFD design code. They are the stress, displacement and local buckling constraints. The optimum designs with and without considering the effects

of warping are listed in Table 7.1. When warping is not taken into account, the ABC algorithm attains the least weight of the cold-formed thin-walled Z-section as 45.34 N (4.623 kg). The minimum weight of the beam is obtained as 50.83 N (5.183 kg) when the effect of warping is considered in the design process. It is clear that consideration of the warping effect increases the minimum weight 12.11%. The normal stress reaches to 344.6 MPa for the case where warping is considered which is almost at its upper bound. This stress value includes both warping and bending stresses which are 325.53MPa and 19.07 MPa, respectively. It is interesting to note that the normal stress due to warping constitutes 94.36% of the total stress. Exclusion of warping effects in this problem certainly yields to unsafe designs. It is also apparent from Table 7.1 that stress constraints are dominant in the design problem. The optimum designs obtained by ABC algorithm are shown in Figure 7.3. The convergence history showing variation of the best feasible design generated so far throughout the optimization process with ABC technique for each warping case is plotted in Figure 7.4.

**Table 7.1.** Optimum design results of thin-walled Z-lip cantilever beam.

Design Variables	ABC algorithm without warping	ABC algorithm with warping
$x_1 (t)$	1 mm	1 mm
$x_2 (d)$	20 mm	30 mm
$x_3 (b)$	77.5 mm	90 mm
$x_4 (h)$	197.5 mm	200 mm
Minimum weight (N (kg))	45.34 (4.623)	50.83 (5.183)
Maximum displacement (mm)	0.0764	0.607
Maximum stress (MPa)	28.15	344.60
Maximum number of iterations	5000	5000

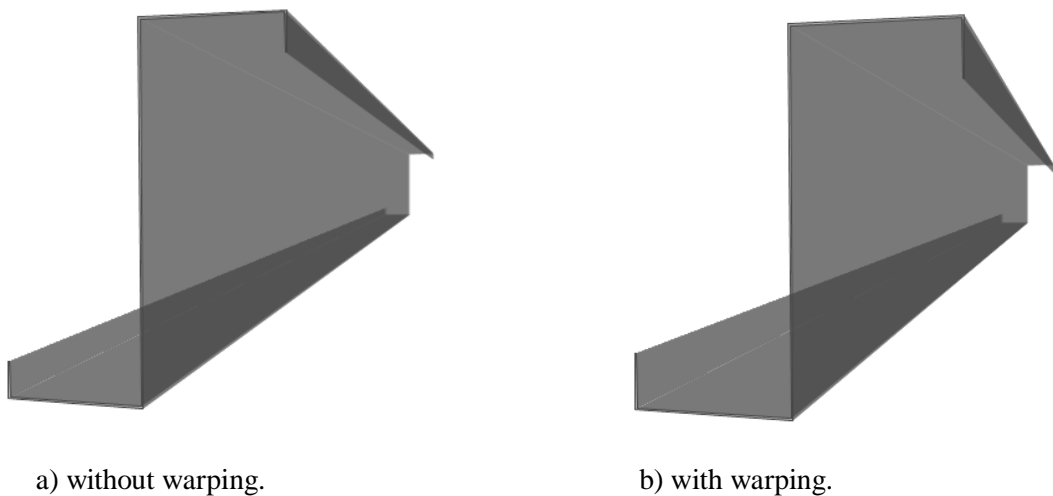


**Figure 7.3.** Optimum designs of cold-formed thin-walled Z-lip cantilever beam; a) without warping, b) with warping.

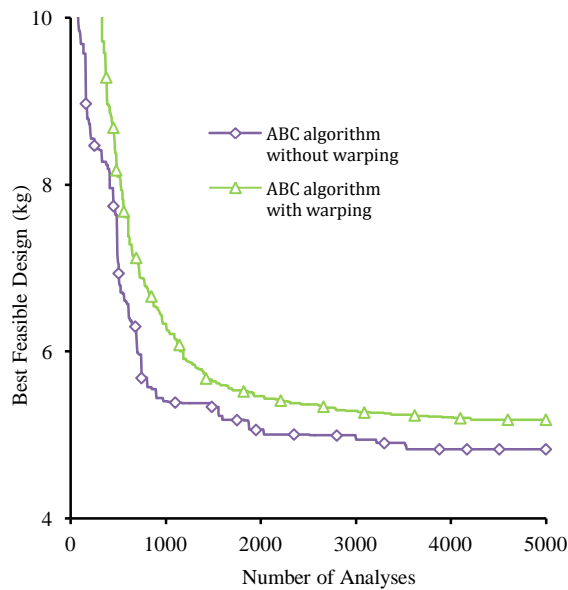


**Figure 7.4.** Design history graph of cold-formed thin-walled Z-lip cantilever beam.

### 7.3. A Thin-Walled Simply Supported Beam with an Arbitrary Open Section

As a second design example a thin-walled simply supported beam with an arbitrary open section is selected as shown in Figure 7.5. The length ( $L$ ) of the beam is selected as 1.5 m. The design variables are assigned as geometric dimensions of thin plates and the prepared design pool that contains separate values for each design variable are taken exactly same as first example. Namely, first column of the pool contains values from 1 mm to 3 mm with the increment of 0.25 mm for  $x_1$  which represents the thickness ( $t$ ) of the section. The second column of the pool has values starting from 15 mm to 30 mm with the increment of 0.25 mm for  $x_2$  which represents the depth ( $d$ ) of the section. The third column of the pool contains values from 30 mm to 90 mm with the increment of 0.25 mm for  $x_3$  which represents flange width ( $b$ ) of the section, and finally the last column has values from 85 mm to 305 mm with the increment of 0.25 mm for  $x_4$  which represents the depth ( $h$ ) of the section. Moreover, similar to first design example the following geometric limits are applied as size constraints [117] to the cold-formed thin-walled arbitrary open section in order to control local buckling of thin walls;  $50 < h/t < 200$ ,  $25 < b/t < 100$ ,  $6.25 < d/t < 50$ ,  $2 < h/b < 8$ . The optimum design problem of the arbitrary thin-walled section is solved by the design algorithm developed. The design constraints are taken as those explained in Chapter 5.2 which are not taken from AISI-LRFD code. The design constraints are the stress, displacement and local buckling constraints.

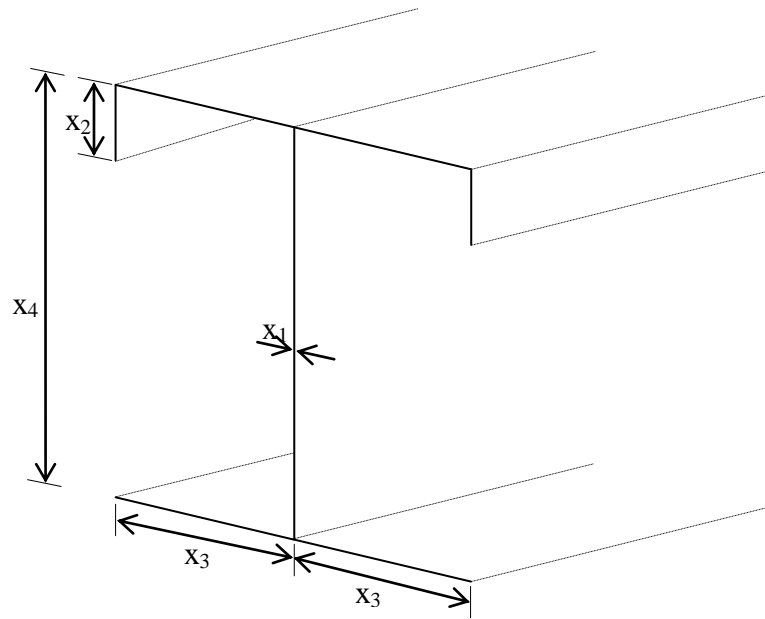


**Figure 7.5.** A thin-walled simply supported beam with arbitrary open section.

The beam is subjected to 8 kN equipment load through its x- and y-axes as shown in Figure 7.6. and 1 kNm moment through its x-axis at its free end. The yield stress of steel is taken as 345 MPa [113] which is considered the upper bound for the normal stresses in the beam. The deflection is limited to  $length/360$  which is 4.167 mm as recommended in the ASCE Ad Hoc Committee report [120] for the lateral displacements and deflection of beams in steel frames.

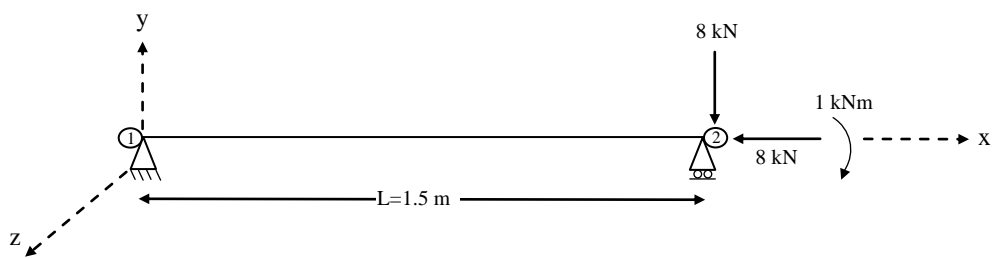


**Figure 7.6.** Loading of thin-walled simply supported beam with arbitrary open section.

The ABC algorithm attains the least weight of the beam with cold-formed thin-walled arbitrary section as 47.36 N (4.828 kg) when warping is not taken into account. The minimum weight of the beam is obtained as 64.98 N (6.624 kg) when the effect of warping is considered in the design process. It is clear that consideration of the warping

effect increases the minimum weight 37.21%. The normal stress reaches to 344.8 MPa for the case where warping is considered which is almost at its upper bound. This stress value includes both warping and bending stresses which are 199.2MPa and 145.6 MPa, respectively. Exclusion of warping effects in this design example certainly yields to unsafe designs. It is obvious from Table 7.2. that while stress constraint is dominant in the case warping is considered, the displacement constraint is dominant in the case warping is not considered. The convergence history showing the variation of the best feasible design generated so far throughout the optimization process with ABC technique for each warping case is plotted in Figure 7.7.

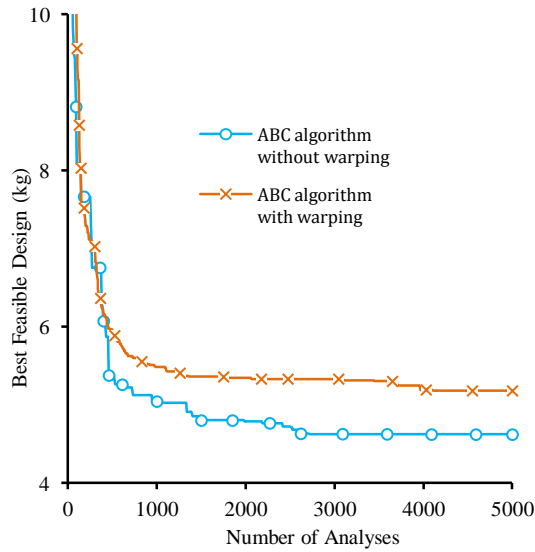


**Figure 7.7.** Design history graph of cold-formed thin-walled simply supported beam with an arbitrary open section.

**Table 7.2.** Optimum design results of cold-formed thin-walled simply supported beam with an arbitrary open section.

Design Variables	ABC algorithm without warping	ABC algorithm with warping
$x_1 (t)$	1 mm	1 mm
$x_2 (d)$	15 mm	15 mm
$x_3 (b)$	45 mm	85 mm
$x_4 (h)$	200 mm	192.5 mm
Minimum weight (N (kg))	47.36 (4.828)	64.98 (6.624)
Maximum displacement (mm)	4.10	2.79
Maximum stress (MPa)	227.2	344.8
Maximum number of iterations	5000	5000

#### 7.4. A Thin-Walled Column with a L-Lip Open Section

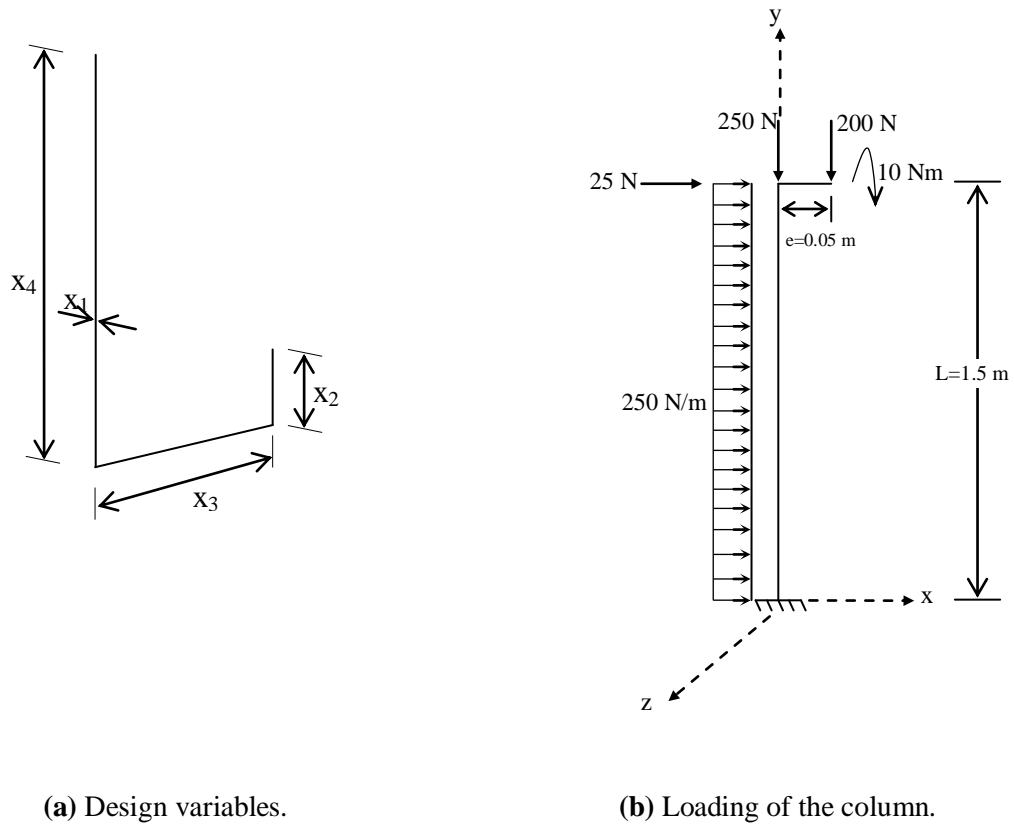


**Figure 7.8.** A thin-walled L-lip column; (a) Design variables, (b) Loading of the column.

The third design example is selected as a cold-formed thin-walled column with L-lip open cross-section as shown in Figure 7.8. The length ( $L$ ) of the column is assigned as 1.5 m. The design variables are assigned as geometric dimensions of thin plates (Figure 7.8. (a)) and the prepared design pool that contains separate values for each design variable are exactly same as above two design examples and these are not repeated here. Also stress, displacement and local buckling constraints are taken exactly same as mentioned in first two design examples. The column is subjected to 25N equipment load through its x-axis and 250 N equipment load through its y-axis as well as a 10 Nm moment through its x-axis at its free end. Besides, a 200 N concentrated load is applied with 0.05 m eccentricity through y-axis at free end of the column and 250 N/m distributed load is applied all over the column. The loading of the column is represented in Figure 7.8. (b).

**Table 7.3.** Optimum design results of thin-walled column with L-lip cross-section.

Design Variables	ABC algorithm without warping	ABC algorithm with warping
$x_1 (t)$	1 mm	1 mm
$x_2 (d)$	15 mm	30 mm
$x_3 (b)$	35 mm	82.5 mm
$x_4 (h)$	130.0 mm	172.5 mm
Minimum weight (N (kg))	26.57 (2.709)	45.92 (4.683)
Maximum displacement (mm)	4.156	1.38
Maximum stress (MPa)	91.0	344.5
Maximum number of iterations	5000	5000

The least weight produced by the ABC algorithm for cold-formed thin-walled column with L-lip open cross-section is 26.57 N (2.709 kg) when warping is not taken into account. The minimum weight of the column is obtained as 45.92 N (4.683 kg) when the effect of warping is taken into account in the design process. It is clear that consideration of the warping effect increases the minimum weight 72.87%. The total normal stress reaches to 344.5 MPa for the case where warping is considered which is almost at its upper bound. This stress value includes both warping and bending stresses which are 329.3 MPa and 15.2 MPa, respectively. The normal stress due to warping constitutes 95.45% of the total stress. It is obvious that including warping produces very higher normal stress along the column. Exclusion of warping effects in this design example certainly yields to unsafe designs. It is obvious from Table 7.3. that while stress constraint is dominant in the case warping is considered, the displacement constraint is dominant in the case warping is not considered. Design histories of the optimum solutions accordance with warping are shown in Figure 7.9.

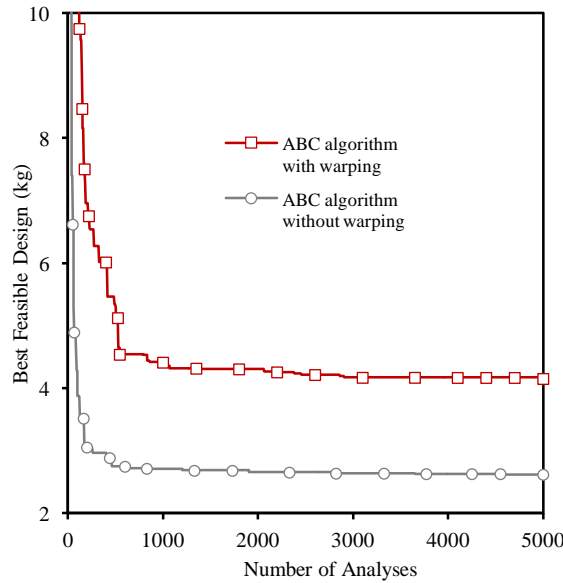


**Figure 7.9.** Design history graph of thin-walled column with L-lip cross-section.



Among three design examples mentioned above, thin-walled column with L-lip open section has the least weight as 2.709 kg which is obtained by ABC algorithm without warping. When warping effect is taken into account ABC algorithm yielded the same weight as 4.683 kg. In the case of cantilever beam with Z-lip open section, the optimum design weights are obtained as 4.623 kg and 5.183 kg by ABC algorithm with and without warping effect, respectively. The heavier design weights are obtained for simply supported beam with an arbitrary thin-walled open section by ABC algorithm including and excluding warping effect as 4.828 kg and 6.624 kg, respectively. It can be concluded from these results that the optimum design weights obtained are directly dependent to section geometry and external loading condition. All design weights are comparatively demonstrated in Figure 7.10.

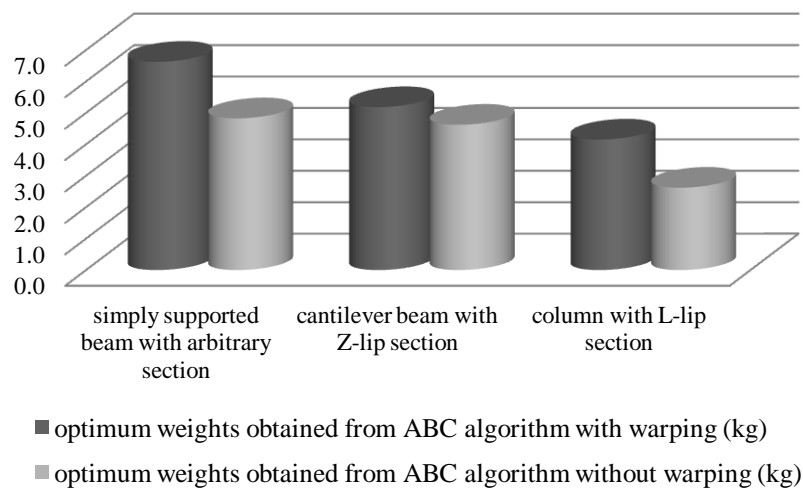


**Figure 7.10.** Comparison of the optimum design weights obtained by ABC algorithm.

### 7.5. Cold-Formed Thin-Walled Cantilever Beam with C-sections with Lips to AISI-LRFD

The forth design example shown in Figure 7.11. is a cantilever beam made of cold-formed thin-walled C-sections with lips accordance with AISI [113]. The C-sections with lips are to be selected from a section list consisting of 85 independent C-shaped cold-formed thin-walled steel sections taken from AISI Design Manual 2007 Excerpts-Gross Section Property Tables [112]. The combined strength and stability constraints adapted from 2007 edition of the North American (AISI) specification [113] are imposed as explained in Chapter 5.3. This example is designed by Artificial Bee Colony (ABC) algorithm to find optimum C-section.

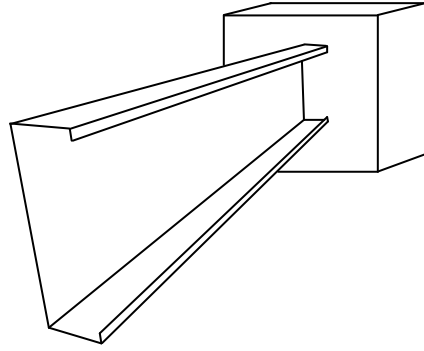


**Figure 7.11.** Cold-formed thin-walled cantilever beam with C-section.

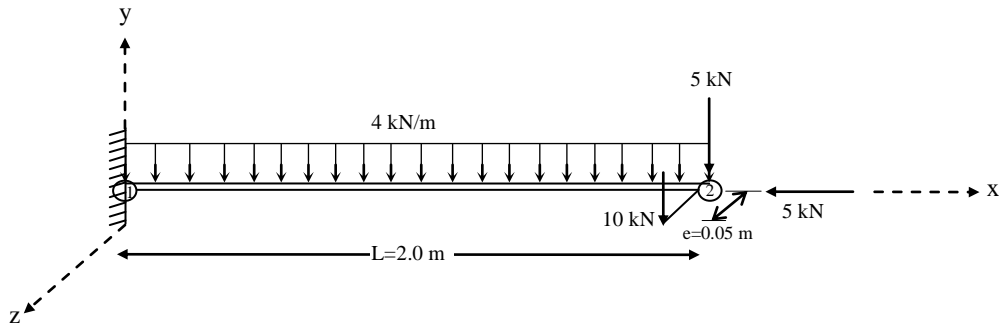


**Figure 7.12.** Loading of cold-formed thin-walled cantilever beam with C-section.

The length ( $L$ ) of the beam is 2.0 m and the upper limit of the maximum displacement is  $L/360$  which is 5.556 mm. Furthermore, both concentrated and distributed loads are considered in designing the beam as shown in Figure 7.12. The beam is subjected to 5 kN concentrated load along  $x$ - and  $y$ -axis as well as a 10 kN equipment load is applied with 0.05 m eccentricity through  $y$ -axis at free end of the beam. Besides, the beam is subjected to 4kN/m distributed loading.

**Table 7.4.** Optimum design results of cold-formed thin-walled cantilever beam.

Algorithm Used	ABC
Minimum weight (N (kg))	218.58 (22.28)
Selected section ID	12CS4X105
Maximum displacement (mm)	5.326
Maximum strength ratio	0.60
Maximum number of iterations	5000

The optimum results obtained by ABC algorithm is tabulated in Table 7.4. The proposed design algorithm selects the 12CS4x105 cold-formed C-section from section list under mentioned loading. The optimum weight of the beam is obtained as 218.58 N (22.281 kg). The maximum strength ratio and the maximum displacement are 0.60 and 5.326 mm, respectively. From this result, it can be concluded that the displacement constraint governs the optimization process for this example. The optimum design obtained by ABC algorithm is shown in Figure 7.13. Design history of the optimum solution is plotted in Figure 7.14.

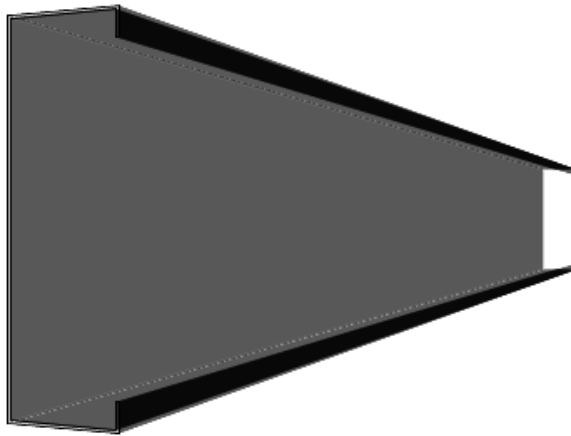


**Figure 7.13.** Optimum design of cold-formed thin-walled cantilever beam with C-section.

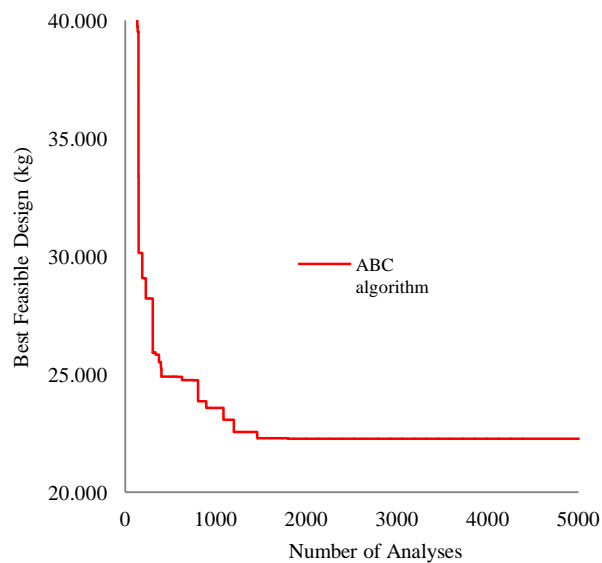


**Figure 7.14.** Design history graph of thin-walled cantilever beam with C-section.

## 7.6. Cold-Formed Thin-Walled Column with C-sections with Lips to AISI-LRFD

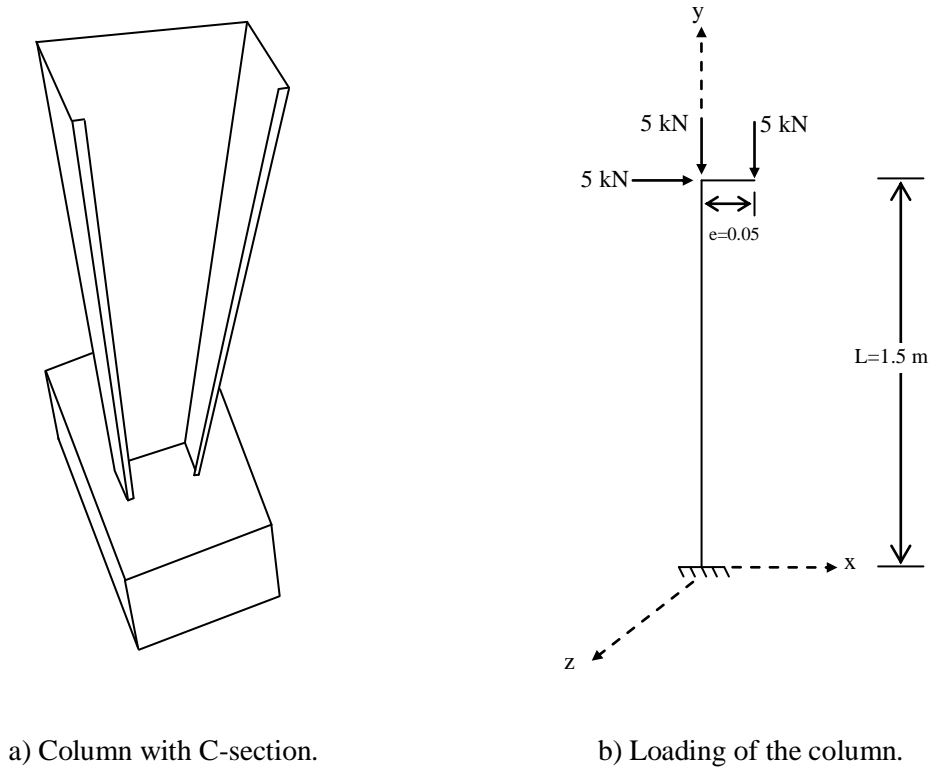


**Figure 7.15.** Cold-formed thin-walled column; a) Column with C-section, b) Loading of the column.

The fifth design example is selected as a column made of cold-formed thin-walled C-sections with lips accordance with AISI [113] as shown in Figure 7.15 (a). The C-sections and the strength constraints are considered in accordance with AISI [112,113] which are exactly same as previous example.

The length ( $L$ ) of the column is 1.5 m and the upper limit of the maximum displacement is  $L/360$  which is 4.166 mm. The section is subjected to 5 kN concentrated load along  $x$ - and  $y$ -axis as well as a 5 kN equipment load is applied with 0.05 m eccentricity through  $y$ -axis at free end of the beam as shown in Figure 7.15. (b).

**Table 7.5.** Optimum design results of cold-formed thin-walled column.

Algorithm Used	ABC
Minimum weight (N (kg))	83.46 (8.51)
Selected section ID	10CS2.5x070
Maximum displacement (mm)	4.152
Maximum strength ratio	0.633
Maximum number of iterations	5000

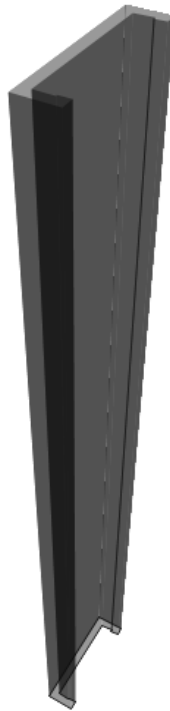


**Figure 7.16.** Optimum designs of cold-formed thin-walled column with C-section.

The optimum results obtained by ABC algorithm is tabulated in Table 7.5. The proposed design algorithm selects the 10CS2.5x070 cold-formed C-section from section list under mentioned loading. The optimum weight of the beam is obtained as 83.46 N (8.51 kg). The maximum strength ratio and the maximum displacement are 0.633 and 4.152 mm, respectively. From this result, it is apparent that the displacement constraint governs the optimization process in this example. The optimum design obtained by ABC algorithm is shown in Figure 7.16. Design history of the optimum solution which shows the convergence variation of the best feasible design generated so far is plotted in Figure 7.17.

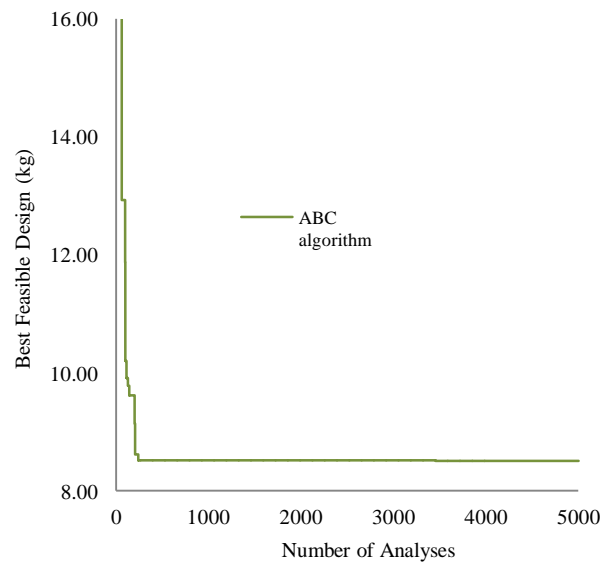


**Figure 7.17.** Design history graph of cold-formed thin-walled column with C-section.

### 7.7. Plane Portal Frame Design to AISI-LRFD

The optimum design algorithm based on ABC technique developed for geometrically nonlinear plane portal frames with cold-formed steel channel (C)-sections is used to determine the optimum design of the pitched roof frame shown in Fig. 7.18. The cold-formed channel steel section designations (C-sections) are treated as design variables in the optimization process by considering that the span ( $L_f$ ), the height of eaves ( $h_f$ ), the pitch angle ( $\theta_f$ ) are given. The design constraints are implemented from AISI-LRFD (American Iron and Steel Institute - Load and Resistance Factor Design) [113] as explained in detail in Chapter 5.3.



**Figure 7.18.** Geometry of a plane portal frame with cold-formed steel sections.

The specific values of span ( $L_r$ ), height of eaves ( $h_r$ ), and pitch angle ( $\theta_r$ ) and the external loading are shown in Figure 7.19. The frame is subjected to two 2 kN and a 4 kN concentrated loads on its joints at eaves and apex. The members of the portal frame are grouped together to achieve the minimum construction cost for the structure. The column members are assigned as the first group and the rafter members are assigned as the second group. Moreover, the modulus of elasticity ( $E$ ) for the steel is taken as  $203 \text{ kN/mm}^2$  and the shear modulus ( $G$ ) is taken as  $78 \text{ kN/mm}^2$  for cold-formed steel sections. The complete C-section with lips list given in AISI Design Manual 2007 [112] which consists of 85 section designations is considered as a design pool for design variables. The inter-storey drift and top-storey drift are restricted as 10 mm. Maximum deflections of rafters are limited as 28.33 mm.

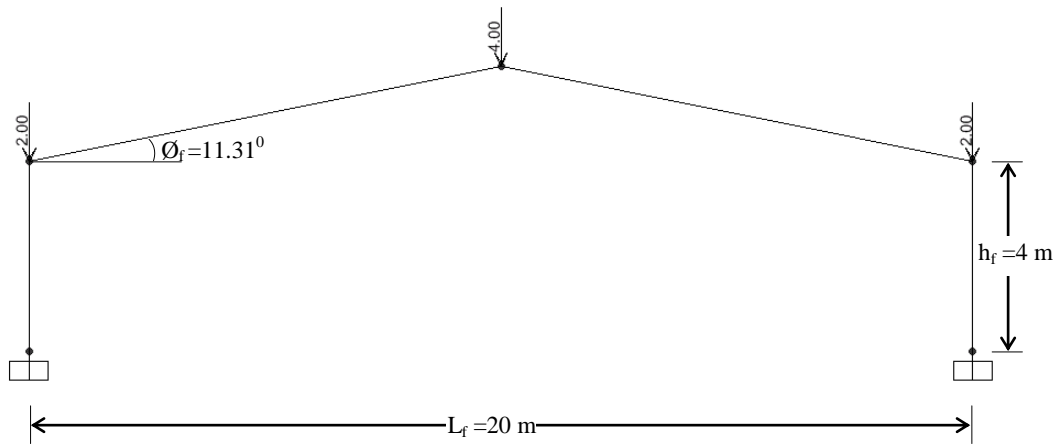


**Figure 7.19.** Loading and geometry of the plane portal frame.

The bee colony size is taken as 30 and the maximum cycle number (MCN) is chosen as 1000. With these selections the total objective function evaluations become is 30000. The value of the limit which is used to abandon the food source is selected as 30. The maximum number of iterations is limited to 5000.

**Table 7.6.** Optimum design results of plane portal frame.

Group Number	Group type	Section selected by ABC algorithm
1	Rafter	12CS4x105
2	Column	12CS4x085
Minimum weight (kN (kg))		2.9365 (299.239)
Maximum top storey drift (mm)		5.535
Maximum inter-storey drift (mm)		5.535
Maximum deflection (mm)		27.63
Maximum strength ratio		0.36
Maximum number of iterations		5000

The minimum weight, maximum constraints values and cold-formed steel section designations of optimum design obtained by the ABC algorithm are illustrated in Table 7.6. It is apparent from this table that the minimum weight obtained by proposed ABC algorithm is 2.9365 kN (299.24 kg). Moreover, artificial bee colony algorithm selects the 12CS4x105 cold-formed C-section with lips for rafter members and 12CS4x085 cold-formed C-section with lips for column members of the plane portal frame. The maximum strength ratio and the maximum deflection values are 0.36 and 27.63 mm, respectively. From these results, it is obvious that the displacement constraint is dominant on the optimization process for this example. Optimum design of the portal frame obtained by ABC algorithm is demonstrated in Figure 7.20. Design history of the optimum solution is graphed in Figure 7.21.

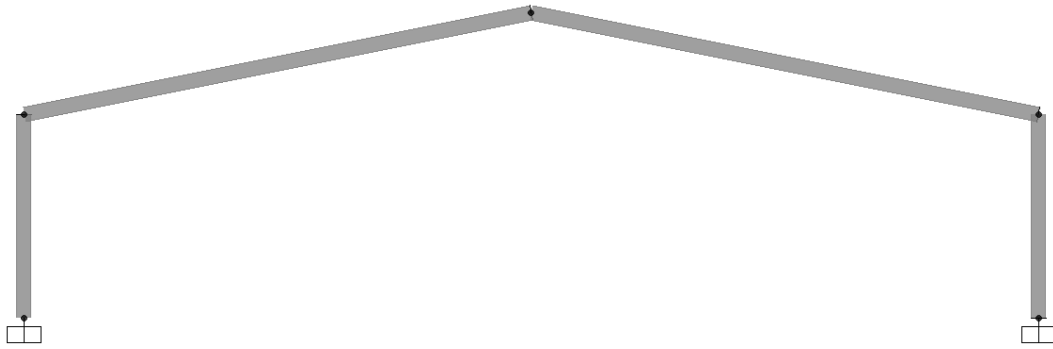


**Figure 7.20.** Optimum design of plane portal frame.



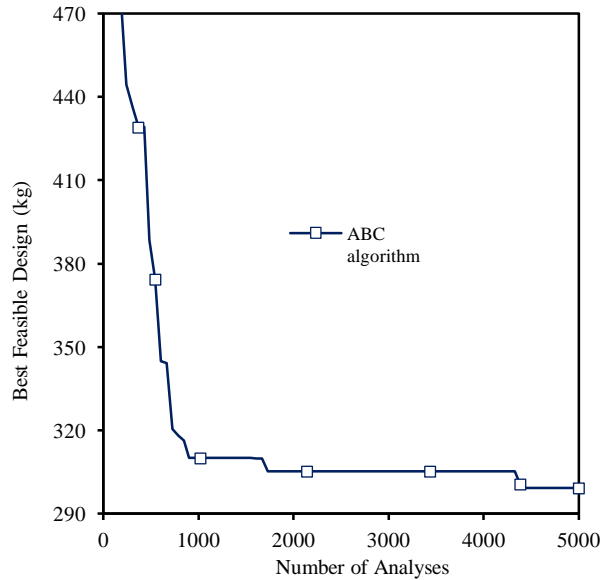
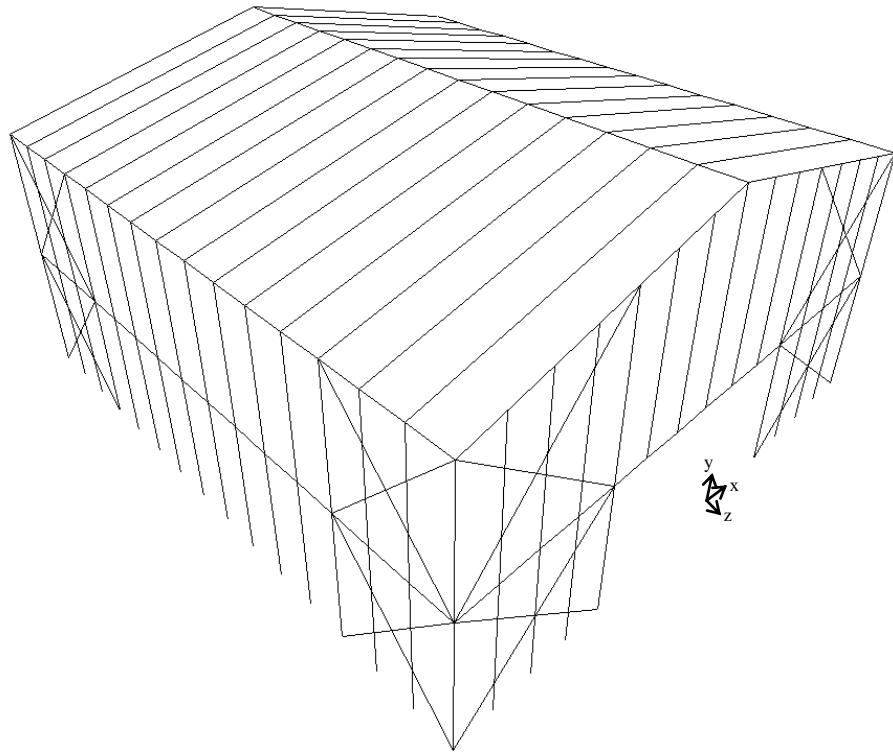


**Figure 7.21.** Design history graph of plane portal frame.

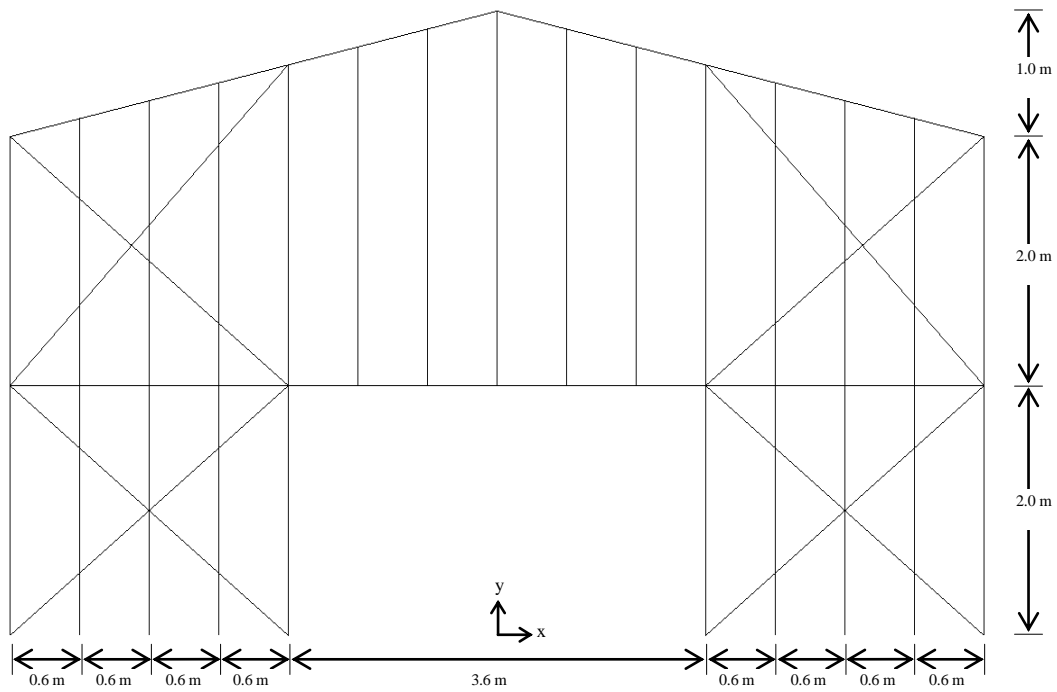
### 7.8. 302-Member Lightweight Steel Frame Built Up With Cold-Formed Thin-Walled Sections

Two storey low-rise braced lightweight steel frame composed of 183 joints and 302 members is considered as a seventh design example. An economical and effective stiffening of the frame against lateral forces is achieved through exterior diagonal bracing members, which also participate in transmitting the gravity forces. The 302 frame members are collected in 8 different member groups considering the symmetry of the structure and practical fabrication requirements. The member grouping details are depicted in Figure 7.22. (d). The C-shaped profile list consisting of 85 cold-formed thin-walled ready sections is used to size column, beam, and diagonal members.

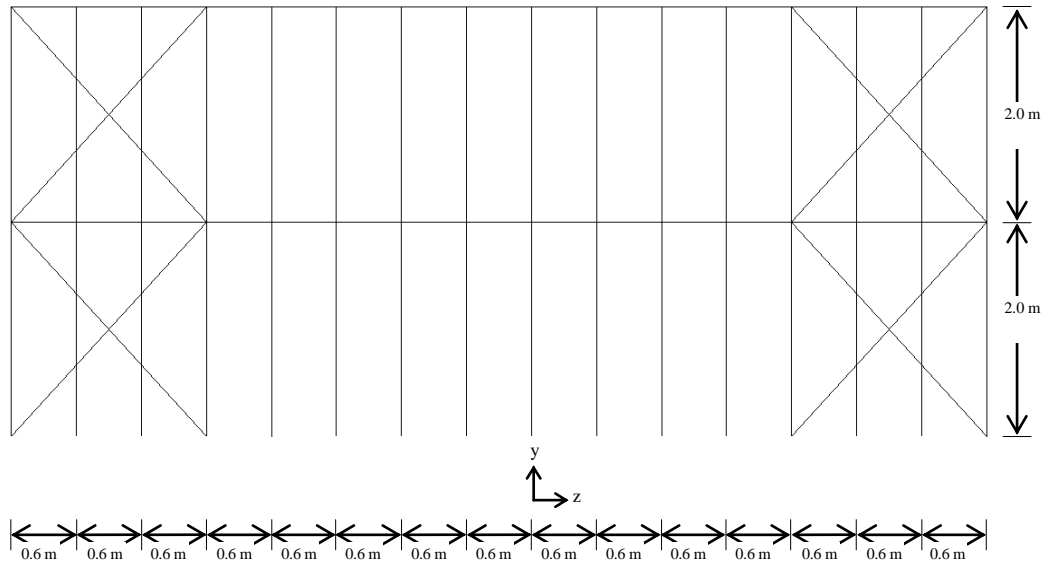
The frame is subjected to a gravity loading condition which is applied as  $2.0 \text{ kN/m}^2$  to floors and  $1.0 \text{ kN/m}^2$  to roof of the frame. Besides, the wind in the  $x$ -direction is considered for design purpose, and the corresponding wind force is applied as  $0.5 \text{ kN}$  to all joints of windward side of the frame. The joint displacements in  $x$  and  $z$  directions are restricted to  $10 \text{ mm}$ , which is obtained as height of frame/400. Furthermore, storey drift constraints are applied to each story of the frame, which is equal to height of each storey/400. Also, maximum deflection of a frame member is equal to member length/360.



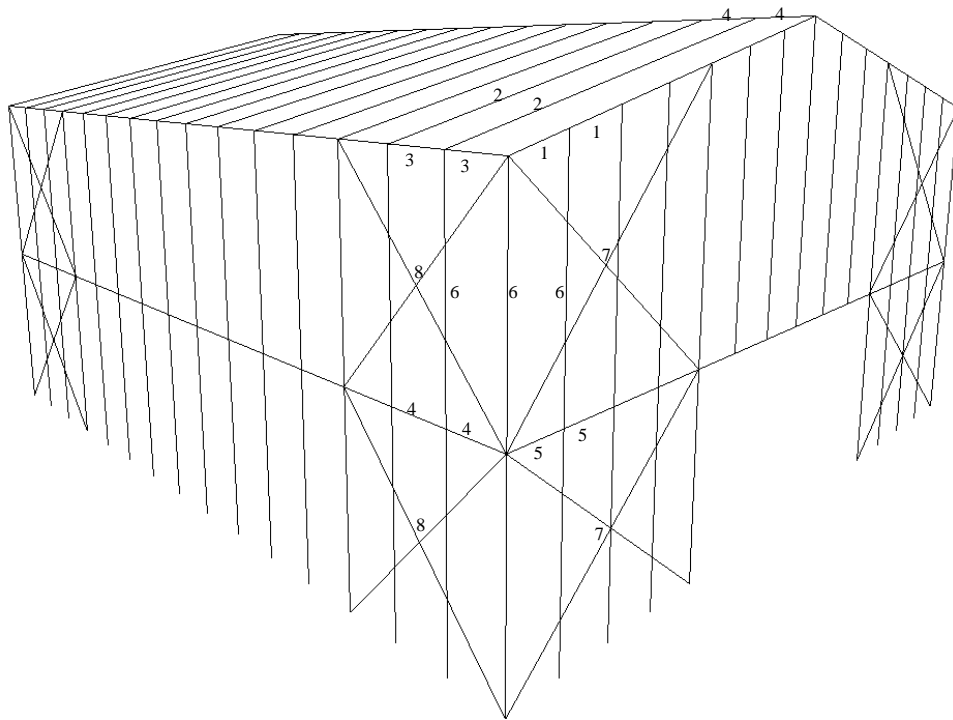
a ) 3D View.



b ) Front View.



c ) Side View.



d ) Member Grouping.

**Figure 7.22.** 302-Member Lightweight Steel Frame; a) 3D View, b) Front View, c) Side View, d) Member Grouping.

A five independent runs are performed with the ABC algorithm using different values of the parameter set, and the best run of the algorithm has been obtained when bee colony size is taken as 50, maximum cycle number (MCN) is taken as 2000, and the limit is taken as 250. The ABC algorithm has yielded the optimum solution of the problem, producing a design with the weight of 44.22 kN (4507.146 kg) for the building. This optimum design is tabulated in Table 7.7. The convergence history showing the variation of the best feasible design generated throughout the optimization process with ABC technique is plotted in Figure 7.23.

**Table 7.7.** Optimum design results of 302-member lightweight steel frame.

Group Number	Group type	Section selected by ABC algorithm
1	Beam	7CS4x105
2	Beam	12CS4x105
3	Beam	8CS4x105
4	Beam	4CS4x085
5	Beam	6CS2.5x059
6	Column	8CS4x105
7	Bracing	4CS2x059
8	Bracing	4CS2x059
Minimum weight (kN (kg))		44.225 (4509.690)
Maximum top storey drift (mm)		5.346
Maximum inter-storey drift (mm)		5.0
Maximum deflection (mm)		10.38
Maximum strength ratio		0.478
Maximum number of iterations		75000

From Table 7.7, it is clear that inter-storey drift and deflection constraints, which are almost at their upper limits indicating the dominance of deflection constraints in the optimum design problem. The ABC algorithm yields the optimum design weight of 44.225 kN (4509.69 kg). The maximum strength ratio and the maximum top-storey drift values are 0.478 and 5.346 mm, respectively. The steel section designations assigned to frame member groups are given in the table.

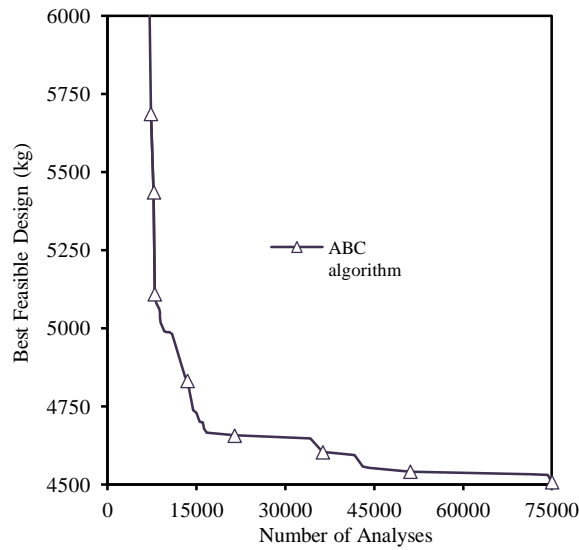


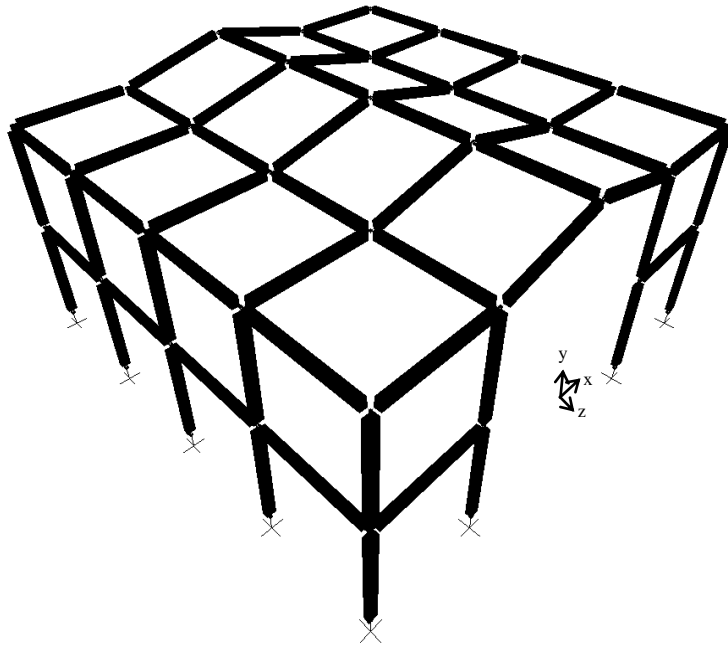
**Figure 7.23.** Design history graph of 302-Member Lightweight Steel Frame.

### 7.9. 106-Member Industrial Building Made of Cold-Formed Thin-Walled Sections to AISI-LRFD

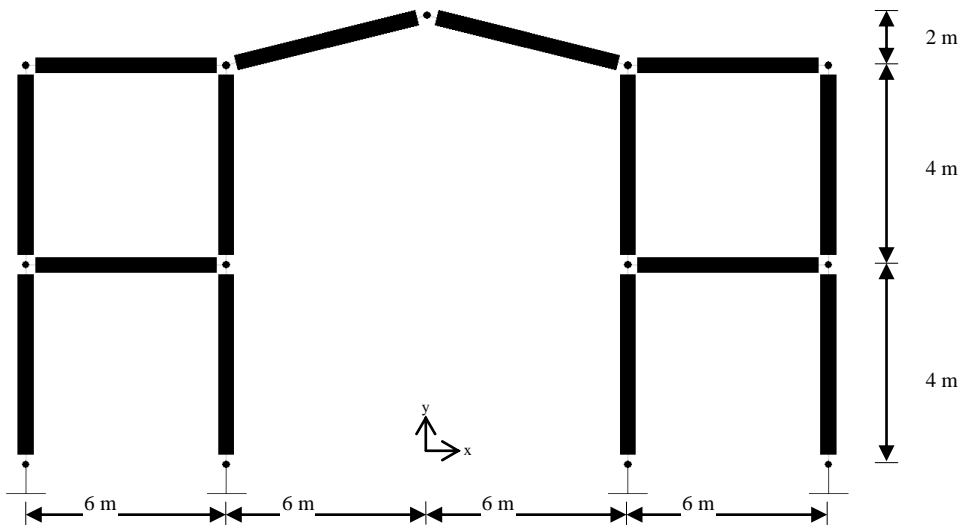
The last design example is an industrial building consisting of 65 joints and 106 members. Shown in Figure 7.24. are the plan, side and 3D views of this structure. The main system of the structure consists of five identical frameworks lying 6.0 m (19.685 ft) apart from each other in the y-z plane and 4.0 m (13.123 ft) in x-y plane. Each framework consists of two side frames and a gable roof in between them, as depicted in Figure 7.24. (b). The lateral stability against wind loads in the y-z plane is provided through columns fixed at the base along with the rigid connections of the side frames. Hence, all the beams and columns in the side frames are designed as moment-resisting axial-flexural members.

Two different types of loads are considered for design of the industrial building; namely gravity and wind loads. A design gravity load of 150 N/m<sup>2</sup> is assumed to be acting on both roof and floors of the frame. Only the wind in the x-direction is considered for design purpose, and the corresponding wind force is applied as 50 N to all joints of windward side of the frame.

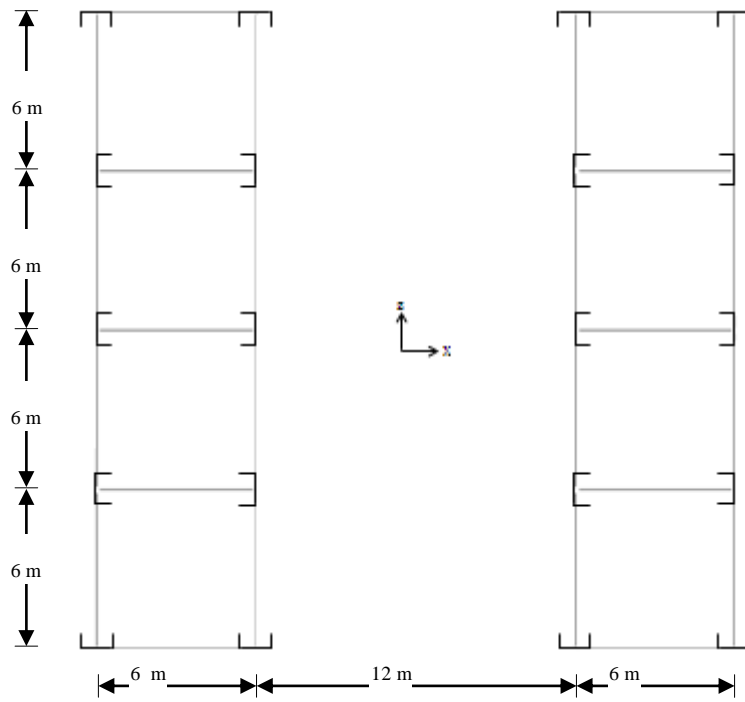
Considering symmetry of the structure as well as fabrication requirements of structural members, 106 members are collected in 15 member groups, Figure 7.23. (e). Section lists consisting of 85 independent C-shaped with lips cold-formed steel sections are used to size the columns and beams, respectively. Combined strength, stability and geometric constraints are imposed according to the provisions of AISI-LRFD [113]. In addition, displacements of all the joints at top storey in x and z directions are limited to 20 mm (0.79 in), and the upper limit of inter-story drifts is set to 10 mm (0.394 in).



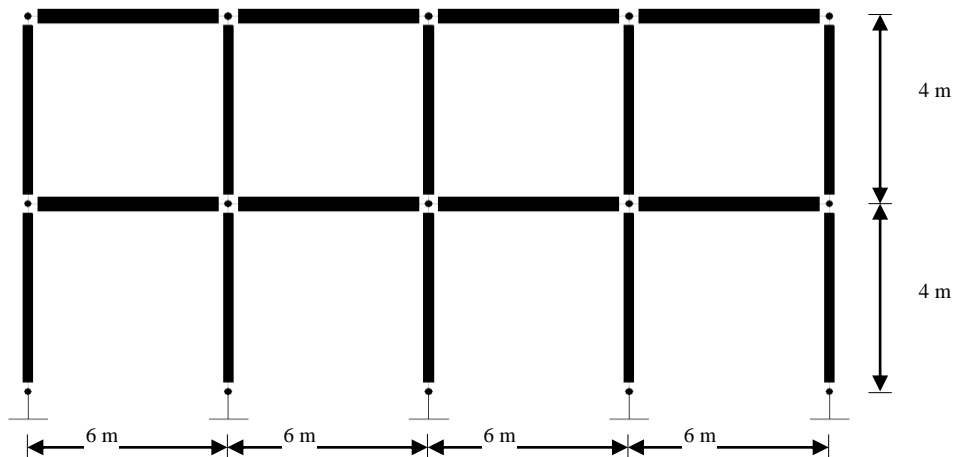
a ) 3D View.



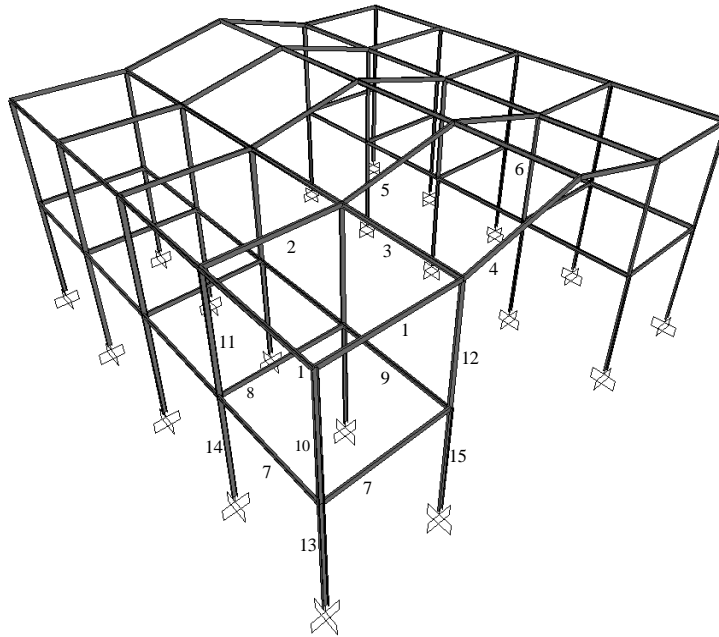
b ) Front View.



c) First Floor Plan View and Column Orientations.



d) Side View.



e ) Member Grouping.

**Figure 7.24.** 106-member industrial building; a) 3D view, b) front view, c) first floor plan and column orientations view, d) side view, e) member grouping.

Several independent runs are performed with the ABC algorithm using different seed values, and the best run of the algorithm has been obtained once again when bee colony size is taken as 50, the maximum cycle number (MCN) is chosen as 2000, and the limit which is used to abandon the food source is selected as 250. The optimum design determined is given in Table 7.8. The minimum weight for the frame is obtained as 21.579 kN (2200.446 kg). It is apparent that in optimum design problems where the number of design variables relatively large, ABC algorithm worked efficiently without any problem. The maximum strength ratio, the maximum top storey drift and the maximum inter-storey drift values are 0.964, 19.18 mm and 9.812 mm, respectively. From these results, it can be concluded that the all constraints are almost at their upper bounds and both displacement and strength constraints are dominant in the optimization process. The convergence history showing the variation of the best feasible design by the ABC technique is plotted in Figure 7.25.



**Table 7.8.** Optimum design results of 106-member industrial building.

Group Number	Group type	Section selected by ABC algorithm
1	Beam	4CS2X059
2	Beam	12CS3.5X070
3	Beam	8CS2X059
4	Rafter	9CS2.5X059
5	Rafter	12CS3.5X070
6	Rafter	6CS2.5X059
7	Beam	4CS2X059
8	Beam	4CS2X059
9	Beam	4CS2X059
10	Column	4CS2X059
11	Column	6CS4X059
12	Column	4CS2X059
13	Column	12CS2.5X070
14	Column	8CS4X059
15	Column	4CS2.5X065
Minimum weight (kN (kg))		221.59 (2200.446)
Maximum top storey drift (mm)		19.180
Maximum inter-storey drift (mm)		9.812
Maximum strength ratio		0.964
Maximum number of iterations		75000

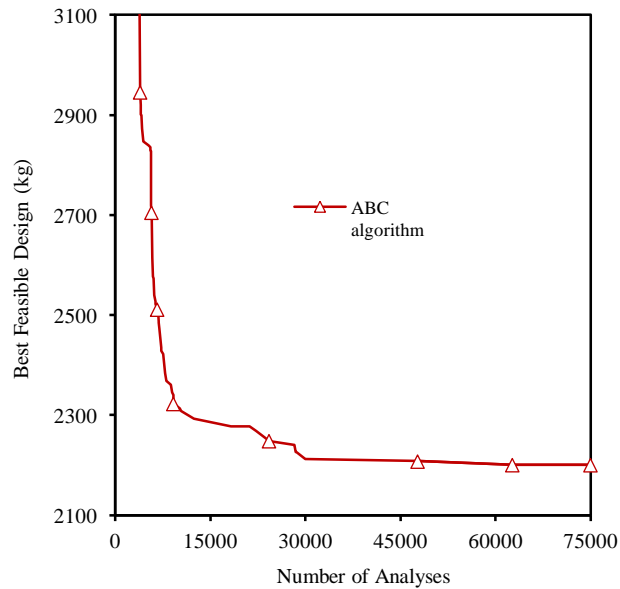


**Figure 7.25.** Design history graph of 106-member industrial building.



## CHAPTER 8

### SUMMARY AND CONCLUSIONS

In this thesis the artificial bee colony algorithm is used to develop an optimum design for the steel frames made of cold-formed thin-walled steel sections. Because cold-formed thin-walled sections do have small torsional and flexural stiffness, they may undergo large deformations. Hence, the algorithm developed should consider geometric nonlinearity. Furthermore warping effects are also taken into account due to the fact that excessive torsional deformations generate large normal stresses. The design algorithm presented is used to determine number of single span beam-columns as well as two and three dimensional space steel frames made of cold-formed thin-walled steel section. It is shown that artificial bee colony algorithm is efficient enough to obtain the optimum designs of all these problems. It is important to notice that the optimum design problem of structures made of cold-formed thin-walled sections is a complex design problem due to the necessity of considering the geometric nonlinearity as well as the warping effect in the prediction of structural response to external loads.

The artificial bee colony algorithm mimics the foraging behavior of a bee colony. To increase the gathered pollen in apiary, bees search for a fruitful food resource. Artificial Bee Colony technique simulates this elementary foraging strategy of a bee colony consisting of employed bees, onlooker bees and scouts. The task of an employed bee in the colony is to find food sources and to identify the pollen content of each new source and to keep in mind the better one (greedy selection). Employed bees carry this data into the hive and inform other bees by dancing in the dance area. The dancing time represents the amount of pollen in the food source. Related with this information onlooker bees attain the new food sources. Then onlooker bees select the most fertile food source (probabilistic selection) among all food resources. In order to detect the most productive food source, a greedy selection is carried out. When a food source is unworthy to gain, it is absconded by the bees. This is a real characteristic of bees, and the employed bee of that source becomes a scout bee and starts searching the environment arbitrarily or instinctively to find a new source. This technique requires pre-determination of only three parameters. These are the bee colony size, the maximum cycle number (MCN), and the limit (predefined iteration) by which if there is no improvement in the amount of nectar from a food source, this food source is discarded by its employed bee. So, the design algorithm developed does not need an initial starting value for the design variables.

The behavior of steel structures made of cold-formed thin-walled open steel sections is nonlinear due to excessive change of their geometry under external loads. This is due to the weak torsional and flexural stiffness of cold-formed-thin-walled sections. It is also necessary to check the overall stability during the analysis to ensure that the structure does not lose its load carrying capacity due to instability. The elastic instability analysis

of steel frames involves iterative linear elastic analysis of the structure and determination of axial forces in structural members. After this identification, the stability functions are calculated and structural analysis is repeated. When the specific convergence is reached at the axial forces of the members, this operation is terminated. The final values of internal actions and displacements obtained at the outlet of the nonlinear analysis of the structure. The details of a nonlinear stiffness matrix of a space member are given in Chapter IV.

In this thesis two different optimum design algorithms are developed. The first one finds out the optimum cross sectional dimensions of a cold-formed thin-walled open section subjected to any general external loading which may consist of axial load, bi-axial bending moment and torsional moment. The optimum design problem in this part of the study is formulated such that the objective function is taken to be the minimum weight of the cold-formed thin-walled section and the design constraints are considered to be the displacement and normal stress limitations. Furthermore, in order to prevent the local buckling the on the depth to thickness ratios are also considered. The yield stress of the steel material is imposed as upper bound on the flexural stresses. The warping effect in the computation of the flexural stresses is taken into account. It is noticed in the design examples that in the case the torsional moments are dominant, the normal stress values become extremely large. Therefore in such cases ignoring the warping effect yields unsafe design. The program developed has a subroutine which computes the sectorial coordinate and warping moment of inertia of a cold-formed thin-walled open section of arbitrary shape. This subroutine takes the geometric dimensions of the cross section as data and computes all the required cross sectional properties such as center of gravity of the section, moment of inertias about both axis and other necessary properties automatically.

In the second part of the study, another optimum design algorithm is developed which determines the optimum design of two or three dimensional steel frames subjected to any general loading whose members are made of cold-formed thin-walled open sections. The design constraints in this optimum design problem are implemented from AISI Design Manual 2007 [112]. The design algorithm selects the optimum cold-formed thin-walled sections from the discrete set of the same code given in Excerpts-Gross Section Property Tables for the members of the frame. This profile list consists of 85 independent C-shaped with lips sections. The combined strength and stability constraints adapted from 2007 edition of the North American (AISI) specification [113] are imposed as explained in Chapter 5.3. It can be concluded from design examples that the strength limitations are dominant in the 106-members industrial building. The optimum design results obtained for this example show that the strength ratios were very close to 1 and the values of the restricted deflections were almost at their upper bounds. But in plane portal frame and 302-members lightweight steel frame displacement constraints governed the optimization process which were almost at their upper limits. This is due to consideration of geometric nonlinearity which affects the behavior of these steel frames drastically.

It is observed that the warping effect in the optimum design of cold-formed thin-walled steel members is very important. This second order torsional effect leads significant stress increase in thin-walled members. It is obvious that excluding warping effect from optimum design of cold-formed thin-walled sections and steel frames made of these sections would be unsafe. In Z-lip cantilever beam the normal stress has reached to 344.60 MPa when effect of warping is taken into account in the computation of normal stresses. 94.47% of this stress was due to warping and the rest of which was due to bending. In simply supported beam with an arbitrary cold-formed thin-walled open section the normal stress is determined as 344.812 MPa when effect of warping is considered in optimum design. This stress is 51.78% higher than the one when the effect of warping is not considered in the optimization process. The normal stress reaches 344.544 MPa in the column with L-lip cold-formed thin-walled open section including both warping and bending stresses which are 329.314 MPa and 15.23 MPa, respectively. These results verify that exclusion of warping effect in the optimum design of cold-formed thin-walled open sections yields unsafe designs.

It can be concluded that the Artificial Bee Colony (ABC), which is a biologically inspired stochastic search technique is promising in finding the optimum design of cold-formed thin-walled open sections and as well as low-rise steel frames made use of these steel sections. No difficulty is observed in obtaining the optimum design even in the design example of 302- member frame which is a relatively large design example. The use of other metaheuristic optimization techniques on the efficiency of the solutions obtained will be the subject of a future work.



## REFERENCES

- [1] Murray, N.W., *Introduction to the Theory of Thin-Walled Structures*, Claredon Press, Oxford, UK, 1984.
- [2] Yu, W-W., *Cold-Formed Steel Structures; Design, Analysis, Construction*, McGraw-Hill Book Company, USA, 1973.
- [3] Stephens, S.F., *Web Crippling and Combined Bending and Web Crippling of Cold-Formed Steel Header Beams*, Ph.D. Thesis, University of Missouri-Rolla, USA, 2002.
- [4] Megson, T.H.G., *Linear Analysis of Thin-Walled Elastic Structures*, John Wiley&Sons, New York, NY, USA, 1974.
- [5] Vlasov, V.Z., *Thin-Walled Elastic Beams, Israel Program for Scientific Translations*, Jerusalem: Israel Program for Scientific Translations, Israel, 1961.
- [6] Timoshenko, S., and Gere, J.M., *Theory of Elastic Stability*, Second Ed., Mcgraw-Hill, New York, NY, USA, 1961.
- [7] Timoshenko, S., *Theory of Bending, Torsion and Buckling of Thin-walled Members of Open Cross Section*, Journal of Franklin Inst., Vol. 239, 249-268, 1945.
- [8] Paz, M., Strehl, C.P., and Schrader, P., *Computer Determination of the Shear Center of Open and Closed Sections*, Computers & Structures, Vol. 6, 117-125, Pergamon Press, Britain, 1976.
- [9] Ghersi, A., Landolfo, R., and Mazzolani, F.M., *Design of Metallic Cold-formed Thin-Walled Members*, Spon Press, London, UK, 2002.
- [10] Gunnlaugsson, G.A., and Pedersen, P.T., *A Finite Element Formulation for Beams with Thin-walled Cross-Sections*, Computers & Structures, Vol. 15, 691-699, 1982.
- [11] Meek, J. L., and Ho, P.T.S., *A Simple Finite Model for the Warping Torsion Problem*, Computer Methods in Applied Mechanics and Engineering, Vol. 37, 25-36, 1983.
- [12] Tralli, A., *A Simple Hybrid Model for Torsion and Flexure of Thin-Walled Beams*, Computers & Structures, Vol. 22 (4),649-658, 1986.
- [13] Eisenberger, M., *Nonuniform Torsional Analysis of Variable and Open Cross-Section Bars*, Thin-Walled Structures, Vol. 21, 93-105, 1995.

- [14] Al-Mosawi, S., and Saka, M.P., *Optimum Shape Design of Cold-Formed Thin-Walled Steel Sections*, Advances in Engineering Software, Vol. 31, 851-862, 2000.
- [15] Lee, J., Kim, S-M., Park, H-S., and Woo, B-H., *Optimum Design of Cold-Formed Steel Channel Beams Using Micro Genetic Algorithm*, Engineering Structures, Vol. 27, 17-24, 2005.
- [16] Lee, J., Kim, S-M., and Park, H-S., *Optimum Design of Cold-Formed Steel Columns by Using Micro Genetic Algorithms*, Thin-Walled Structures, Vol. 44, 952-960, 2006.
- [17] Magnucki, K., and Monczak, T., *Optimum Shape of Open Cross Section of Thin-Walled Beam*, Engineering Optimization, Vol. 32, 335-351, 2000.
- [18] Magnucki, K., *Optimization of Open Cross Section of the Thin-Walled Beam with Flat Web and Circular Flange*, Thin-Walled Structures, Vol. 40 (3), 297-310, 2002.
- [19] Magnucki, K., Szyk, W., and Stasiewicz, P., *Stress state and elastic buckling of a thin-walled beam with monosymmetrical open cross-section*, Thin-Walled Structures, Vol. 42 (1), 25-38, 2004.
- [20] Adeli, H., and Park, H-S., *A Neural Dynamics Model for Structural Optimization—Theory*, Computers & Structures, Vol. 57 (1), 383-90, 1995.
- [21] Adeli, H., and Park, H-S., *Neurocomputing for Design Automation*. CRC Press, Boca Raton, FL, USA, 1998.
- [22] Tran, T., and Li, L-Y., *Global Optimization of Cold-Formed Steel Channel Sections*, Thin-Walled Structures, Vol. 44, 399-406, 2006.
- [23] Chang, S-P., Park, H-G., Kim, P-Y., and Kim, S-B., *Geometrically Nonlinear Analysis of Thin-Walled Space Frames*, Transactions of the 15<sup>th</sup> International Conferences on Structural Mechanics in Reactor Technology (SMIRT 15), Seoul, Korea, August 15-20, 1999.
- [24] Stasiewicz, P., Magnucki, K., Lewiski, J., and Kasprzak, J., *Local Buckling of a Bent Blange of a Thin-Walled Beam*, Proceedings in Applied Mathematics and Mechanics, Vol. 4, 554-555, 2004.
- [25] Silvestre, N., and Camotim, D., *Distortional Buckling Formulae for Cold-Formed Steel C- and Z-Section Memebers. Part I – Derivation*, Thin-Walled Structures, Vol. 42, 1567-1597, 2004.
- [26] Silvestre, N., and Camotim, D. *Distortional Buckling Formulae for Cold-Formed Steel C- and Z-Section Memebers. Part II - Validation and application*, Thin-Walled Structures, Vol. 42, 1599-1629, 2004.



- [27] Camotim, D., Silvestre, N., Basaglia, C., and Bebiano R., *GBT-Based Buckling Analysis of Thin-Walled Members with Non-standard Support Conditions*, Thin-Walled Structures, Vol. 46, 800-815, 2008.
- [28] Macdonald, M., Heiyantuduwa, M.A., and Rhodes, J., *Recent Developments in the Design of Cold-Formed Steel Members and Structures*. Thin-Walled Structures, Vol. 46, 1047-1053, 2008.
- [29] Lim, J.B.P., and Nethercot, D.A., *Design and Development of a General Cold-Formed Steel Portal Framing System*, The Structural Engineer, Vol. 80 (21), 31-40, 2002.
- [30] Lim, J.B.P., and Nethercot, D.A., *Ultimate Strength of Bolted Moment-Connections Between Cold-Formed Steel Members*, Thin-Walled Structures, Vol. 41, 1019–1039, 2003.
- [31] Dogan, E., *Optimum Design of Rigid and Semi-Rigid Steel Sway Frames Including Soil-Structure Interaction*, Ph.D. Thesis, Middle East Technical University (METU), Ankara, Turkey, 2010.
- [32] Spillers, W.R., and MacBain, K.M., *Structural Optimization*, Springer, New York, NY, USA, 2009.
- [33] Saka, M.P., Dogan, E., and Aydogdu, I., *Review and Analysis of Swarm-Intelligence Based Algorithms*, in Yang, X-S., Cui, Z., Xiao, R., Gandomi, A.H., and Karamanoglu, M., (Eds.), *Swarm Intelligence and Bio Inspired Computation: Theory and Applications*, Elsevier, 2013.
- [34] Saka, M.P., and Hasancebi, O., *Adaptive harmony search algorithm for design code optimization of steel structures*, in Geem, Z.W. (Ed.), *Harmony search algorithms for structural design optimization*, Springer-Verlag, Berlin, Heidelberg, Germany, 79–120, 2009.
- [35] Saka, M.P., and Dogan, E., *Recent Developments in Metaheuristic Algorithms: A Review*, in Topping, B.H.V. (Ed.), *Computational Technology Reviews*, Vol. 5, 31-78, 2012.
- [36] Saka, M.P., *Optimum Design of Steel Skeleton Structures*, in Geem, Z.W. (Ed.), *Music-Inspired Harmony Search Algorithm, Theory and Applications*, Springer-Verlag Berlin, Heidelberg, Germany, 2009.
- [37] Horst, R., and Tuy, H., *Global Optimization; Deterministic Approaches*, Springer-Verlag, Berlin, Germany, 1995.
- [38] Paton, R., *Computing with Biological Metaphors*, Chapman & Hall, London, UK, 1994.

- [39] Adami, C., *An Introduction to Artificial Life*, Springer-Verlag/Telos, Berlin, Germany, 1998.
- [40] Matheck, C., *Design in Nature: Learning from Trees*, Springer-Verlag, Berlin, Germany, 1998.
- [41] Mitchell, M., *An Introduction to Genetic Algorithms*, The MIT Press, Cambridge, MA, USA, 1998.
- [42] Hasancebi, O., Carbas, S., and Saka, M.P., *A Reformulation of the Ant Colony Optimization Algorithm for Large Scale Structural Optimization*, Proceedings of the Second International Conference on Soft Computing Technology in Civil, Structural and Environmental Engineering, in Tsompanakis, Y., and Topping, B.H.V. (Eds.), Stirlingshire: Civil-Comp Press, 2011.
- [43] Kochenberger, G.A., and Glover, F., *Handbook of Metaheuristics*, Kluwer Academic Publishers, Norwell, MA, USA, 2003.
- [44] De Castro, L.N., and Von Zuben, F.J., *Recent Developments in Biologically Inspired Computing*, Idea Group Publishing, Hershey, PA, USA, 2005.
- [45] Saka, M.P., *Optimum Design of Steel Frames Using Stochastic Search Techniques Based on Natural Phenomena: A Review*, in Topping, B.H.V. (Ed.), *Civil Engineering Computations: Tools and Techniques*, Saxe-Coburgh Publications, Scotland, UK, 2007.
- [46] Atrek, E., *New Directions in Optimum Structural Design*, John Wiley & Sons, New York, NY, USA, 1984.
- [47] Dréo, J., Petrowski, A., Siary, P., and Taillard, E., *Metaheuristics for Hard Optimization; Methods and Case Studies*, Springer-Verlag, Berlin, Germany, 2006.
- [48] Nocedal, J., and Wright, S.J., *Numerical Optimization*, Springer-Verlag, Berlin, Germany, 1999.
- [49] Chong, E.K.P., and Żak, S.H., *An introduction to Optimization*, John Wiley and Sons, New York, NY, USA, 2001.
- [50] Sun, W., and Yuan, Y-X., *Optimization Theory and Methods; Nonlinear Programming*, Springer-Verlag, Berlin, Germany, 2006.
- [51] Xie, Y.M., and Steven, G.P., *Evolutionary Structural Optimization*, Springer-Verlag, Berlin, Germany 1997.
- [52] Evolution vs. Creationism, *An Introduction. Eugenie Carol Scott*, University of California Press, ISBN 0520233913, CA, USA, 2005.

- [53] Goldberg, D.E., *Genetic Algorithms in Search, Optimization and Machine Learning*, Addison-Wesley Publishing Co. Inc., MA, USA, 1989.
- [54] Gen, M., and Cheng, R., *Genetic Algorithms & Engineering Optimization*, John Wiley&Sons, Inc., New York, NY, USA, 2000.
- [55] Rechenberg, I., *Evolutions Strategie, Optimierung Technischer Systeme Nach Prinzipien der Biologischen Evolution*, Frommann-Holzboog, Germany, 1973.
- [56] Schwefel, H.P., *Numerical Optimization of Computer Models*, Wiley, Chichester, UK, 1981.
- [57] Rajasekaran, S., Mohan, V.S., and Khamis, O., *The Optimization of Space Structures Using Evolution Strategies with Functional Networks*, Engineering with Computers, Vol. 20, 75-87, 2004.
- [58] Ebenau, C., Rottschäferb, J., and Thierauf, G., *An Advanced Evolutionary Strategy with Adaptive Penalty Function for Mixed Discrete Structural Optimization*, Advances in Engineering Software, Vol. 36, 29-38, 2005.
- [59] Hasancebi, O. Carbas, S., Dogan, E., Erdal, F., and Saka, M.P., *Performance Evaluation of Metaheuristic Search Techniques in The Optimum Design of Real Size Pin Jointed Structures*, Computers & Structures, Vol. 87, 284-302, 2009.
- [60] Fogel, L.J., Owens, A.J., and Walsh, M.J., *Artificial Intelligence through Simulated Evolution*, John Wiley, New York, NY, USA, 1996.
- [61] Back, T., *Evolutionary Algorithms in Theory and Practice: Evolution Strategies, Evolutionary Programming, Genetic Algorithms*, Oxford University Press, Oxford, UK, 1996.
- [62] Kim, J-H., and Myung, H., *Evolutionary Programming Techniques for Constrained Optimization*, IEEE Transaction on Evolutionary Computations, Vol. 1,129-140, 1997.
- [63] Saka, M.P., *Optimum Design of Steel Frames using Stochastic Search Techniques Based on Natural Phenomena: A Review*, Civil Engineering Computations: Tools and Techniques Saxe-Coburg Publications, 2007.
- [64] Kirkpatrick, S., and Gelatt, C.D., *Optimization by Simulated Annealing*, Vecchi, M.P. Science, New Series, Vol. 220, 4598, 671-680, 1983.
- [65] Balling, R.J., *Optimal Steel Frame Design by Simulated Annealing*, Journal of Structural Engineering, ASCE, Vol. 117, 1780-1795, 1991.

- [66] May, S.A., and Balling, R.J., *A Filtered Simulated Annealing for Discrete Optimization of 3D Steel Frameworks*, Structural Optimization, Vol. 4, 142-148, 1992.
- [67] Topping, B.H.V., Khan, A.I., and Leite, J.P.B., *Topological Design of Truss Structures Using Simulated Annealing*, in Topping, B.H.V., and Khan, A. (Eds.), *Neural Networks and Combinatorial Optimization in Civil and structural Engineering*, Civil-Comp Press, 151-165, 1993.
- [68] Hasancebi, O., and Erbatur, F., *On Efficient Use of Simulated Annealing in Complex Structural Optimization Problems*, Acta Mechanica, Vol. 157, 27-50, 2002.
- [69] Hasancebi, O., and Erbatur, F., *Layout Optimization of Trusses Using Simulated Annealing*, Advances in Engineering Software, Vol. 33, 681-696, 2002.
- [70] Kennedy, J., Eberhart, R., and Shi, Y., *Swarm Intelligence*, Morgan Kaufmann Publishers, San Fransisco, CA, USA, 2001.
- [71] Fourie, P., and Groenwold, A., *The Particle Swarm Optimization Algorithm in Size and Shape Optimization*, Structural and Multidisciplinary Optimization, Vol. 23 (4), 259-267, 2002.
- [72] Perez, R.E., and Behdinan, K., *Particle Swarm Approach for Structural Design Optimization*, Computers & Structures, Vol. 85 (19-20), 1579-1588, 2007.
- [73] Glover, F., *Tabu Search-Part I*, ORSA Journal on Computing, Vol. 1 (3), 190-206, 1989.
- [74] Glover, F., *Tabu Search-Part II*, ORSA Journal on Computing, Vol. 2 (1), 4-32, 1990.
- [75] Degertekin, S.O., Hayalioglu, M.S., and Ulker, M., *Tabu search based optimum design of geometrically non-linear steel space frames*, Structural Engineering and Mechanics, Vol. 27 (5), 575-588, 2007.
- [76] Degertekin, S.O., Saka, M.P., and Hayalioglu, M.S., *Optimal Load and Resistance Factor Design of Geometrically Nonlinear Steel Space Frames via Tabu Search and Genetic Algorithm*, Engineering Structures , Vol. 30 (1), 197-205, 2008.
- [77] Degertekin, S.O., Ulker, M., and Hayalioglu, M.S., *Uzay çelik Çerçevelerin Tabu Arama ve Genetik Algoritma Yöntemleriyle Optimum Tasarımı*, Teknik Dergi-TMMOB İnşaat Mühendisleri Odası, Vol. 17 (3), 3917-3934, 2006.
- [78] Degertekin, S.O., Hayalioglu, M.S., and Ulker, M., *Geometrik Olarak Lineer Olmayan Uzay Çelik Çerçevelerin Tabu Arama Yöntemiyle Optimum Tasarımı*, Sigma Mühendislik ve Fen Bilimleri Dergisi, Vol. 6 (1), 107-118, 2006.

- [79] Degertekin, S.O., Ulker, M., and Hayalioglu, M.S., *Uzay Çelik çerçevelerin Tabu Arama Yöntemiyle Optimum Tasarımı*, XV. Ulusal Mekanik Kongresi, Isparta, Turkey, 2007.
- [80] Dorigo, M., *Optimization, Learning and Natural Algorithms*, (in Italian), Ph.D. Thesis, Dipartimento di Elettronica e Informazione, Politecnico di Milano, IT, 1992.
- [81] Camp, C.V., and Bichon, B.J., *Design of Space Trusses Using Ant Colony Optimization*, Journal of Structural Engineering, ASCE, Vol. 130 (5), 741-751, 2004.
- [82] Camp, C.V., Bichon, B.J., and Stovall, S.P., *Design of Steel Frames Using Ant Colony Optimization*, Journal of Structural Engineering, ASCE, Vol. 131 (3), 369-379, 2004.
- [83] Kaveh, A., and Shojaee, S., *Optimal Design of Skeletal Structures Using Ant Colony Optimization*, International Journal for Numerical Methods in Engineering, Vol. 70, 563-581, 2007.
- [84] Kaveh, A., and Talatahari, S., *A Discrete Particle Swarm Ant Colony Optimization for Design of Steel Frames*, Asian Journal of Civil Engineering, Vol. 9 (6), 563-575, 2007.
- [85] Kaveh, A., and Talatahari, S., *A Hybrid Particle Swarm and Ant Colony Optimization for Design of Truss Structures*, Asian Journal of Civil Engineering, Vol. 9 (4), 329-348, 2008.
- [86] Kaveh, A., and Talatahari, S., *A Particle Swarm Ant Colony Optimization for Truss Structures with Discrete Variables*, Journal of Constructional Steel Research, Vol. 65, 1558-1568, 2009.
- [87] Aydogdu, I., and Saka, M.P., *Ant Colony Optimization of Irregular Steel Frames Including Effect of Warping*, Civil-Comp 09, Proceedings of the Twelfth International Conference on Civil, Structural and Environmental Engineering Computing, in Topping, B.H.V., Costa Neves, L.F., and Barros, R.C. (Eds.), September 1-4, Madeira, Portugal, 2009.
- [88] Yang, X-S., *Nature-Inspired Metaheuristic Algorithms*, Luniver Press, UK, 2008.
- [89] Gandomi, A.H., Yang, X-S., and Alavi, A.H., *Mixed Variable Structural Optimization Using Firefly Algorithm*, Computers & Structures, Vol. 89, 2325-2336, 2011.

- [90] Sayadi, M.K., Remazanian, R., and Ghaffari-Nasab, N., *A Discrete Firefly Metaheuristic with Local Search for Make-Span Minimization in Permutation Flow Shop Scheduling Problems*, International Journal of Industrial Engineering Computations, Vol. 1, 1-10, 2010.
- [91] Yang, X-S., and Deb, S., *Engineering Optimization by Cuckoo Search*, International Journal of Mathematical Modeling and Numerical Optimization, Vol. 1 (4), 330–343, 2010.
- [92] Civicioglu, P., and Besdok, E., *A Conceptual Comparison of the Cuckoo Search, Particle Swarm Optimization, Differential Evolution and Artificial Bee Colony Algorithms*, Artificial Intelligence Review, Vol. 39 (4), 315-346, 2013.
- [93] Kaveh, A., and Bakhspoori, T., *Optimum Design of Steel Frames using Cuckoo Search Algorithm with Levy Flights*, The Structural Design of Tall and Special Buildings, Vol. 22 (13), 1023-1036, 2013.
- [94] Yang, X-S., and Deb, S., *Multi-Objective Cuckoo Search for Design Optimization*, Computers & Operations Research, Vol. 40 (6), 1616–1624, 2013.
- [95] Nakrani, S., and Tovey, C., *On Honey Bees and Dynamic Server Allocation in Internet Hosting Centers*, Adaptive Behaviour, Vol. 12 (3-4), 223-240, 2004.
- [96] Yang, X.S., *Engineering Optimization via Nature-Inspired Virtual Bee Algorithms*, Artificial Intelligence and Knowledge Engineering Applications: A Bio-inspired Approach, Lecture Notes in Computer Science, 3562, 317-323, Springer Berlin, Heidelberg, Germany, 2005.
- [97] Karaboga, D., *An Idea Based on Honey Bee Swarm for Numerical Optimization*, Technical Report TR06, Erciyes University, Kayseri, Turkey, 2005.
- [98] Pham, D.T., Ghanbarzadeh, A., Koc, E., Otri, S., Rahim, S., and Zaidi, M., *The Bees Algorithm: A Novel Tool for Complex Optimisation Problems*, Proceedings of IPROMS 2006 Conference, 454-461, 2006.
- [99] Karaboga, D., and Basturk, B., *A Powerful and Efficient Algorithm for Numerical Function Optimization: Artificial Bee Colony (ABC) Algorithm*, Global Optimization, Vol. 39, 459-471, 2007.
- [100] Basturk, B., and Karaboga, D., *An Artificial Bee Colony (ABC) Algorithm for Numeric Function Optimization*, IEEE Swarm Intelligence Symposium, Indianapolis, IN, USA, 2006.
- [101] Karaboga, D., and Basturk, B., *On the Performance of Artificial Bee Colony (ABC) Algorithm*, Applied Soft Computing, Vol. 8 (1), 687–697, 2008.

- [102] Karaboga, D., and Basturk, B., *Artificial Bee Colony (ABC) Optimization Algorithm for Solving Constrained Optimization Problems*, LNCS: Advances in Soft Computing: Foundations of Fuzzy Logic and Soft Computing, 789–798, Springer-Verlag, 2007.
- [103] Hibbeler, R.C., *Mechanics of Materials, Ninth Edition*, Prentice Hall, USA, 2013.
- [104] Coates, R.C., Coutine, M.G., and Kong, F. K., *Structural Analysis, 2nd Edition*, Vokingham, Berks, Van Nostrand Reinhold, 1980.
- [105] Goltermann, P., *Linear Distortional Beam Theory*, Journal of Constructional Steel Research, Vol. 24 (1), 1-23, 1993.
- [106] Vlasov, V.Z., *Thin-Walled Elastic Beams*, National Science Foundation, USA, 1961.
- [107] Koscia, K.Z., *Thin-Walled Beams*, Crosby-Lockwood Ltd, London, UK, 1967.
- [108] Waldron, P., *Sectorial Properties of Straight Thin-Walled Beams*. Computers&Structures, Vol. 24 (1), 147-156, 1986.
- [109] Saka, M.P., and Ulker, M., *Optimum Design of Geometrically Nonlinear Space Trusses*, Computer and Structures, Vol. 42 (3), 289-299, 1992.
- [110] Ekhande, S.G., Selvappalam, M., and Madugula, K.S., *Stability Functions for Three-Dimensional Beam-Columns*, Journal of Structural Engineering, Vol. 115 (2), 467-479, 1989.
- [111] SAP2000 v14, *Integrated Finite Element Analysis and Design of Structures: Steel Design Manual*, Computers & Structures Inc., Berkeley, CA, USA, 2010.
- [112] AISI (American Iron and Steel Institute) D100-08, *Excerpts-Gross Section Property Tables*, Cold-Formed Steel Design Manual, Part I; Dimensions and Properties, 2008.
- [113] AISI (American Iron and Steel Institute) S100-07, *North American Specification for the Design of Cold-Formed Steel Structural Members*, 2007.
- [114] AISC (American Institute of Steel Construction), *LRFD, Volume 1, Structural Members, Specifications & Code*, Manual of Steel Construction, 1991.
- [115] Prokic, A., *Computer Program for Determination of Geometric Properties of Thin-walled Beams with Open Profile*, Advances in Engineering Software, Vol. 30, 109-119, 1999.

- [116] Saka, M.P., and Geem, Z.W., *Mathematical and Metaheuristic Applications in Design Optimization of Steel Frame Structures: An Extensive Review*, Mathematical Problems in Engineering, Hindawi Publishing Corporation, 2013.
- [117] Yu, W-W., and LaBoube, R.A., *Cold-Formed Steel Design, Fourth Edition*, John Wiley & Sons Inc., Hoboken, NJ, USA, 2010.
- [118] Carbas, S., Aydogdu, I., and Saka, M.P., *A Comparative Study of Three Metaheuristics for Optimum Design of Engineering Structures*, 10th World Congress on Structural and Multidisciplinary Optimization, Orlando, FL, USA, May 19 -24, 2013.
- [119] Hasancebi, O., and Carbas, S., *Ant colony search method in practical structural optimization*, International Journal of Optimization in Civil Engineering, Vol. 1 (1), 91-105, 2011.
- [120] Ad Hoc Committee on Serviceability, *Structural Serviceability: A critical appraisal and research needs*, Journal of Structural Engineering, ASCE, Vol. 112 (12), 2646-2664, 1986.



## CURRICULUM VITAE

### PERSONAL INFORMATION

Surname, Name : Çarbaş, Serdar  
Nationality : Turkish (T.C.)  
Date of Birth and Place : 04.06.1979, Erzurum  
Marital Status : Married  
e-mail : [serdarcarbas@gmail.com](mailto:serdarcarbas@gmail.com), [carbas@metu.edu.tr](mailto:carbas@metu.edu.tr)

### EDUCATION

<b>Degree</b>	<b>Institution</b>	<b>Year of Graduation</b>
PhD.	METU, Engineering Sciences Dept.	2013
MSc.	METU, Engineering Sciences Dept.	2008
BSc.	Ataturk University, Civil Engineering Dept.	2003
High School	Anatolian High School, Erzurum	1997

### WORK EXPERIENCE

<b>Year</b>	<b>Enrollment</b>	<b>Place</b>
1. 2006-2013,	Research Assistant,	Department of Engineering Sciences, Middle East Technical University (METU), Ankara, Turkey
2. 2012-2013,	Visitor Graduated Researcher,	Civil and Environmental Engineering, University of California Los Angeles (UCLA), Los Angeles, California, USA

### FOREIGN LANGUAGES

1. Advanced English.

## **PUBLICATIONS**

### **1. International Referred Journal Articles**

1. Hasacebi, O., **arbař, S.**, Dođan, E., Erdal, F., and Saka, M.P., *Performance Evaluation of Metaheuristic Search Techniques in the Optimum Design of Real Size Pin Jointed Structures*, Computers & Structures, Vol. 87 (5-6), 284-302, 2009.
2. Hasacebi, O., **arbař, S.**, Dođan, E., Erdal, F., and Saka, M.P., *Comparison of Non-deterministic Search Techniques in the Optimum Design of Real Size Steel Frames*, Computers & Structures, Vol.88 (17-18), 1033-1048, 2010.
3. Hasacebi, O., **arbař, S.**, and Saka, M.P., *Improving the Performance of Simulated Annealing in Large-Scale Structural Optimization*, Structural and Multidisciplinary Optimization, Vol.41 (2), 189-203, 2010.
4. **arbař, S.**, and Saka, M.P., *Optimum Topology Design Of Various Geometrically Nonlinear Latticed Domes Using Improved Harmony Search Method*, Structural and Multidisciplinary Optimization, Vol.45 (3), 377-399, 2012.
5. Dong, S.B., **arbař, S.**, and Taciroglu, E., *On Principal Shear Axes for Correction Factors in Timoshenko Beam Theory*, International Journal of Solids and Structures, Vol.50 (10), 1681-1688, 2013.
6. Hasacebi, O., and **arbař, S.**, *Bat Inspired Algorithm for Discrete Size Optimization of Steel Frames*, Advances in Engineering Software, 2013.  
<http://dx.doi.org/10.1016/j.advengsoft.2013.10.003>
7. **arbař, S.**, and Saka, M.P., *Optimum Design of Single Layer Network Domes Using Harmony Search Method*, Asian Journal of Civil Engineering (Building and Housing), Vol.10 (1), 97-112, 2009.
8. Hasacebi, O., and **arbař, S.**, *Ant Colony Search Method in Practical Structural Optimization*, International Journal of Optimization in Civil Engineering, Vol.1 (1), 91-105, 2011.
9. **arbař, S.**, and Saka, M.P., *Efficiency of Improved Harmony Search Algorithm for Solving Engineering Optimization Problems*, International Journal of Optimization in Civil Engineering, Vol.3 (1), 99-114, 2013.

## **2. Proceedings in Symposiums, Conferences, and Congresses**

### **2.1. International Proceedings**

1. **Çarbaş, S.**, and Saka, M.P., *A Harmony Search Algorithm for Optimum Topology Design of Single Layer Lamella Domes*, The 9<sup>th</sup> International Conference on Computational Structures Technology, Athens, Greece, September 2-5, 2008.

2. **Çarbaş, S.**, Aydogdu, I., and Saka, M.P., *An Adaptive Harmony Search Algorithm Based Optimum Design of Steel Frames to LRFD-AISC*, The 8<sup>th</sup> World Congress on Structural and Multidisciplinary Optimization, LNEC, Lisbon, Portugal, June 1-5, 2009.

3. **Çarbaş, S.**, Aydogdu, I., and Saka, M.P., *Optimum Design of Cold-Formed Open Thin-Walled Sections Using Harmony Search Algorithm*, The 9<sup>th</sup> International Congress on Advances in Civil Engineering, Trabzon, Turkey, September 27-30, 2010

4. **Çarbaş, S.**, Doğan, E., Erdal, F., and Saka, M.P., *Comparison of Metaheuristic Search Techniques in Finding Solution of Optimization Problems*, The 2<sup>nd</sup> International Symposium on Computing in Science and Engineering, Kuşadası, Aydın, Turkey, June 1-4, 2011.

5. Hasańçebi, O., **Çarbaş, S.**, and Saka, M.P., *A Reformulation of the Ant Colony Optimization Algorithm for Large Scale Structural Optimization*, The 2<sup>nd</sup> International Conference on Soft Computing Technology in Civil, Structural and Environmental Engineering, Chania, Crete, Greece, September 6-9, 2011.

6. **Çarbaş, S.**, Aydogdu, I., and Saka, M.P., *A Comparative Study of Three Metaheuristics for Optimum Design of Engineering Structures*, The 10<sup>th</sup> World Congress on Structural and Multidisciplinary Optimization, Orlando, Florida, USA, May 19-24, 2013.

7. Hasańçebi, O., and **Çarbaş, S.**, *Optimum Design of Steel Space Frames Via Bat Inspired Algorithm*, The 10<sup>th</sup> World Congress on Structural and Multidisciplinary Optimization, Orlando, Florida, USA, May 19-24, 2013.

8. Hasańçebi, O., and **Çarbaş, S.**, *Optimal Design of Steel Trusses Using Stochastic Search Techniques*, The 4<sup>th</sup> International Conference on Mathematical and Computational Applications, Manisa, Turkey, June 11-13, 2013.

### **2.2. National Proceedings**

1. **Çarbaş, S.**, and Saka, M.P., *Tek Katmanlı Yapraksı Kubbe Yapıların Harmoni Arama Yöntemi Kullanılarak Optimum Topoloji Boyutlandırması*, 16. Ulusal Mekanik Kongresi, Kayseri, Turkey, June 22-26, 2009.

2. Dođan, E., Erdal, F., **Çarbaş, S.**, and Saka, M.P., *Izgara Sistemlerin LRFD-AISC Şartnamesine Göre Parçacık Küme Yöntemi Kullanılarak Optimum Boyutlandırılması*, 17. Ulusal mekanik Kongresi, Elazığ, Turkey, September 6-9, 2011.

3. **Çarbaş, S.**, Dođan, E., Erdal, F., and Saka, M.P., *Yapısal Optimizasyon Problemlerinin Çözümlerini Bulmak İçin Kullanılan Meta-Bulgusal Araştırma Yöntemlerinin Karşılaştırılması*, 17. Ulusal mekanik Kongresi, Elazığ, Turkey, September 6-9, 2011.

4. **Çarbaş, S.**, Dođan, E., Erdal, F., Hasańçebi, O., and Saka, M.P., *Yapı Mühendisliđi Problemlerinin Çözümü İçin Kullanılan Optimizasyon Tekniklerinin Karşılaştırılması*, 18. Ulusal Mekanik Kongresi, Manisa, Turkey, August 26-30, 2013.

### **FINANCED RESEARCH PROJECTS UNDERTAKEN**

1. Hasańçebi, O., Saka, M.P., Kurç, O., **Çarbaş, S.**, Dođan, E., Erdal, F., and Bahçeliođlu, T., *Stokastik Optimizasyon Yöntemleri Kullanılarak Üç Boyutlu Çelik Taşıyıcı Sistemlerin Optimum Tasarımı ve Ülkemiz Yapı Mühendisliđine Uygulanması*, The Scientific and Technological Research Council of Turkey (TUBITAK), Ankara, Turkey, Project No: 108M070, Start: June 1, 2008, End: December 1, 2010 (Duration: 2.5 years).

2. Hasańçebi, O., Saka, M.P., **Çarbaş, S.**, Dođan, E., Erdal, F., Yıldırım, I., and Kızıllkan, M., *Çok Katlı Çelik Taşıyıcı Sistemli Binaların Stokastik Optimizasyon Yöntemleri ile Optimum Boyutlandırılması*, Middle East Technical University (METU), Coordinatorship of Scientific Research Projects (BAP), Ankara, Turkey, Project No: BAP-2008-03-03-02, Start: April 1, 2008, End: March 31, 2010 (Duration: 2 years).

### **TEACHING EXPERIENCES**

#### **2006-2013**

Course/Teaching Assistant  
Department of Engineering Sciences,  
Middle East Technical University (METU),  
Ankara, Turkey

- ES202 Mathematics for Engineers
- ES223 Statics and Strength of Materials
- ES224 Strength of Materials
- ES225 Engineering Mechanics
- ES361 Computing Methods in Engineering
- ES501 Analytical Methods in Engineering – I
- ES502 Analytical Methods in Engineering – II
- ES503 Finite Elements Method
- ES504 Numerical Solution of Partial Differential Equations

## **MEMBERSHIP IN SCIENTIFIC AND PROFESSIONAL SOCIETIES**

1. Chamber of Turkish Engineers and Architects (TMMOB), Chamber of Civil Engineers (IMO), Member ID # 80201

## **SCHOLARSHIPS, AWARDS and HONOURS**

1. International Scientific Fellowship Program, Scientific Fellowship and Grant Programs (BIDEB), The Scientific and Technological Research Council of Turkey (TUBITAK), Turkey.

Place; Athens, Greece

Date (Duration); September 1-6, 2008 (1 week)

2. International Scientific Publication Awards, Development Foundation, Middle East Technical University (METU), Turkey.

in 2009, 2010 (2), 2012, 2013

3. International Scientific Publication Awards, The Scientific and Technological Research Council of Turkey (TUBITAK), Turkey.

in 2009, 2010 (2), 2012, 2013

4. The Council of Higher Education (YÖK), Doctoral Research Fellowship, Turkey.

Place; University of California Los Angeles (UCLA), Los Angeles, California, USA,

Date (Duration); August 1, 2011 – July 31, 2012 (12 Months)

5. Included in *Marquis Who's Who in the World 2014 (31<sup>st</sup> Edition)*

## **SOFTWARE AND PROGRAMMING SKILLS**

1. Microsoft Office
2. Visual and Intel FORTRAN
3. MATHCAD
4. MATLAB
5. SAP2000
6. ABAQUS
7. AUTOCAD
8. MAPLE